



# Exclusive processes at hermes

# Generalized parton distributions

- I believe Peter has done a good job this morning introducing generalized parton distributions (GPDs) ...



# Generalized parton distributions

- I believe Peter has done a good job this morning introducing generalized parton distributions (GPDs) ...

● ... thanks!



# Generalized parton distributions

- I believe Peter has done a good job this morning introducing generalized parton distributions (GPDs) ...

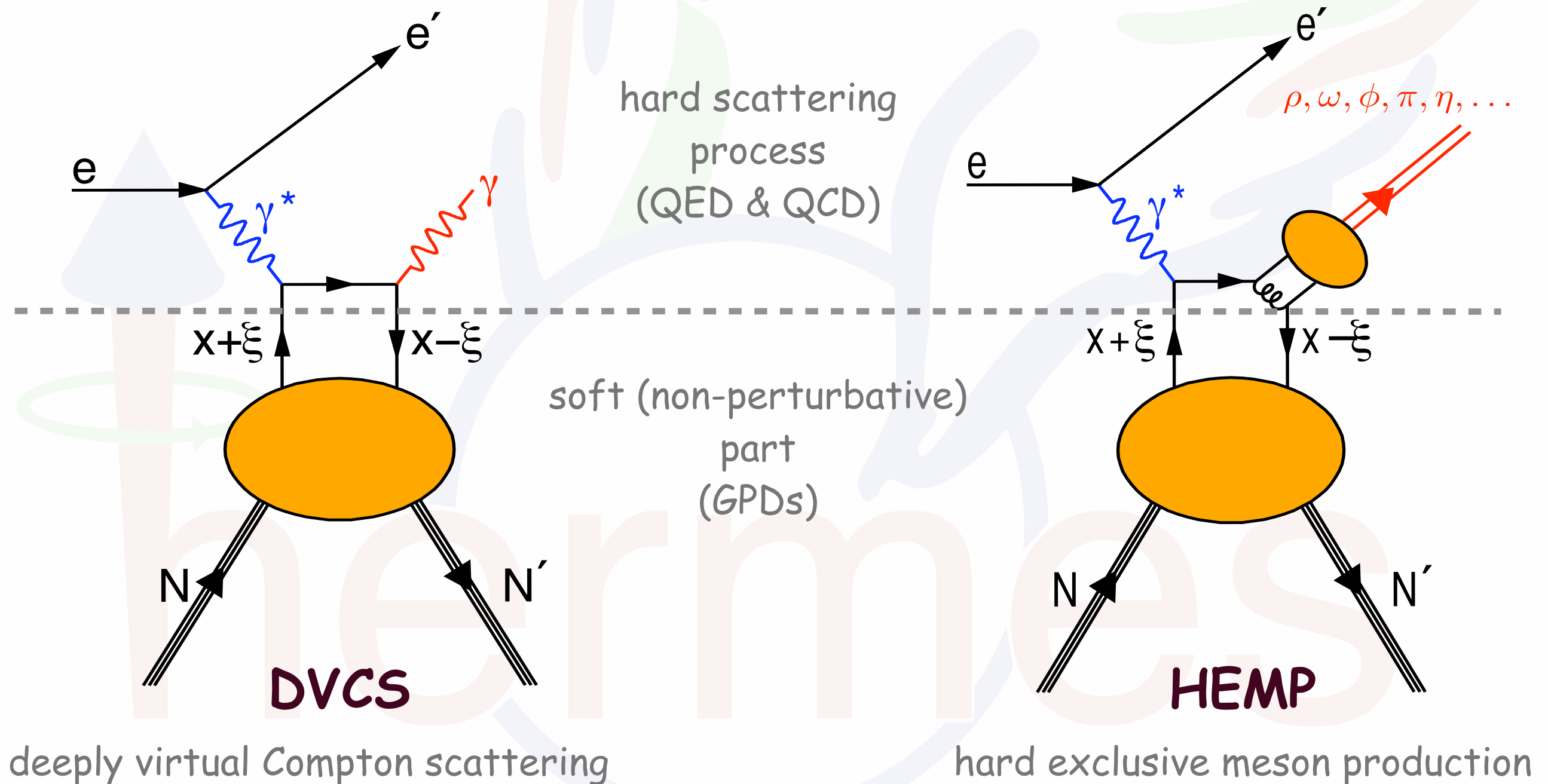
● ... thanks!

- ... also to Erik Etzelmüller and Charlotte Van Hulse for "slides support"

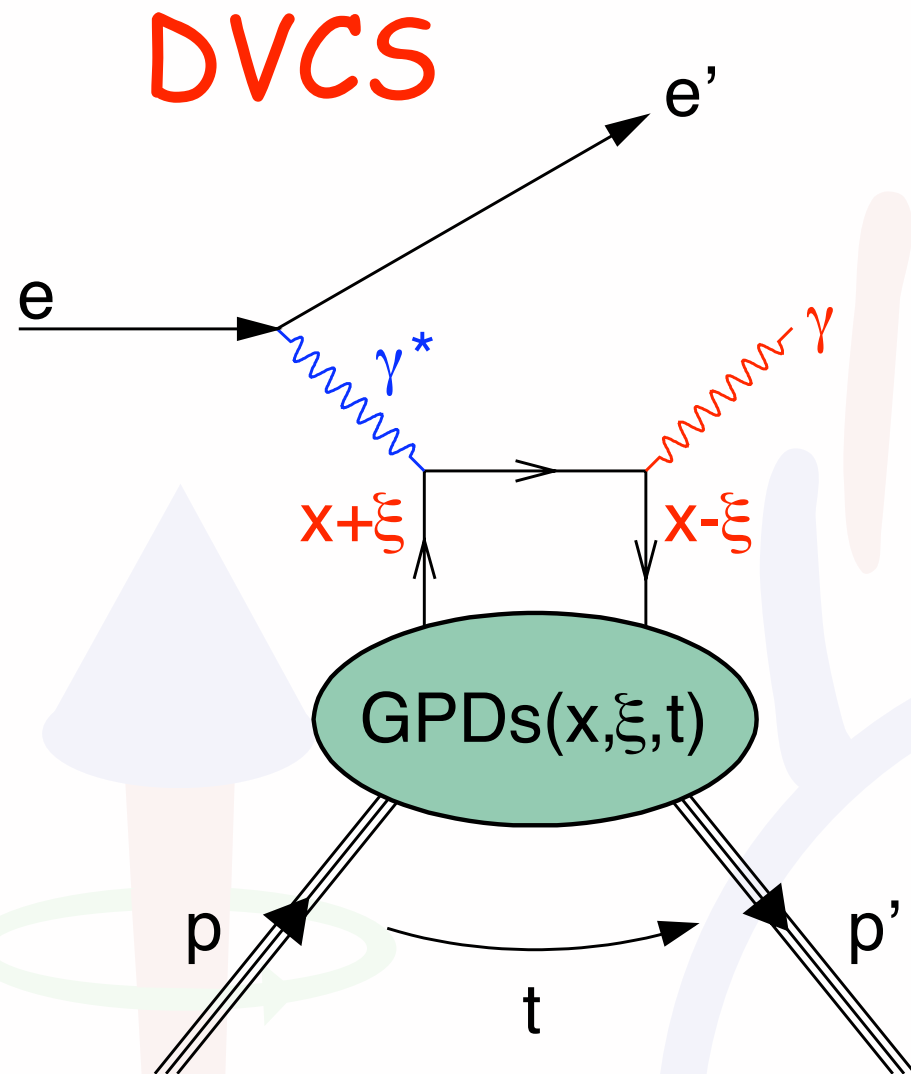


# GPDs in exclusive reactions

Experimentally GPDs can be accessed through measurements of hard exclusive lepton-nucleon scattering processes.

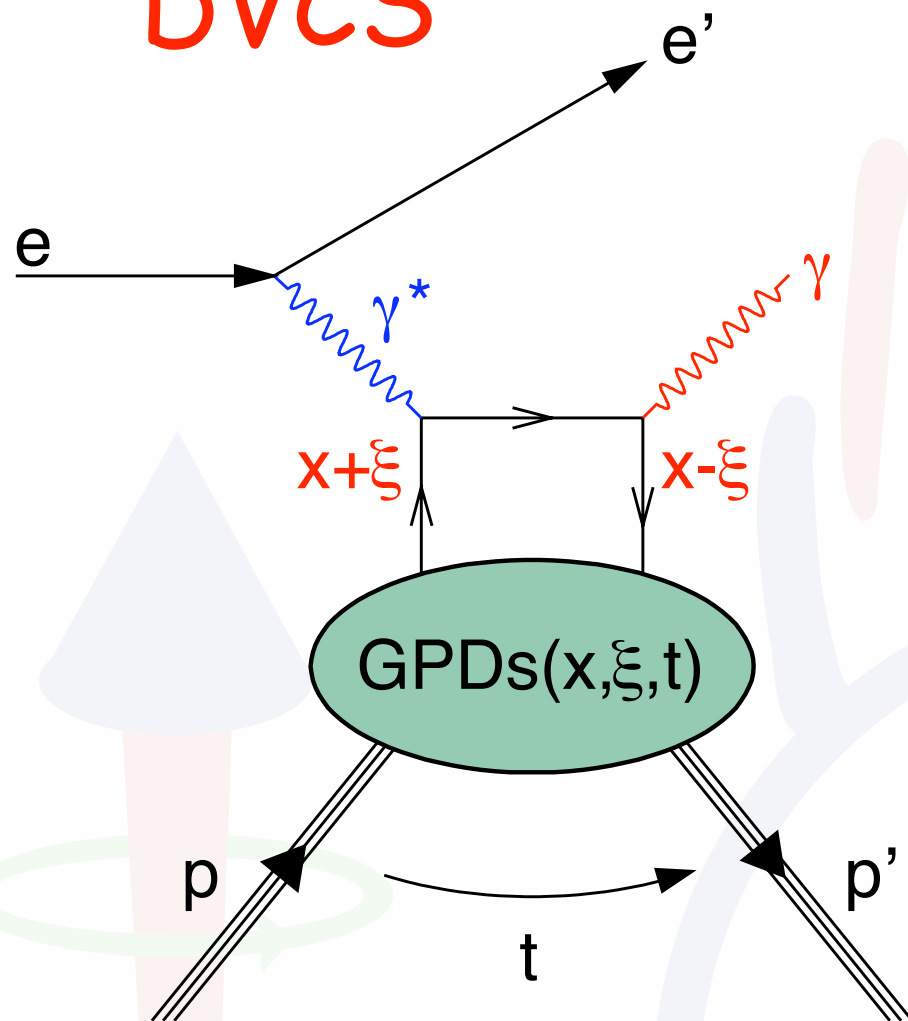


# Real-photon production

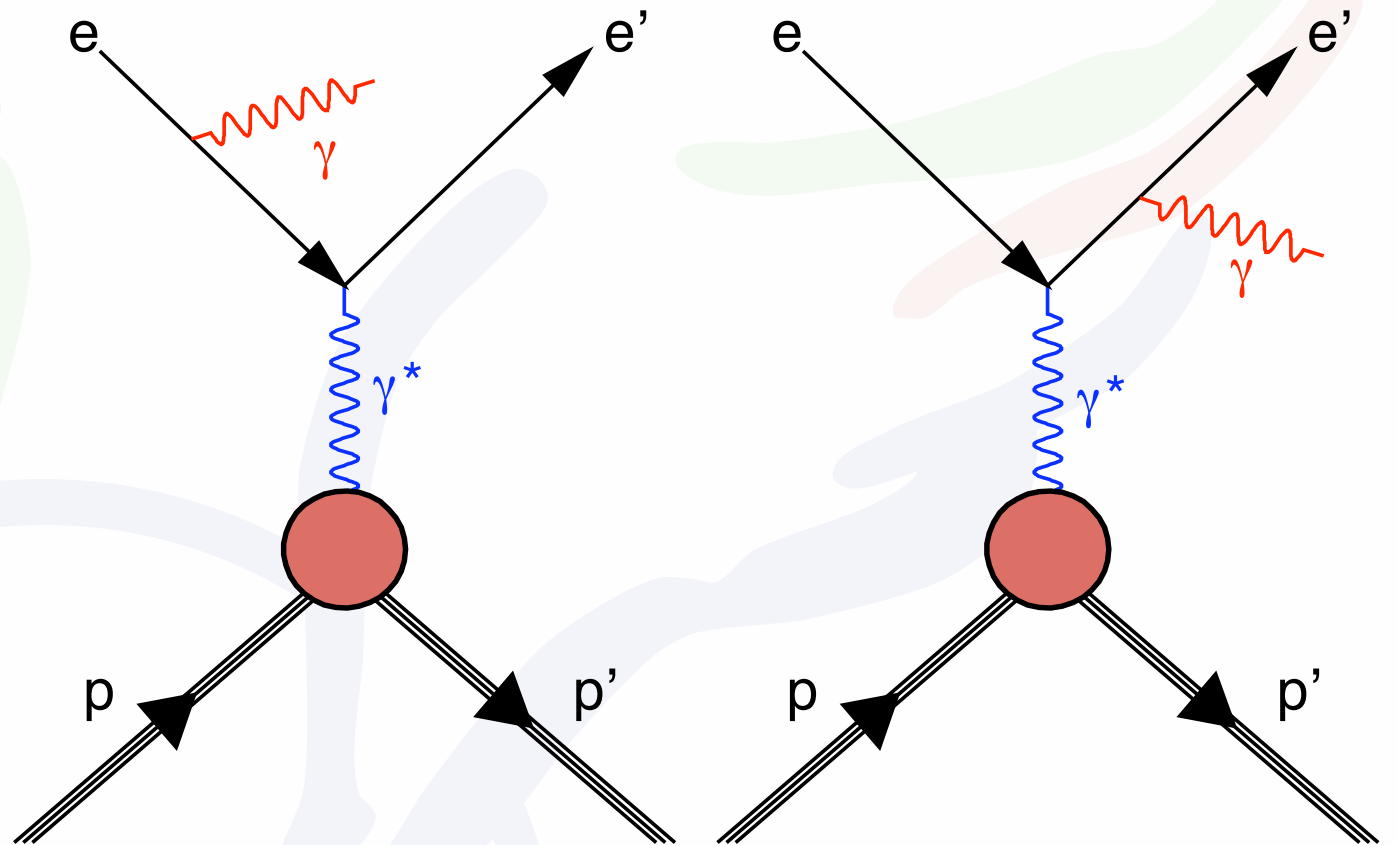


# Real-photon production

DVCS



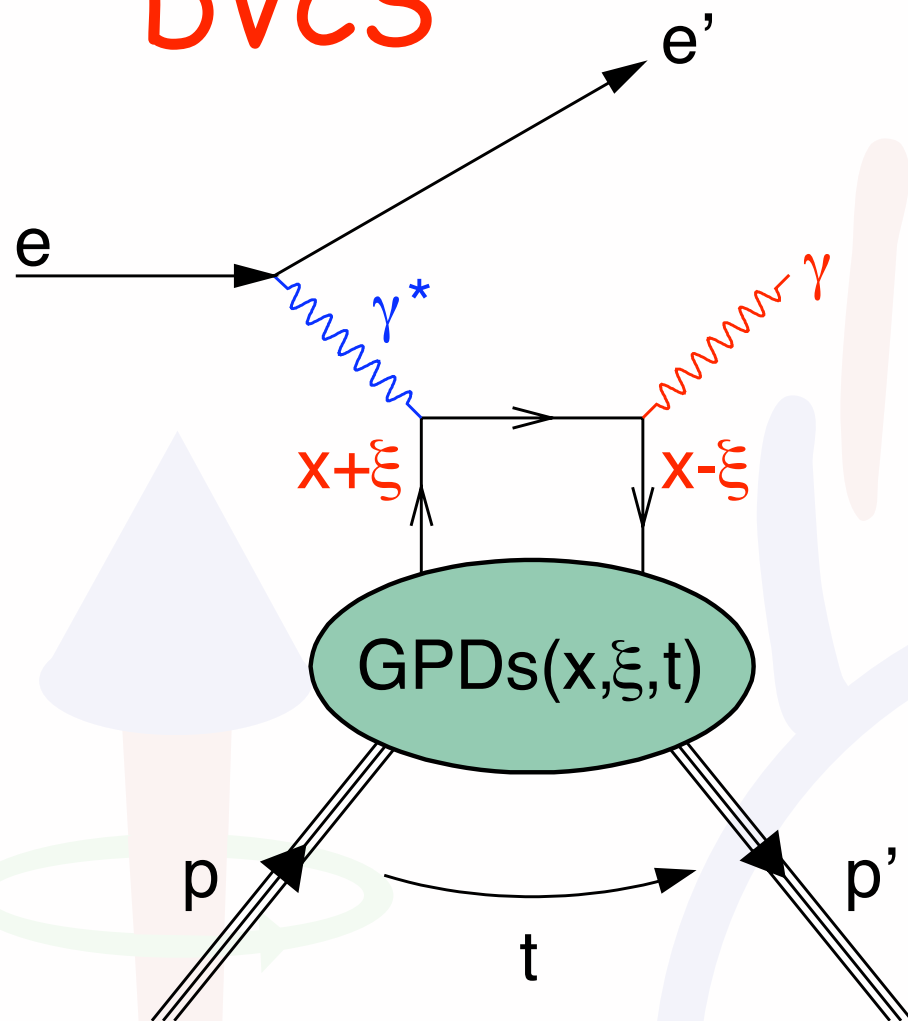
Bethe-Heitler



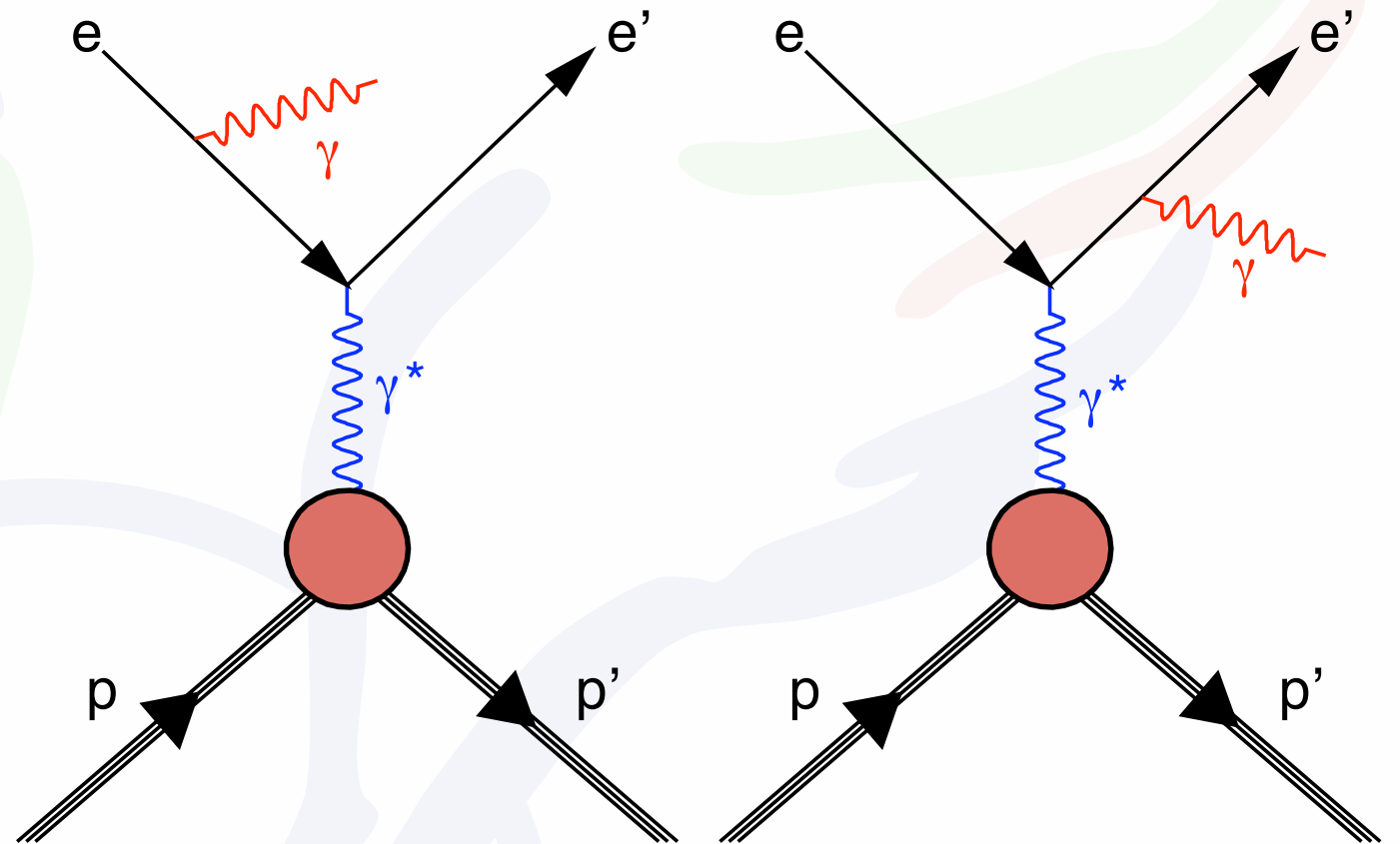
$$\frac{d^4\sigma}{dQ^2 dx_B dt d\phi} = \frac{y^2}{32(2\pi)^4 \sqrt{1 + \frac{4M^2 x_B^2}{Q^2}}} (|\mathcal{T}_{\text{DVCS}}|^2 + |\mathcal{T}_{\text{BH}}|^2 + \mathcal{I})$$

# Real-photon production

DVCS



Bethe-Heitler



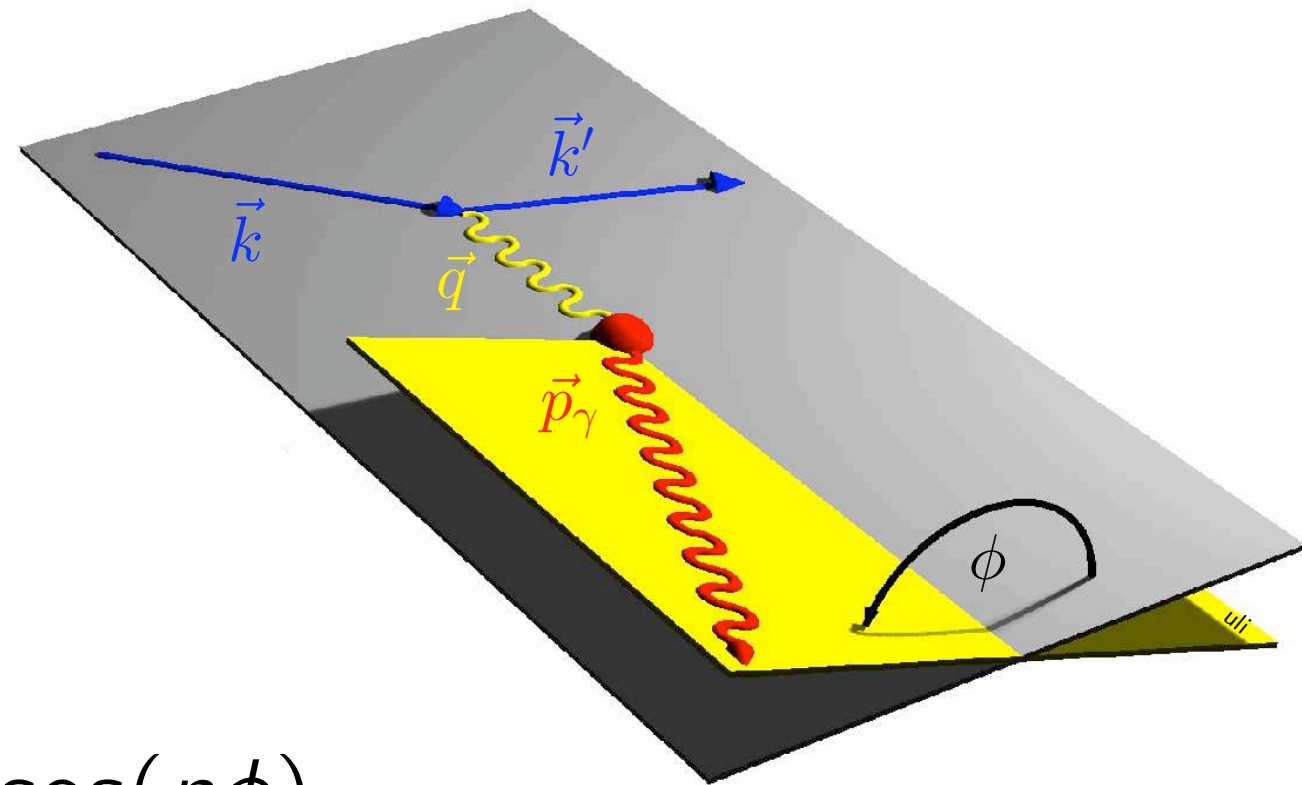
Amplitude of Bethe-Heitler scattering is dominant at HERMES kinematics

$$\frac{d^4\sigma}{dQ^2 dx_B dt d\phi} = \frac{y^2}{32(2\pi)^4 \sqrt{1 + \frac{4M^2 x_B^2}{Q^2}}} (|\mathcal{T}_{\text{DVCS}}|^2 + |\mathcal{T}_{\text{BH}}|^2 + \boxed{\mathcal{I}})$$

DVCS amplitude is amplified by  
BH in the interference term

# Azimuthal dependences in DVCS/BH

- beam polarization  $P_B$
- beam charge  $C_B$
- here: unpolarized target



Fourier expansion for  $\phi$ :

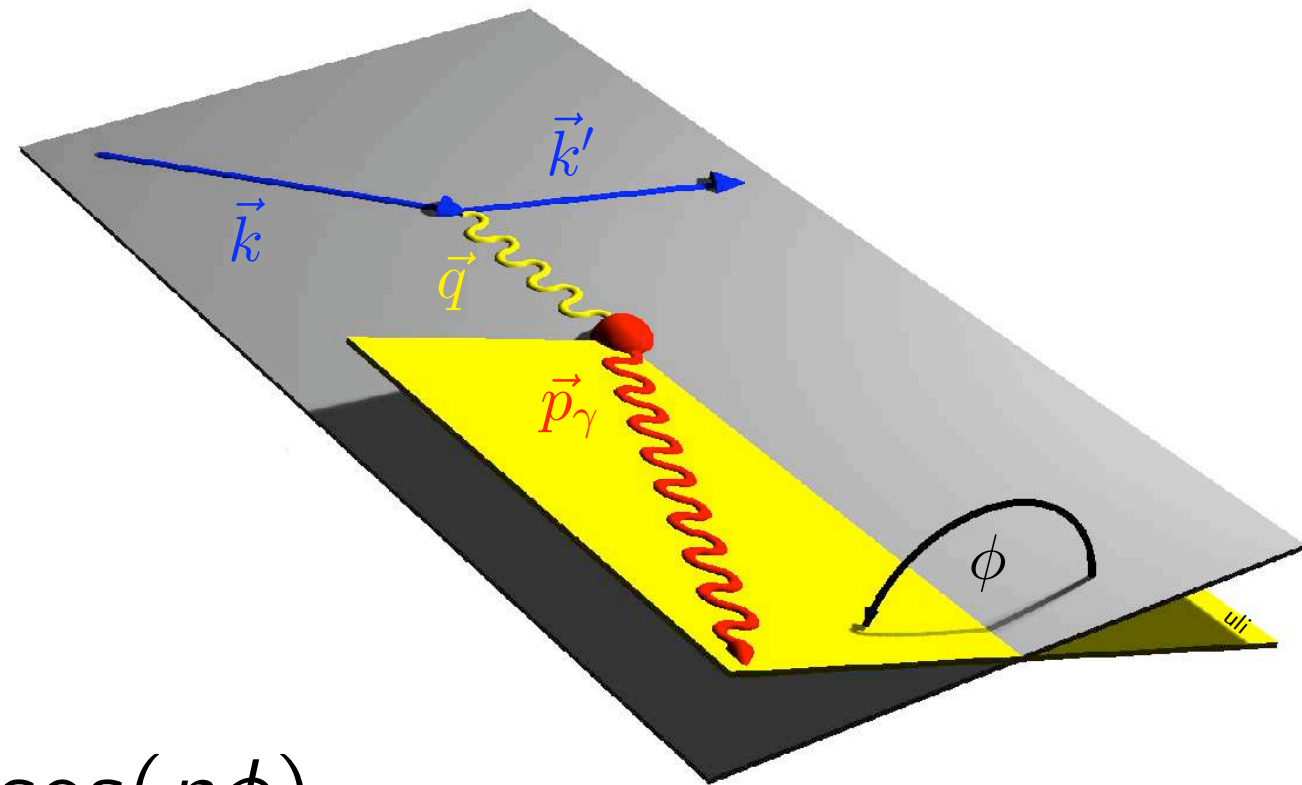
$$|\mathcal{T}_{\text{BH}}|^2 = \frac{K_{\text{BH}}}{\mathcal{P}_1(\phi)\mathcal{P}_2(\phi)} \sum_{n=0}^2 c_n^{\text{BH}} \cos(n\phi)$$

calculable in QED  
(using form-factor measurements)



# Azimuthal dependences in DVCS/BH

- beam polarization  $P_B$
- beam charge  $C_B$
- here: unpolarized target



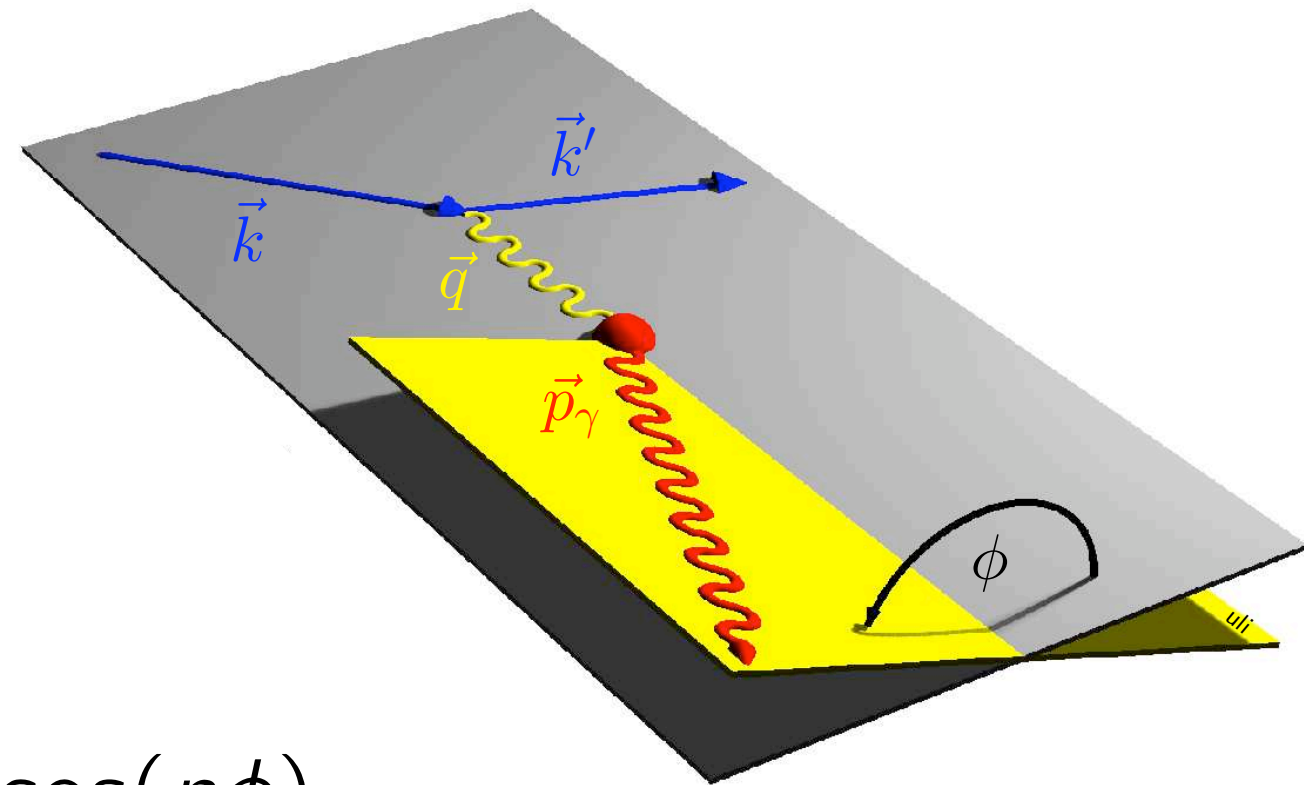
Fourier expansion for  $\phi$ :

$$|\mathcal{T}_{\text{BH}}|^2 = \frac{K_{\text{BH}}}{\mathcal{P}_1(\phi)\mathcal{P}_2(\phi)} \sum_{n=0}^2 c_n^{\text{BH}} \cos(n\phi)$$

$$|\mathcal{T}_{\text{DVCS}}|^2 = K_{\text{DVCS}} \left[ \sum_{n=0}^2 c_n^{\text{DVCS}} \cos(n\phi) + P_B \sum_{n=1}^1 s_n^{\text{DVCS}} \sin(n\phi) \right]$$

# Azimuthal dependences in DVCS/BH

- beam polarization  $P_B$
- beam charge  $C_B$
- here: unpolarized target



Fourier expansion for  $\phi$ :

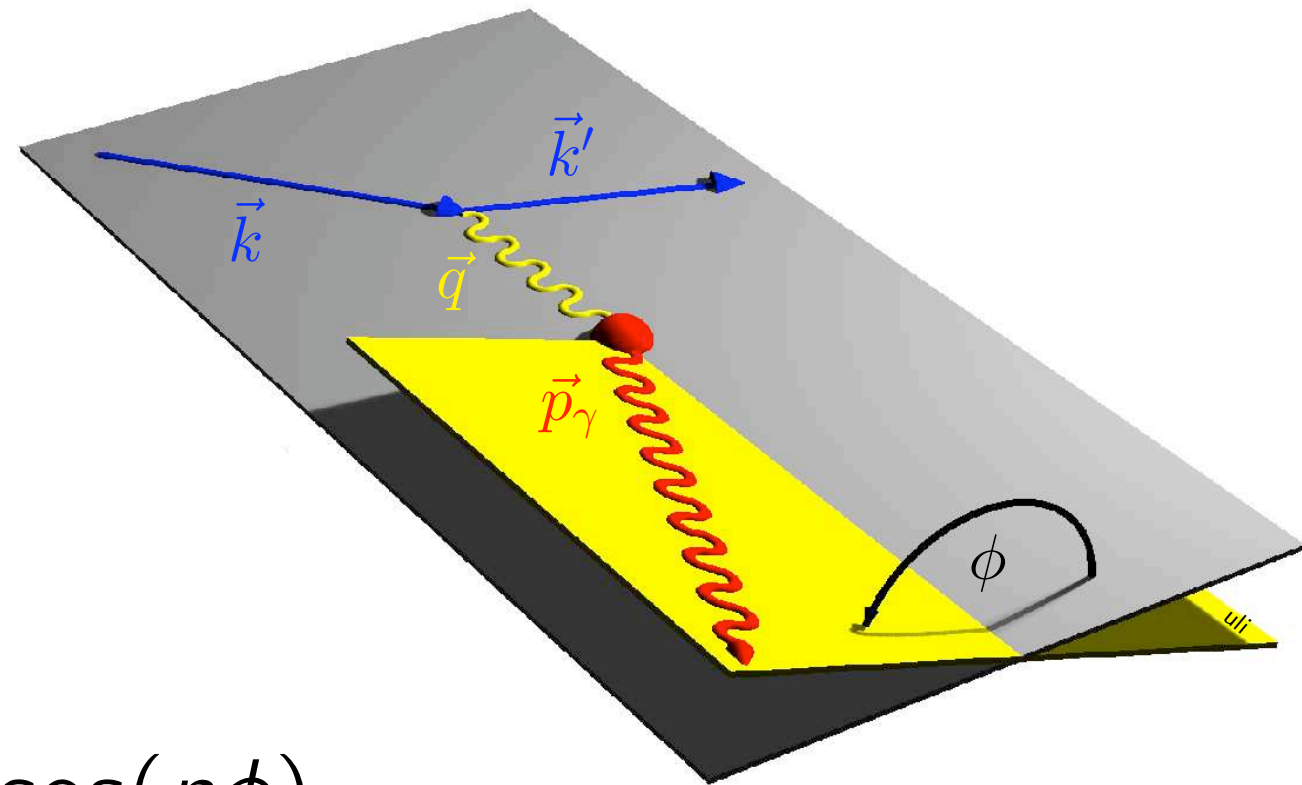
$$|\mathcal{T}_{\text{BH}}|^2 = \frac{K_{\text{BH}}}{\mathcal{P}_1(\phi)\mathcal{P}_2(\phi)} \sum_{n=0}^2 c_n^{\text{BH}} \cos(n\phi)$$

$$|\mathcal{T}_{\text{DVCS}}|^2 = K_{\text{DVCS}} \left[ \sum_{n=0}^2 c_n^{\text{DVCS}} \cos(n\phi) + P_B \sum_{n=1}^1 s_n^{\text{DVCS}} \sin(n\phi) \right]$$

$$\mathcal{I} = \frac{C_B K_{\mathcal{I}}}{\mathcal{P}_1(\phi)\mathcal{P}_2(\phi)} \left[ \sum_{n=0}^3 c_n^{\mathcal{I}} \cos(n\phi) + P_B \sum_{n=1}^2 s_n^{\mathcal{I}} \sin(n\phi) \right]$$

# Azimuthal dependences in DVCS/BH

- beam polarization  $P_B$
- beam charge  $C_B$
- here: unpolarized target



Fourier expansion for  $\phi$ :

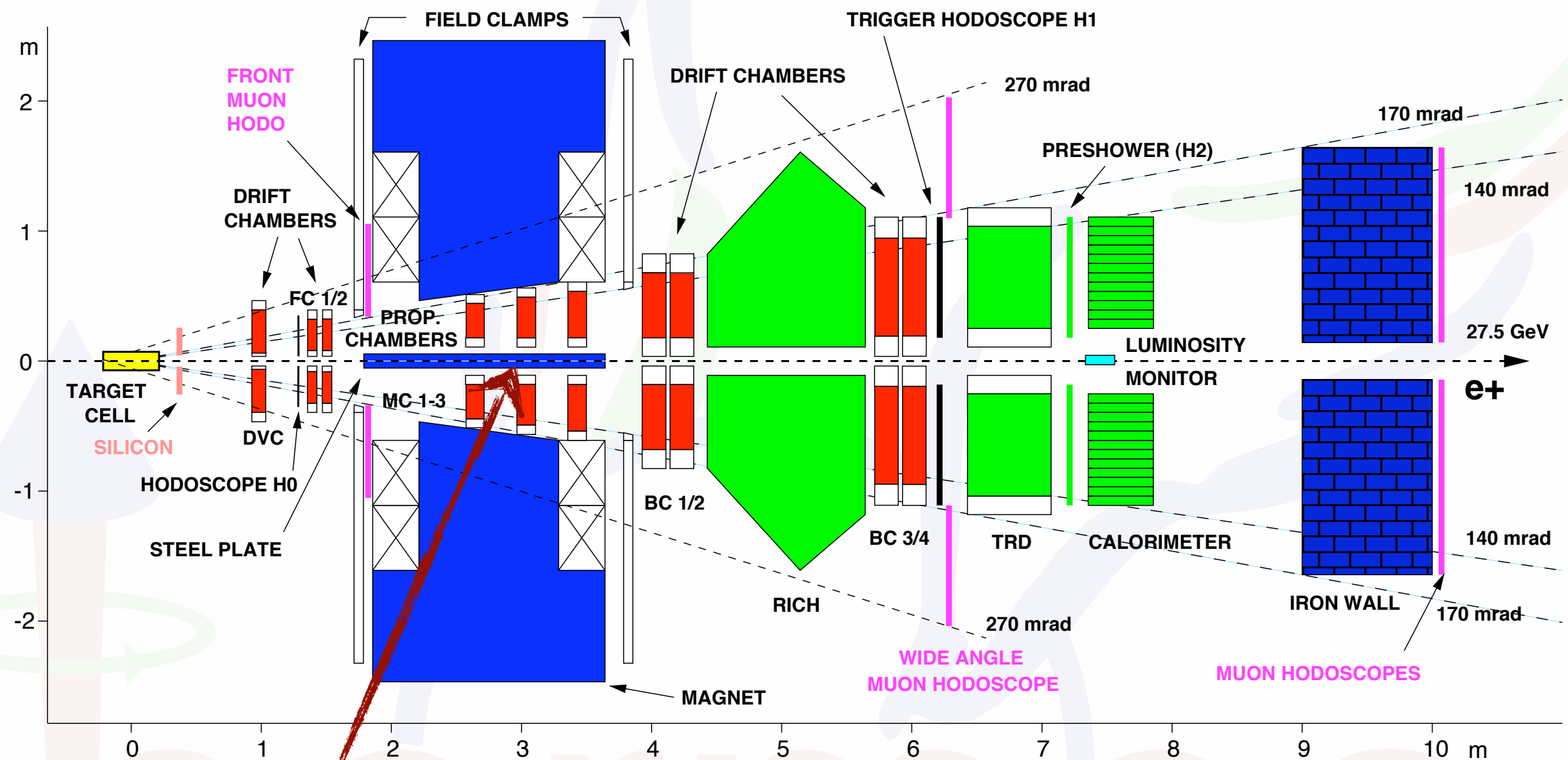
$$|\mathcal{T}_{\text{BH}}|^2 = \frac{K_{\text{BH}}}{\mathcal{P}_1(\phi)\mathcal{P}_2(\phi)} \sum_{n=0}^2 c_n^{\text{BH}} \cos(n\phi)$$

$$|\mathcal{T}_{\text{DVCS}}|^2 = K_{\text{DVCS}} \left[ \sum_{n=0}^2 c_n^{\text{DVCS}} \cos(n\phi) + P_B \sum_{n=1}^1 s_n^{\text{DVCS}} \sin(n\phi) \right]$$

$$\mathcal{I} = \frac{C_B K_{\mathcal{I}}}{\mathcal{P}_1(\phi)\mathcal{P}_2(\phi)} \left[ \sum_{n=0}^3 c_n^{\mathcal{I}} \cos(n\phi) + P_B \sum_{n=1}^2 s_n^{\mathcal{I}} \sin(n\phi) \right]$$

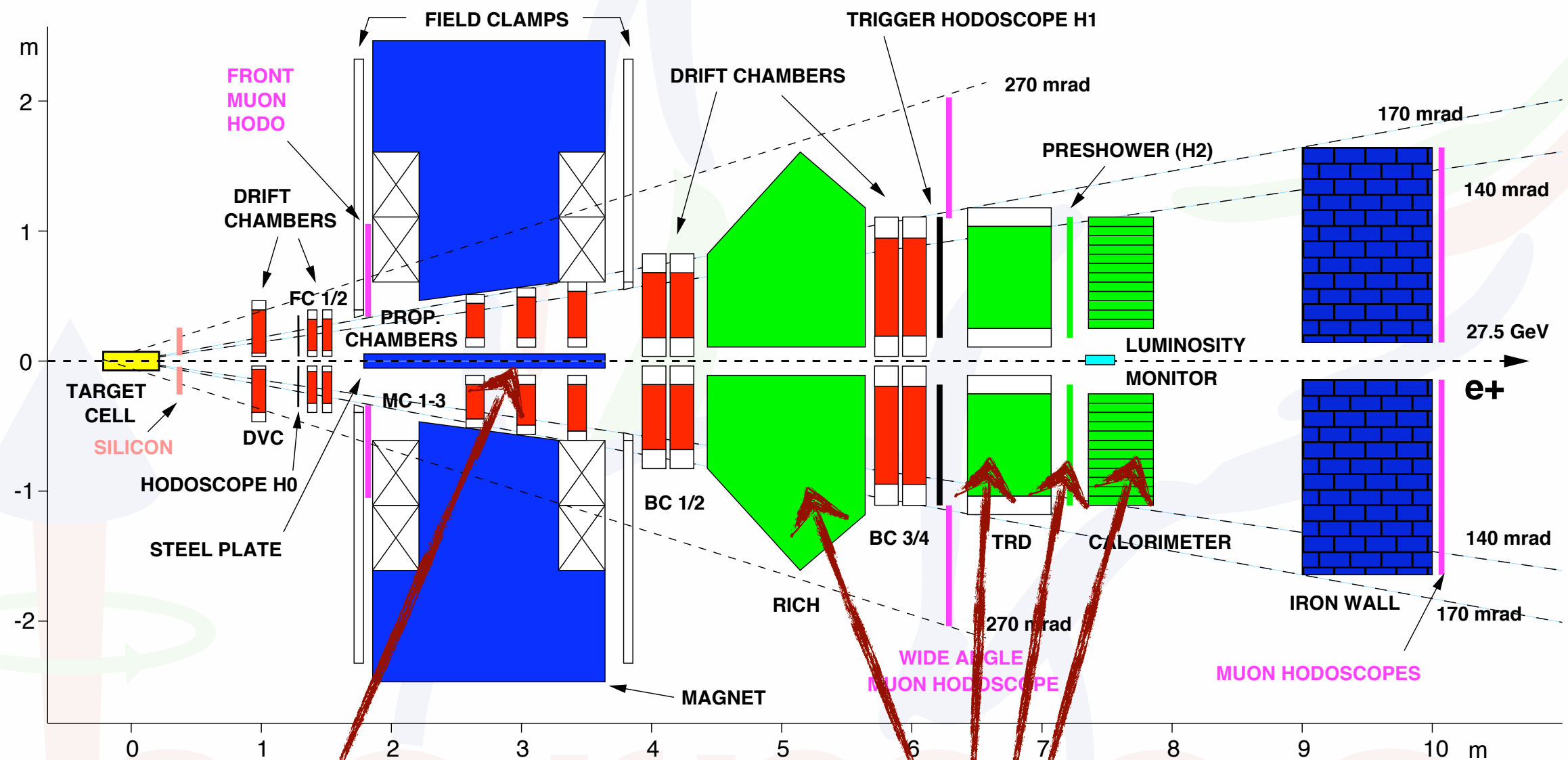
bilinear ("DVCS") or linear ("I") in GPDs

# HERMES (1998-2005) schematically



two (mirror-symmetric) halves  
-> no homogenous azimuthal  
coverage

# HERMES (1998-2005) schematically



two (mirror-symmetric) halves  
 -> no homogenous azimuthal coverage

Particle ID detectors allow for

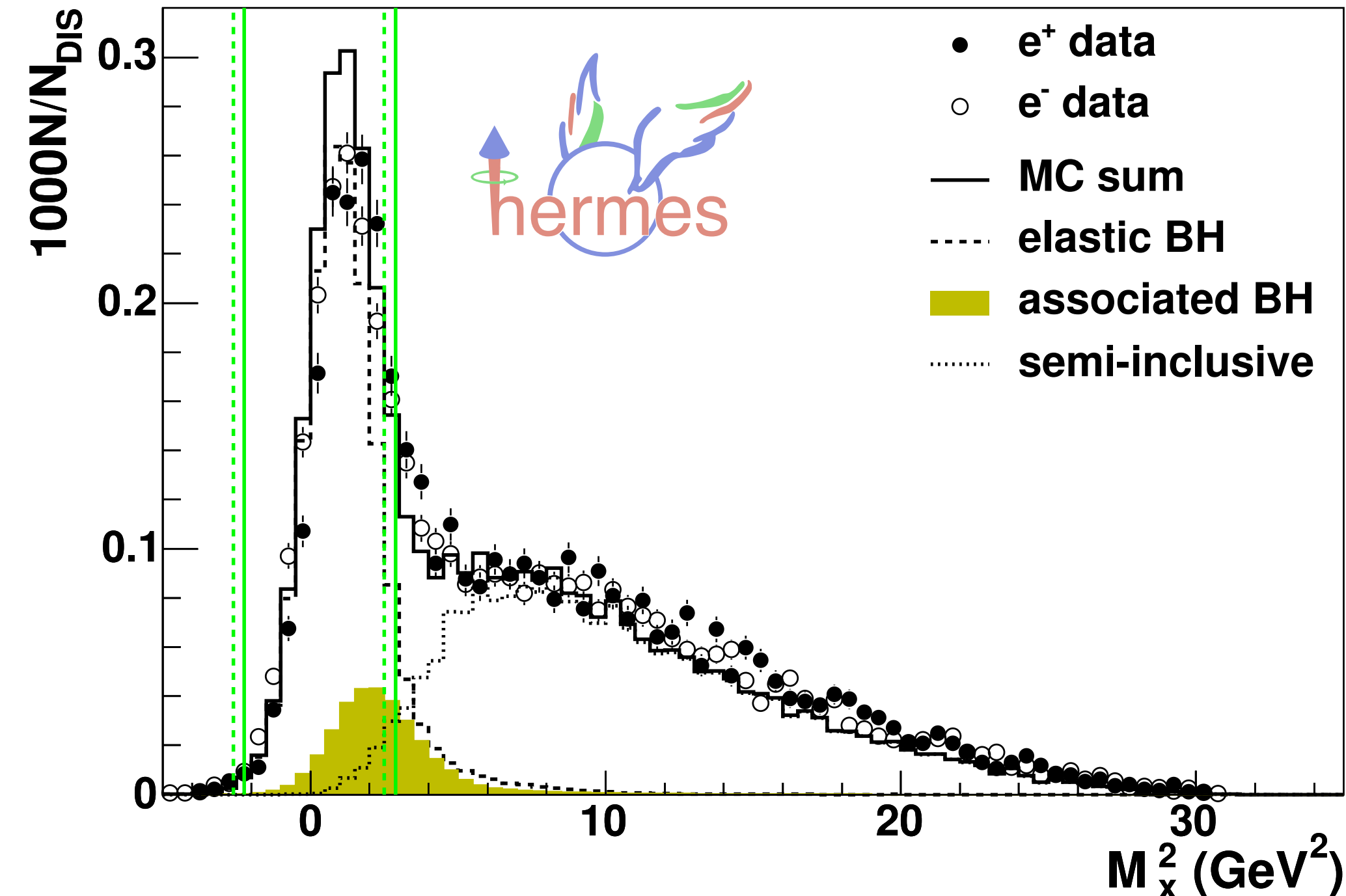
- lepton/hadron separation
- RICH: pion/kaon/proton discrimination  $2\text{GeV} < p < 15\text{GeV}$



# Exclusivity: missing-mass technique

$$M_x^2 = (k - k' + P_0 - P_\gamma)^2 = M^2 + 2M(\nu - E_\gamma) + t$$

$ep \rightarrow e \gamma X$

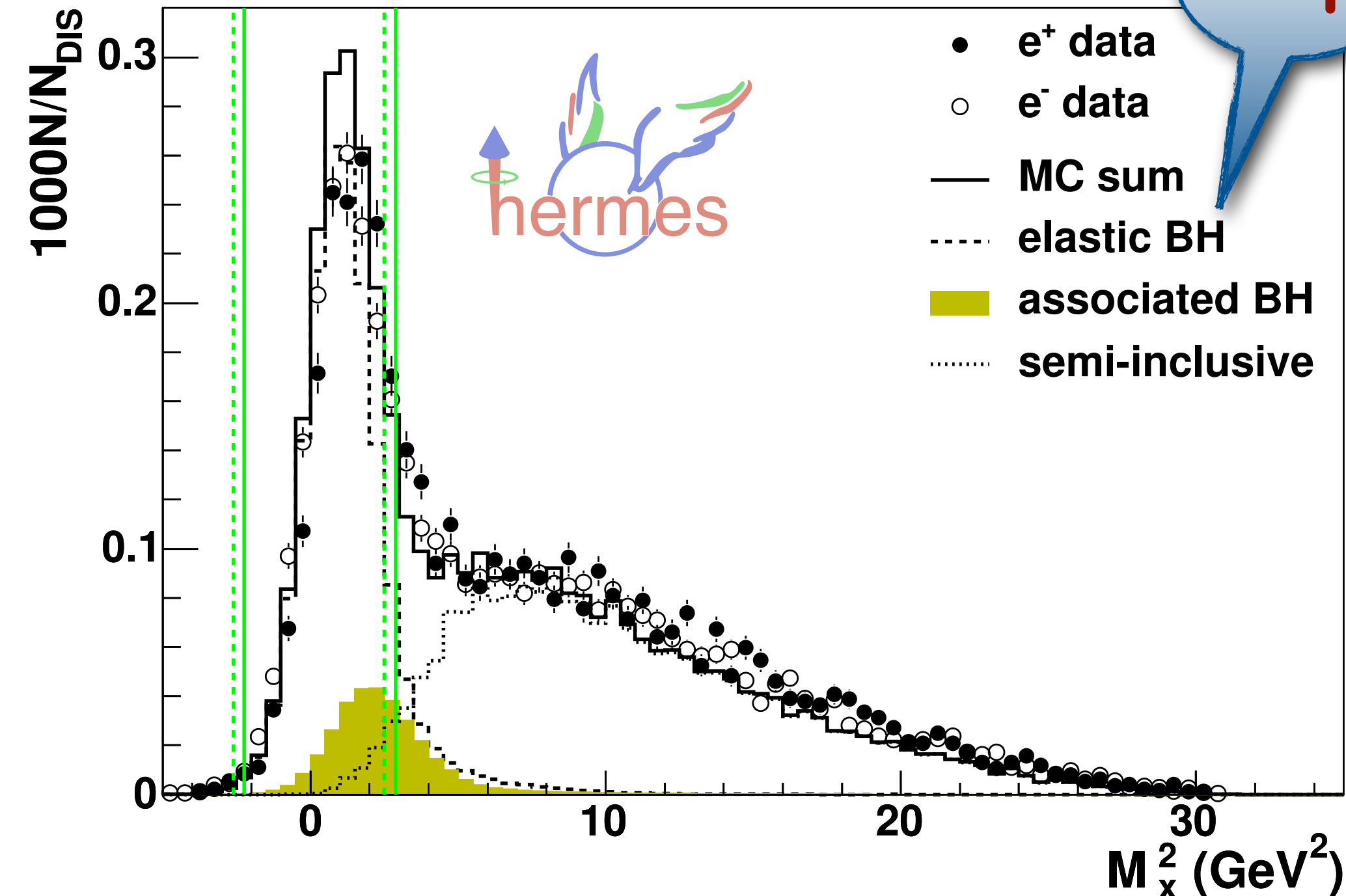


# Exclusivity: missing-mass technique

$$M_x^2 = (k - k' + P_0 - P_\gamma)^2 = M^2 + 2M(\nu - E_\gamma) + t$$

$ep \rightarrow e \gamma X$

$X=p$



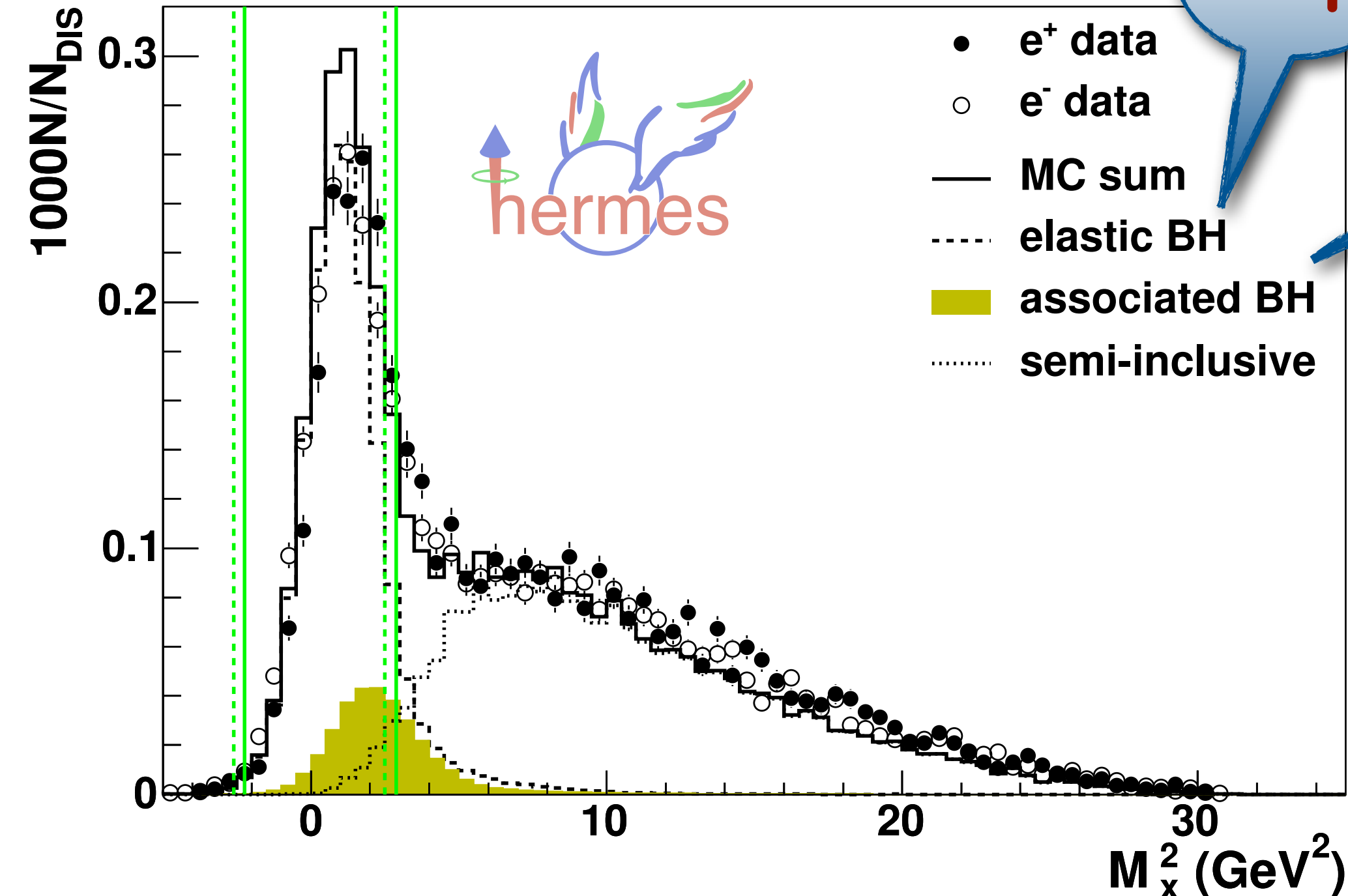
# Exclusivity: missing-mass technique

$$M_x^2 = (k - k' + P_0 - P_\gamma)^2 = M^2 + 2M(\nu - E_\gamma) + t$$

$ep \rightarrow e \gamma X$

$X=p$

$X=\Delta^+$



# Exclusivity: missing-mass technique

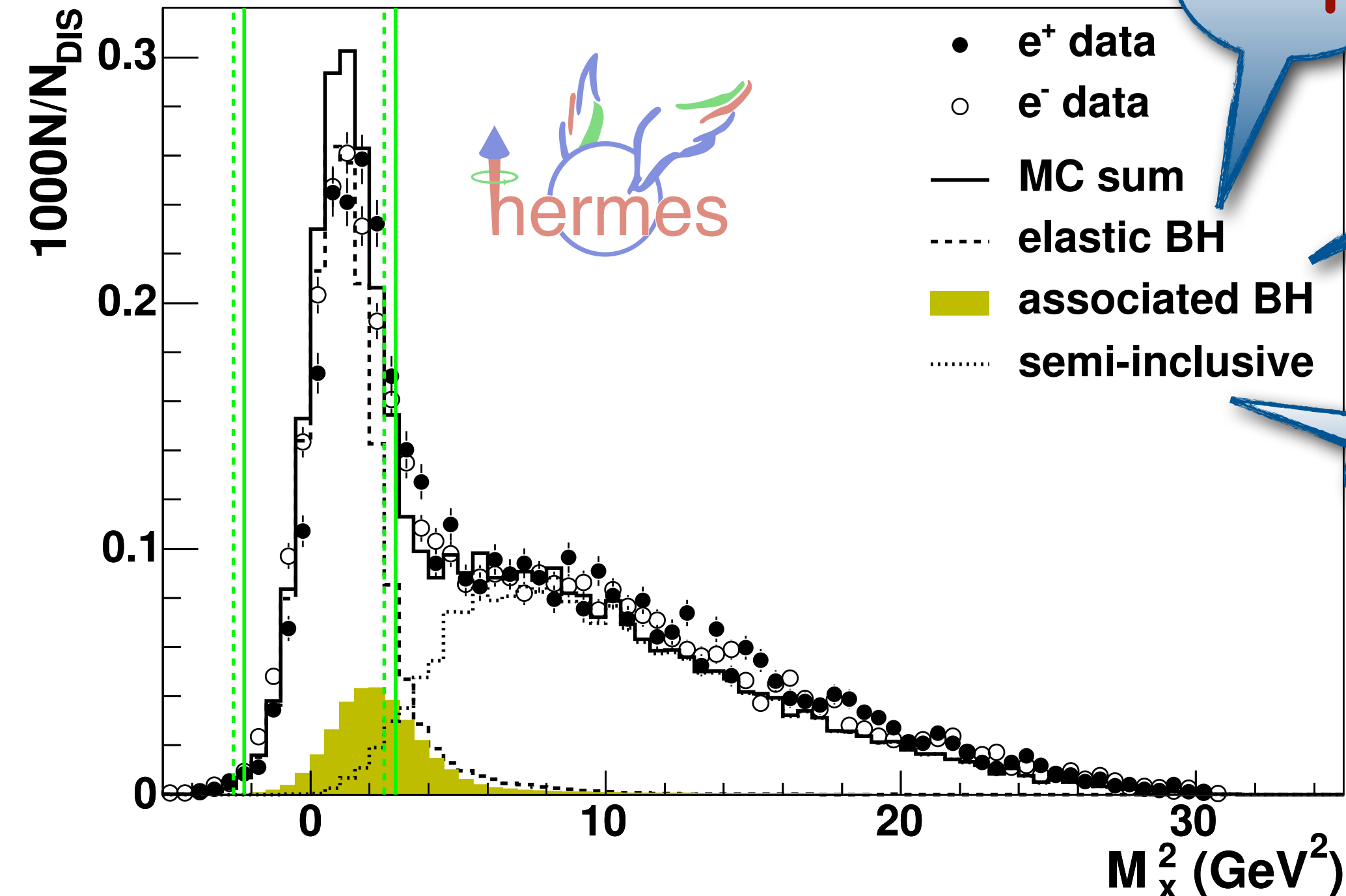
$$M_x^2 = (k - k' + P_0 - P_\gamma)^2 = M^2 + 2M(\nu - E_\gamma) + t$$

$ep \rightarrow e \gamma X$

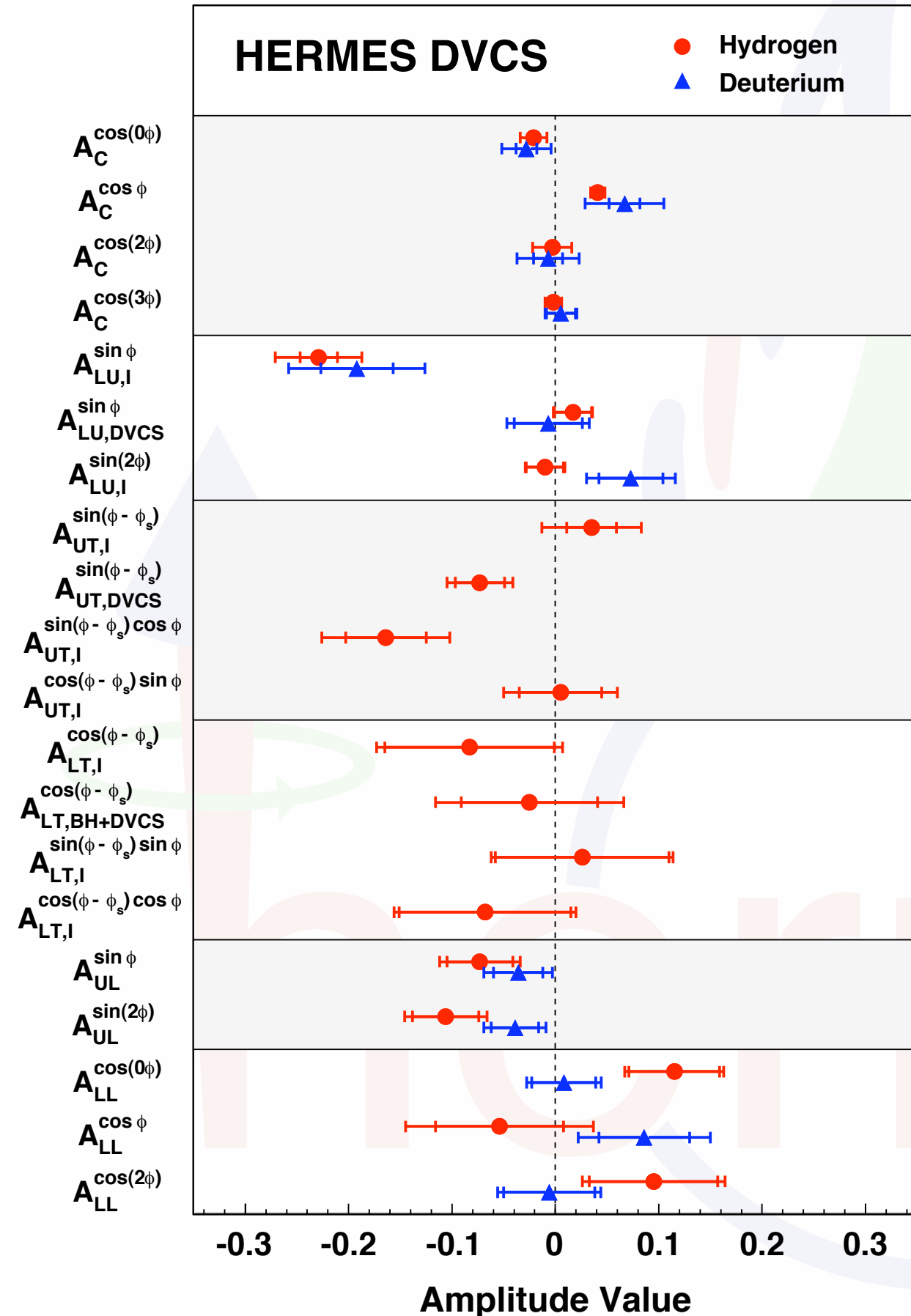
$X=p$

$X=\Delta^+$

$\pi^0 + \dots$



# A wealth of azimuthal amplitudes



Beam-charge asymmetry:

**GPD H**

PRD 75 (2007) 011103

NPB 829 (2010) 1

JHEP 11 (2009) 083

PRC 81 (2010) 035202

Beam-helicity asymmetry:

**GPD H**

PRL 87 (2001) 182001

JHEP 07 (2012) 032

Transverse target spin asymmetries:

**GPD E from proton target**

JHEP 06 (2008) 066

PLB 704 (2011) 15

Longitudinal target spin asymmetry:

**GPD  $\tilde{H}$**

JHEP 06 (2010) 019

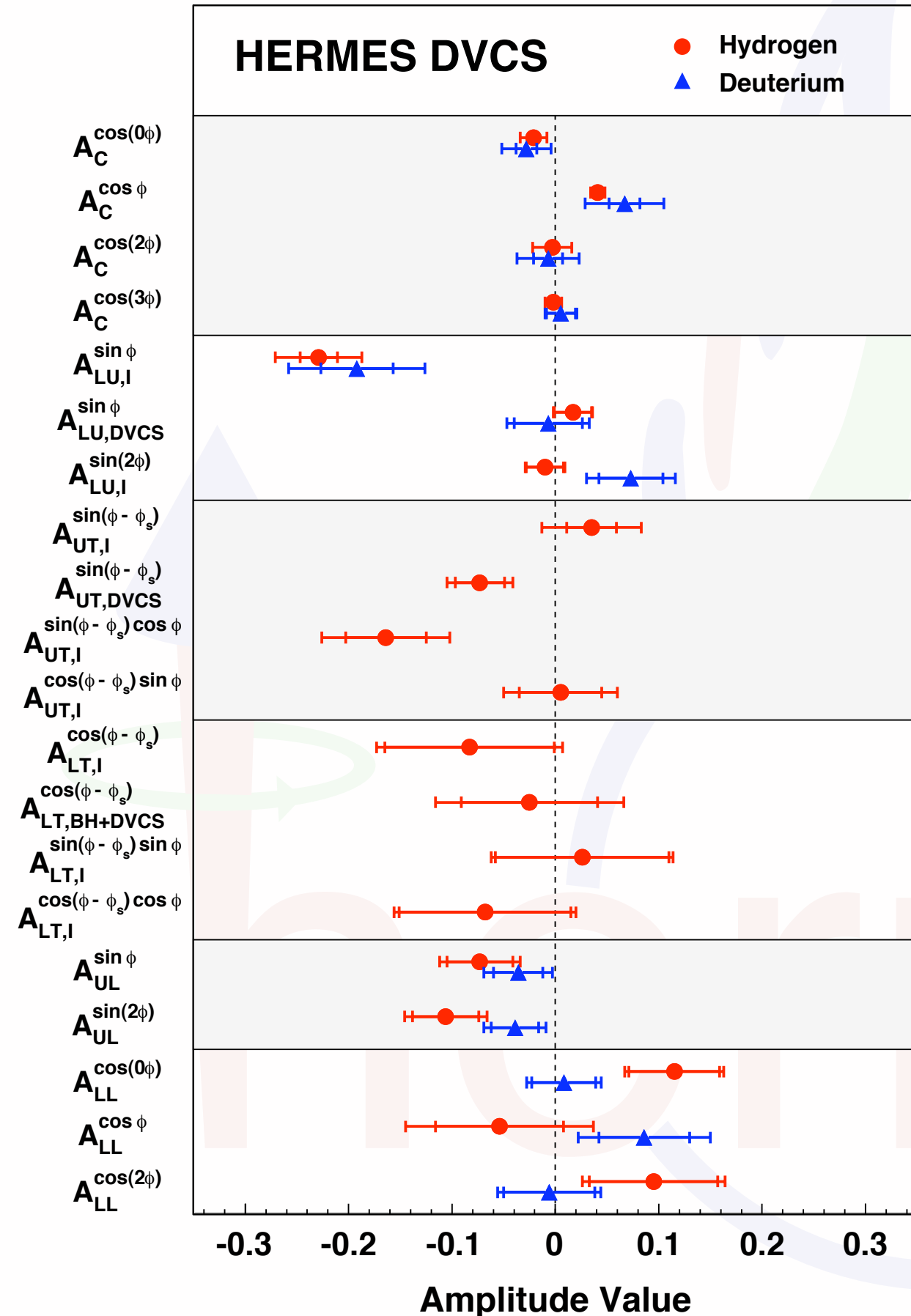
Double-spin asymmetry:

**GPD  $\tilde{H}$**

NPB 842 (2011) 265



# A wealth of azimuthal amplitudes



Beam-charge asymmetry:

**GPD H**

PRD 75 (2007) 011103

NPB 829 (2010) 1

JHEP 11 (2009) 083

PRC 81 (2010) 035202

Beam-helicity asymmetry:

**GPD H**

PRL 87 (2001) 182001

JHEP 07 (2012) 032

Transverse target spin asymmetries:

**GPD E from proton target**

JHEP 06 (2008) 066

PLB 704 (2011) 15

Longitudinal target spin asymmetry:

**GPD  $\tilde{H}$**

JHEP 06 (2010) 019

Double-spin asymmetry:

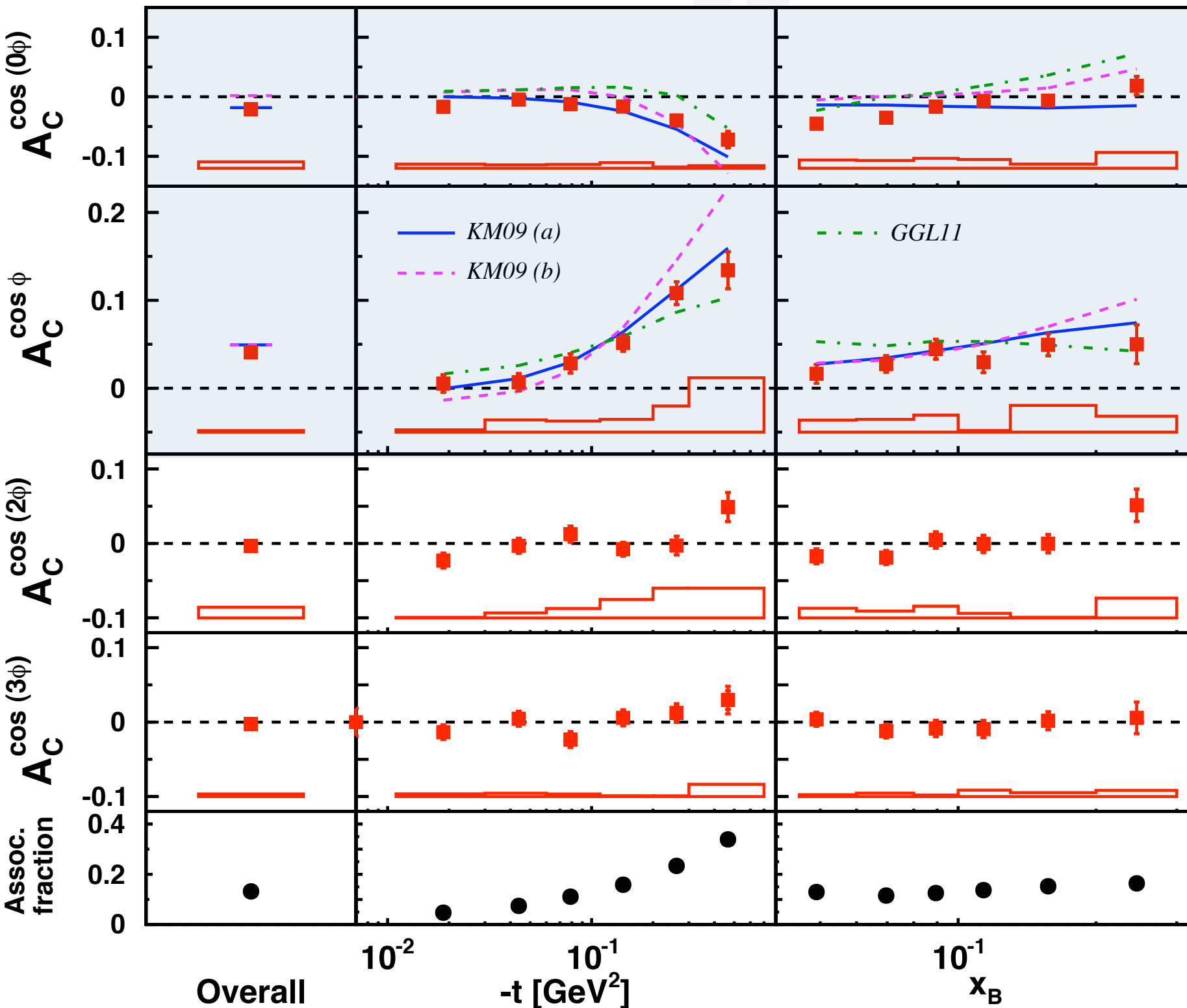
**GPD  $\tilde{H}$**

NPB 842 (2011) 265

complete data set!

# Beam-charge asymmetry

[Airapetian et al., JHEP 07 (2012) 032]



constant term:

$$\propto -A_C^{\cos\phi}$$

$$\propto \text{Re}[F_1 \mathcal{H}]$$

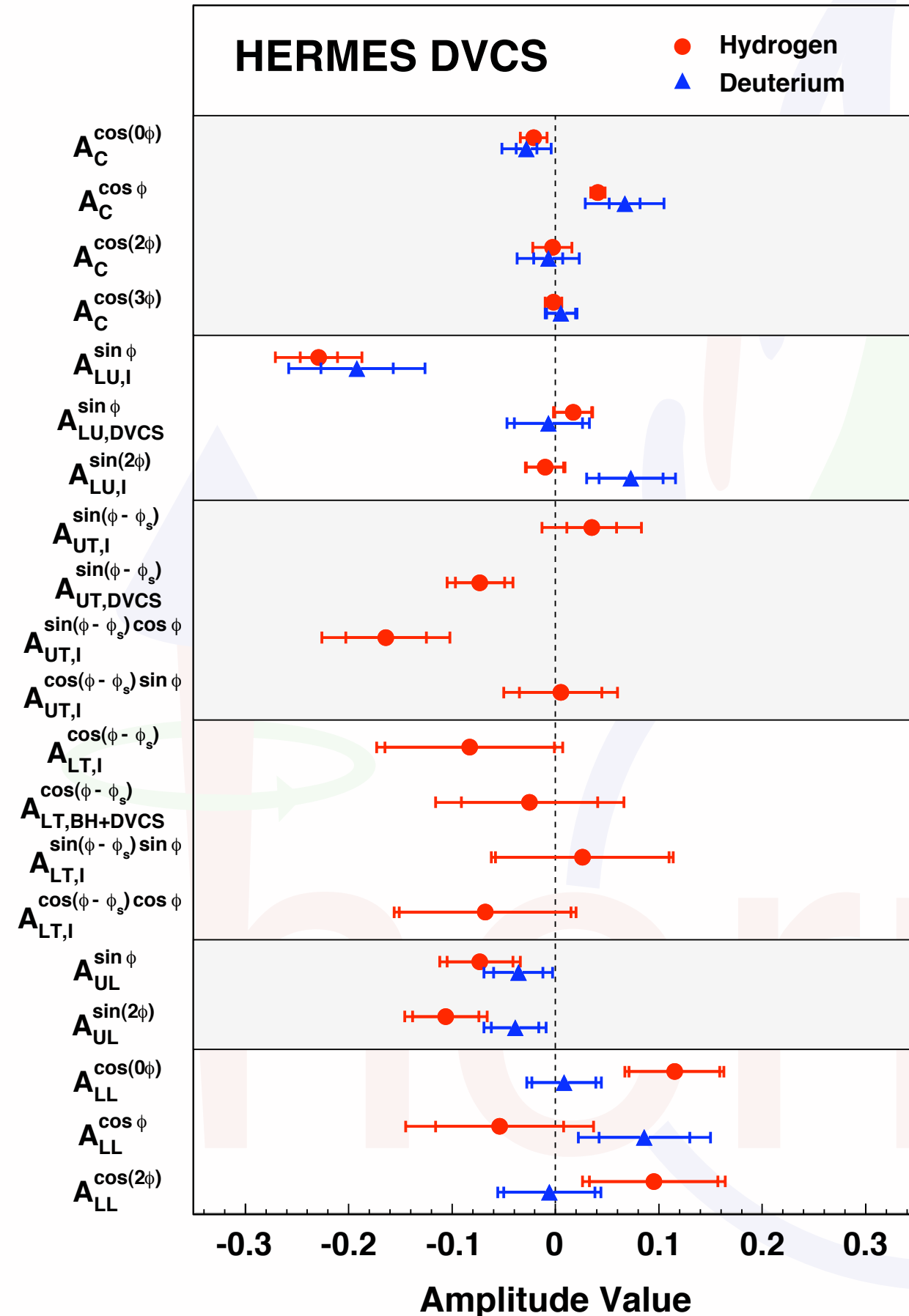
[higher twist]

[gluon leading twist]

Resonant fraction:

$$ep \rightarrow e\Delta^+\gamma$$

# A wealth of azimuthal amplitudes



Beam-charge asymmetry:

**GPD H**

PRD 75 (2007) 011103

NPB 829 (2010) 1

JHEP 11 (2009) 083

Beam-helicity asymmetry:

**GPD H**

PRC 81 (2010) 035202

PRL 87 (2001) 182001

JHEP 07 (2012) 032

Transverse target spin asymmetries:

**GPD E from proton target**

JHEP 06 (2008) 066

PLB 704 (2011) 15

Longitudinal target spin asymmetry:

**GPD  $\tilde{H}$**

JHEP 06 (2010) 019

Double-spin asymmetry:

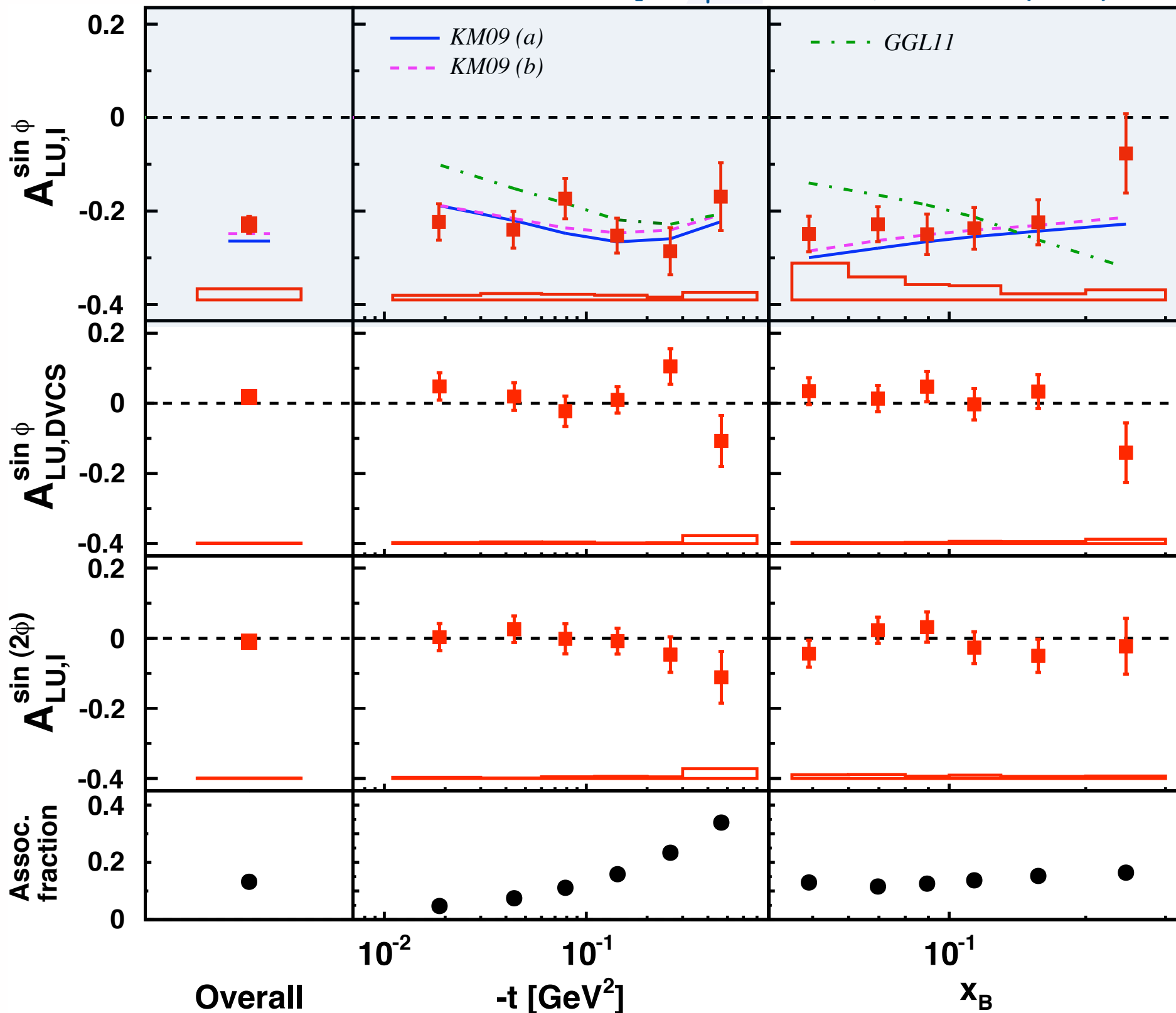
**GPD  $\tilde{H}$**

NPB 842 (2011) 265

complete data set!

# Beam-spin asymmetry

[Airapetian et al., JHEP 07 (2012) 032]



$$\propto \text{Im}[F_1 \mathcal{H}]$$

[higher twist]

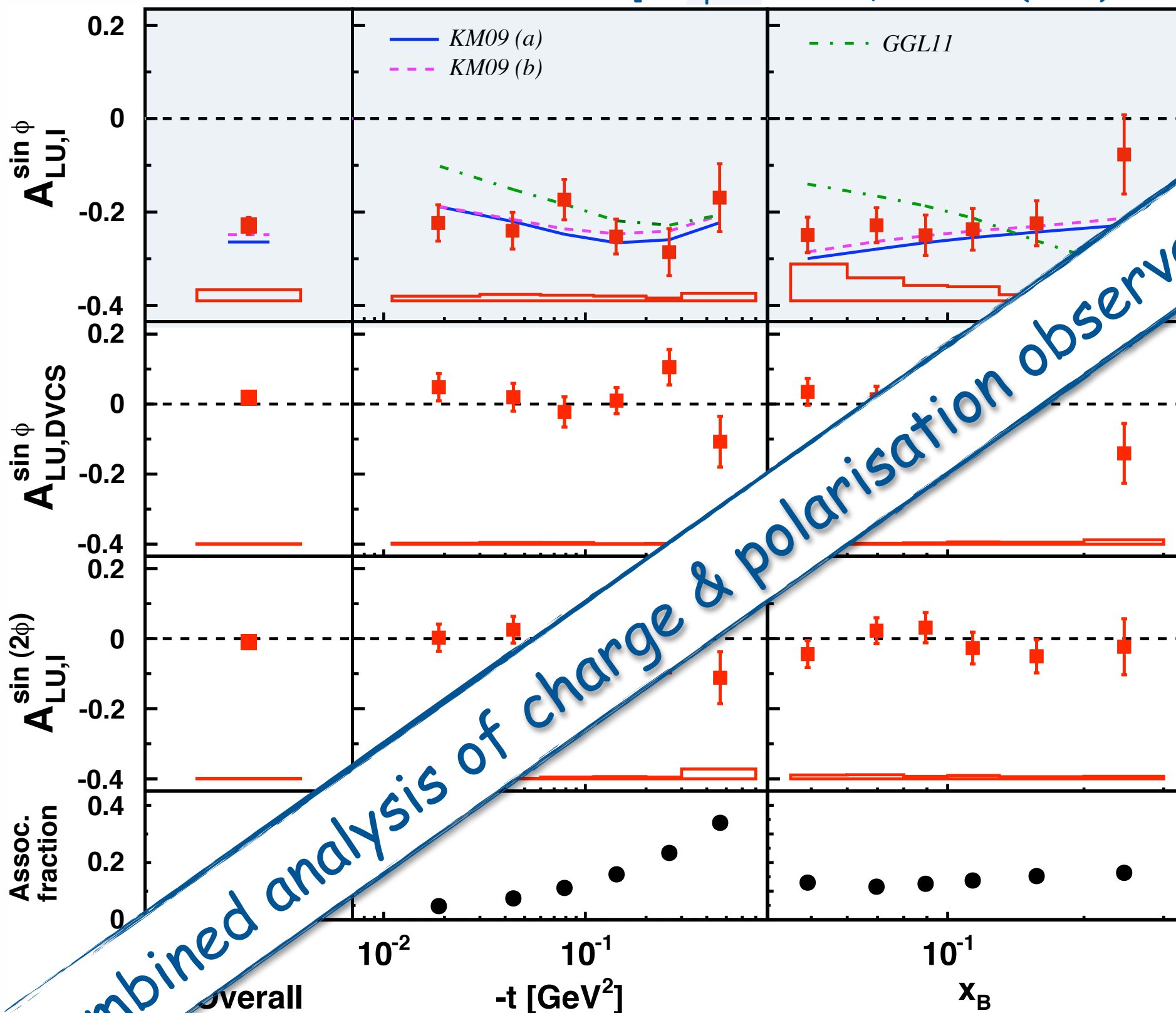
Resonant fraction:

$$ep \rightarrow e\Delta^+\gamma$$

complete data set!

# Beam-spin asymmetry

[Airapetian et al., JHEP 07 (2012) 032]



combined analysis of charge & polarisation observables unique to HERA!

[higher twist]

Resonant fraction:

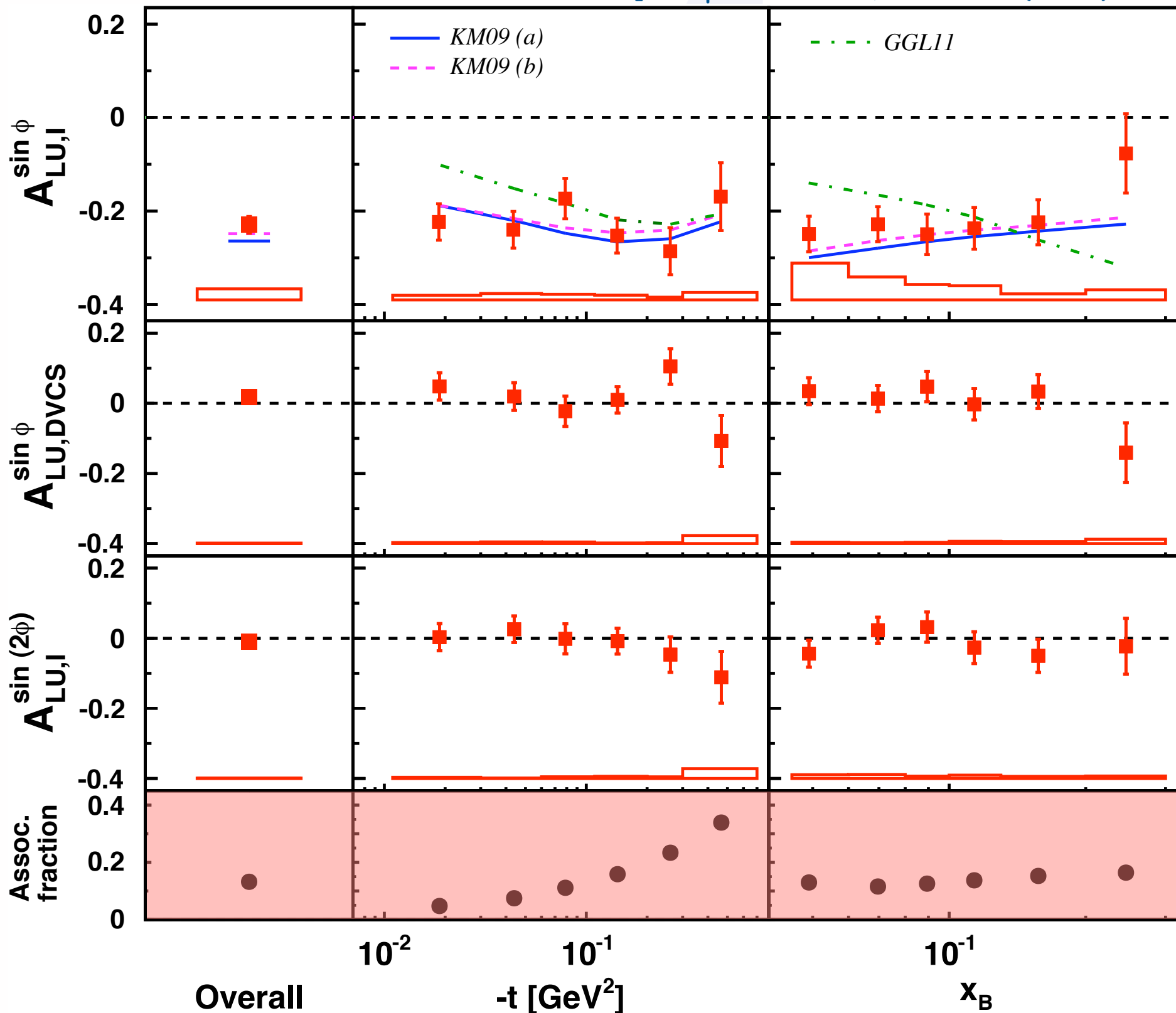
$$ep \rightarrow e\Delta^+\gamma$$



complete data set!

# Beam-spin asymmetry

[Airapetian et al., JHEP 07 (2012) 032]



$\propto \text{Im}[F_1 \mathcal{H}]$

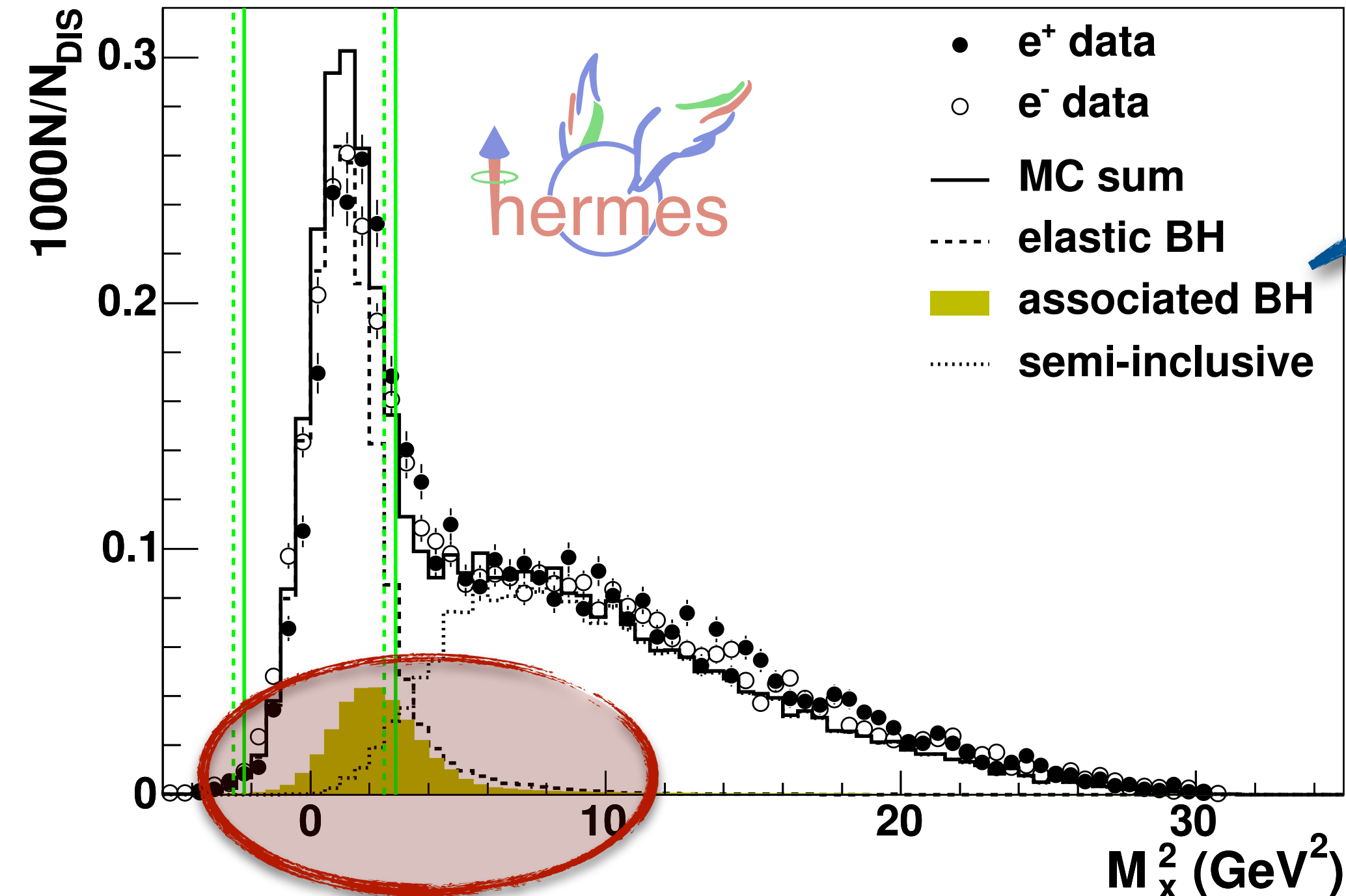
[higher twist]

Resonant fraction:

$$ep \rightarrow e\Delta^+ \gamma$$

# Exclusivity: missing-mass technique

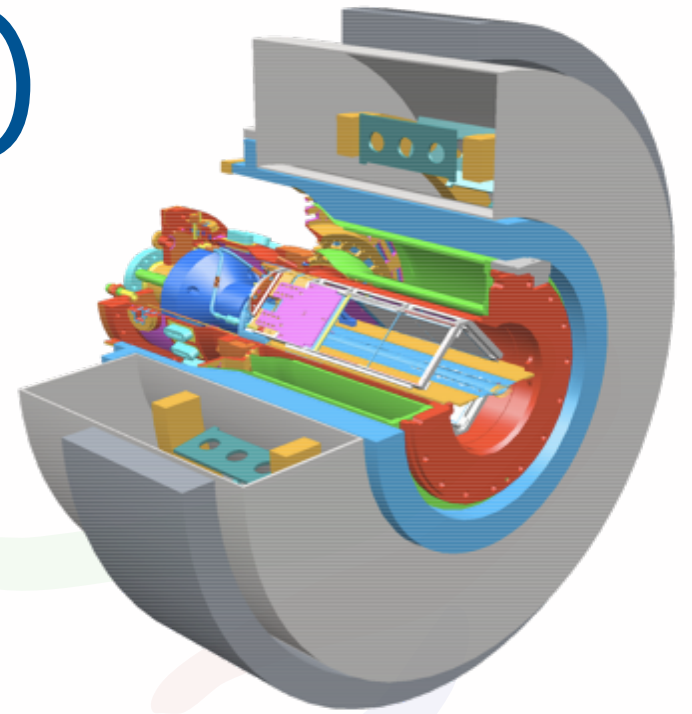
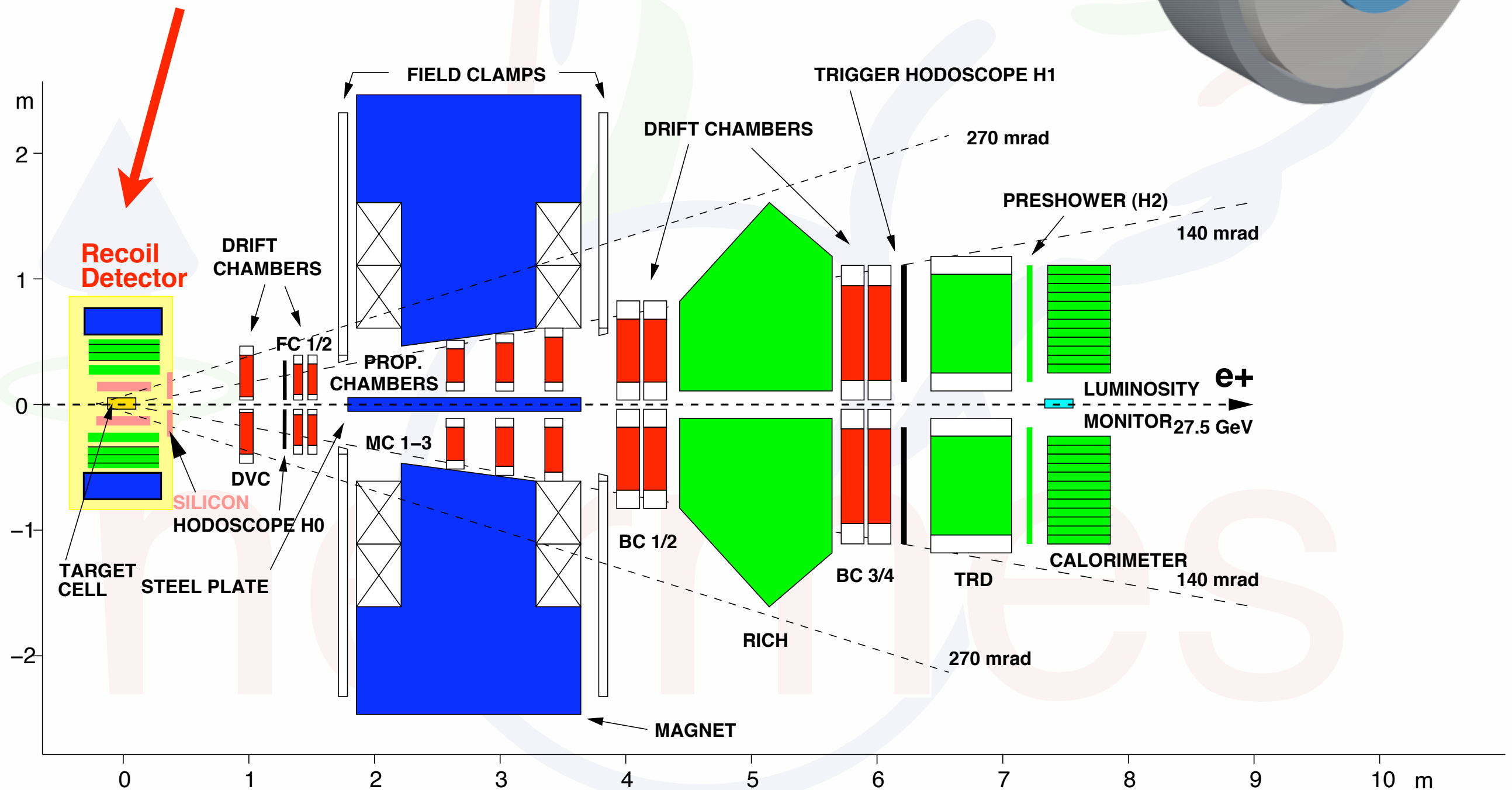
$ep \rightarrow e \gamma X$



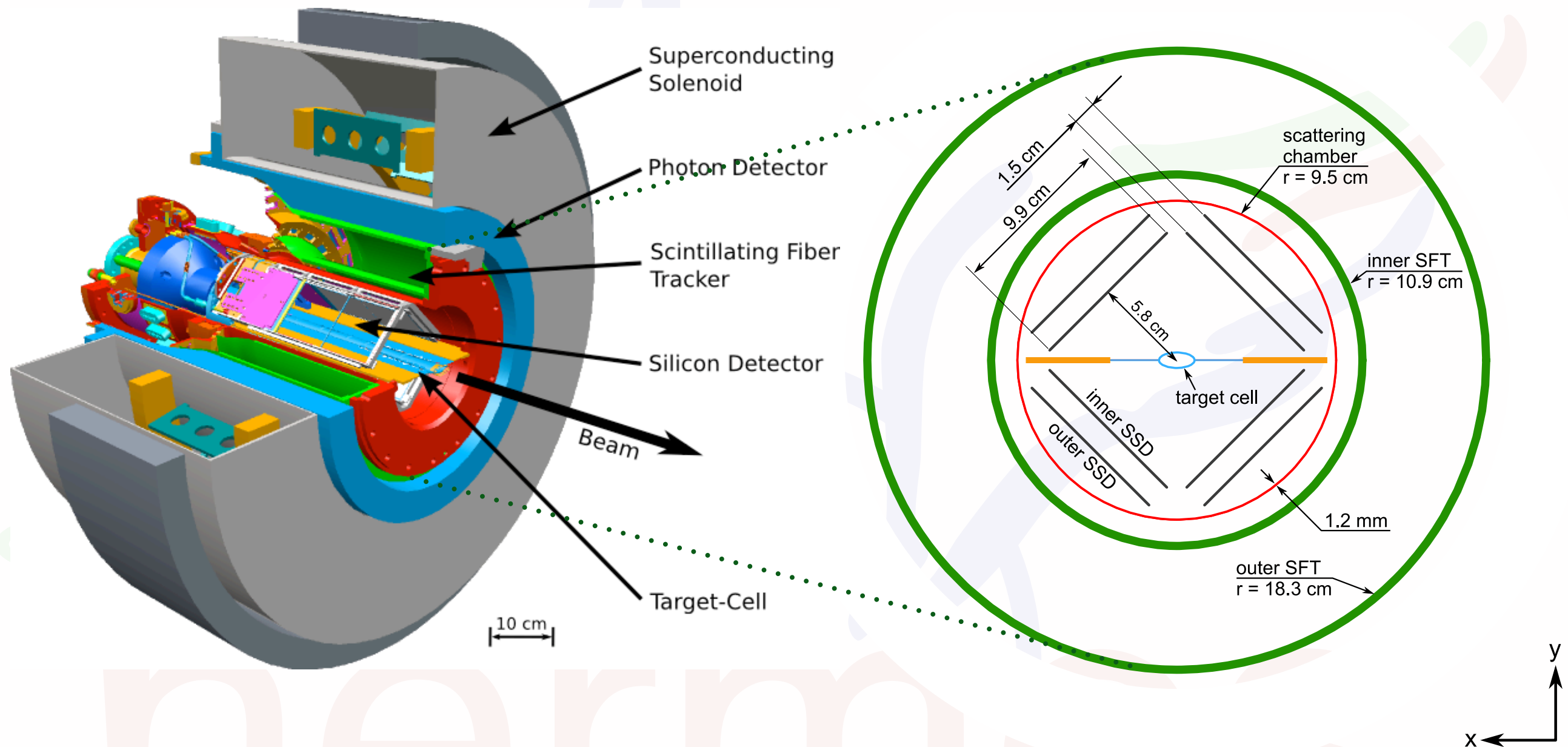
$X = \Delta^+, \dots$

# HERMES detector (2006/07)

detection of  
recoiling proton



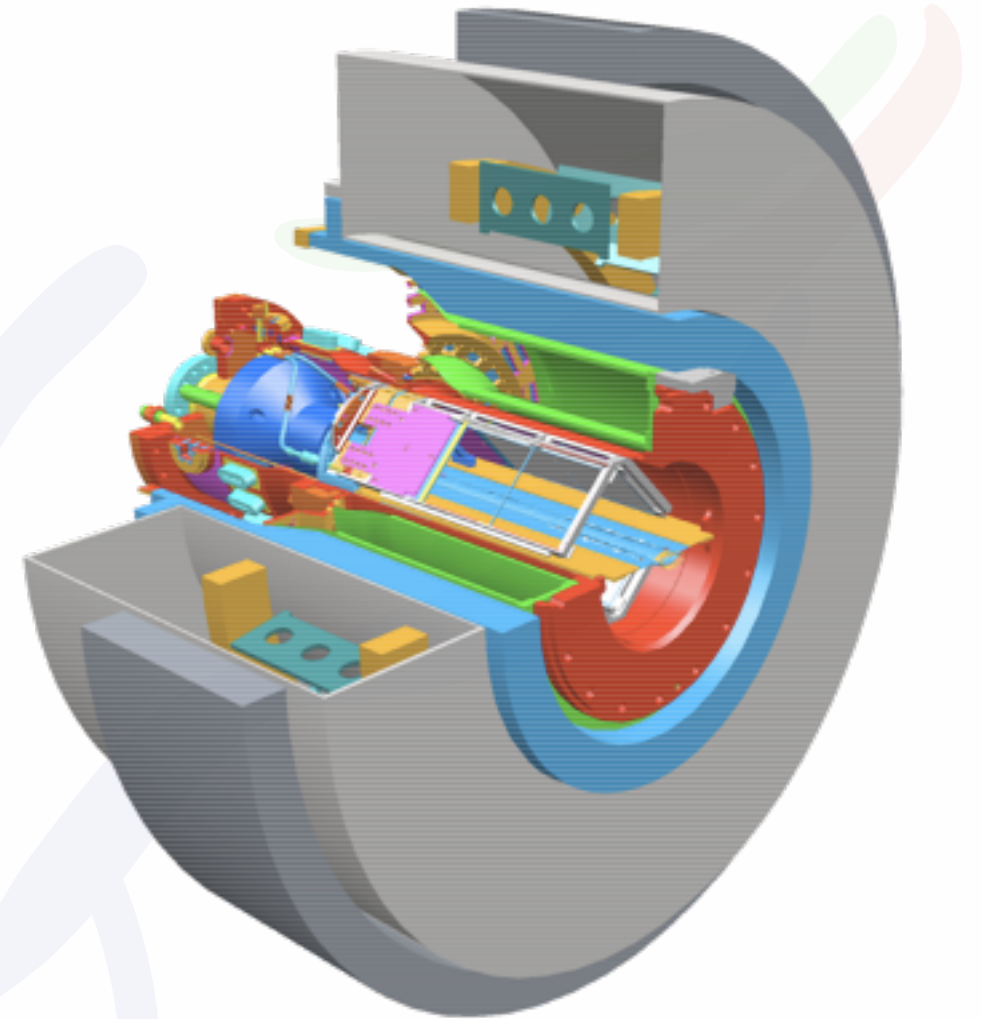
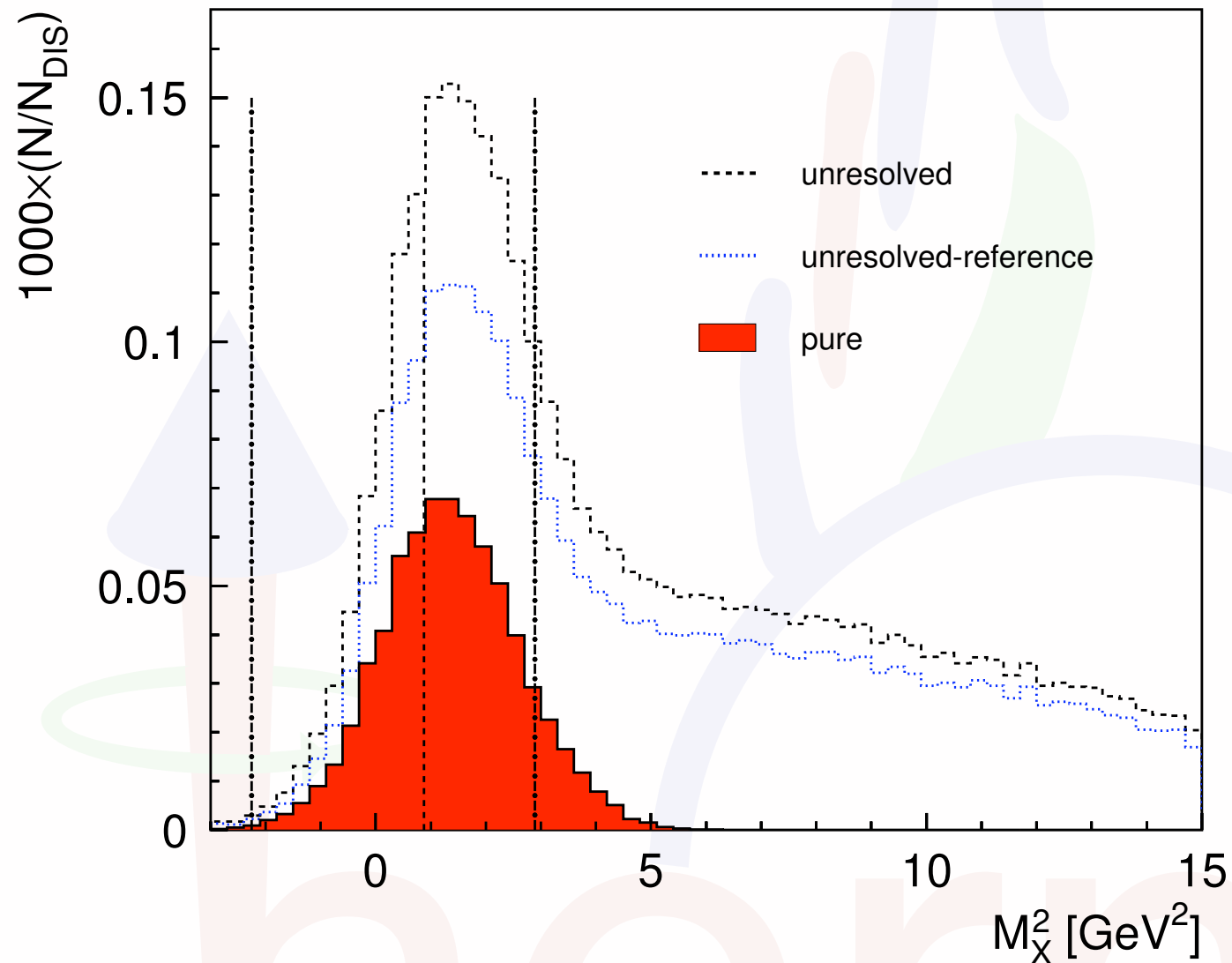
# The HERMES Recoil detector



Enables the measurement of the recoiling charged particle and therefore full  $ep \rightarrow ep \gamma$  event reconstruction

# HERMES detector (2006/07)

## kinematic fitting



- All particles in final state detected  $\rightarrow$  4 constraints from energy-momentum conservation
- Selection of **pure BH/DVCS** ( $ep \rightarrow ep \gamma$ ) with **high efficiency** ( $\sim 83\%$ )
- Allows to suppress background from associated and semi-inclusive processes to a negligible level ( $< 0.2\%$ )



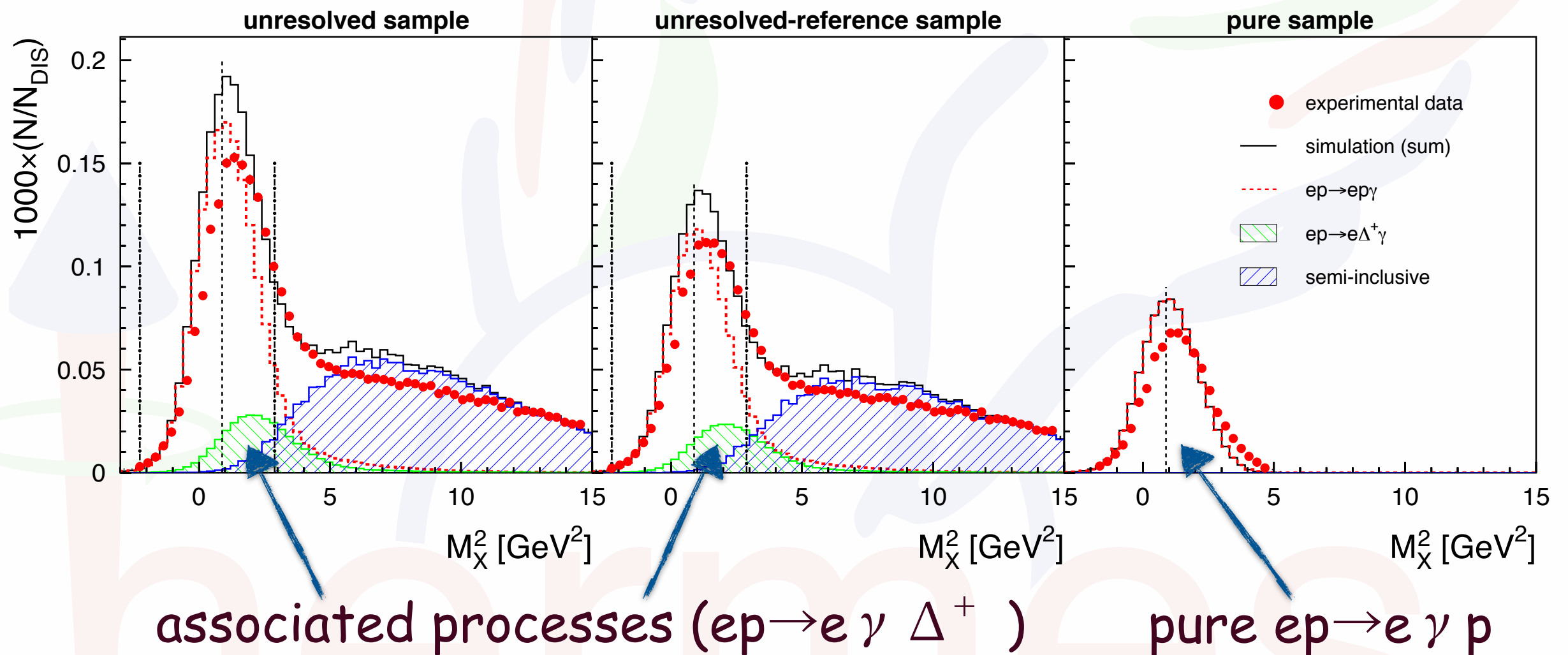
# Exclusivity with recoil detector

forward spectrometer only

similar background

measured  
proton

same kinematic acceptance



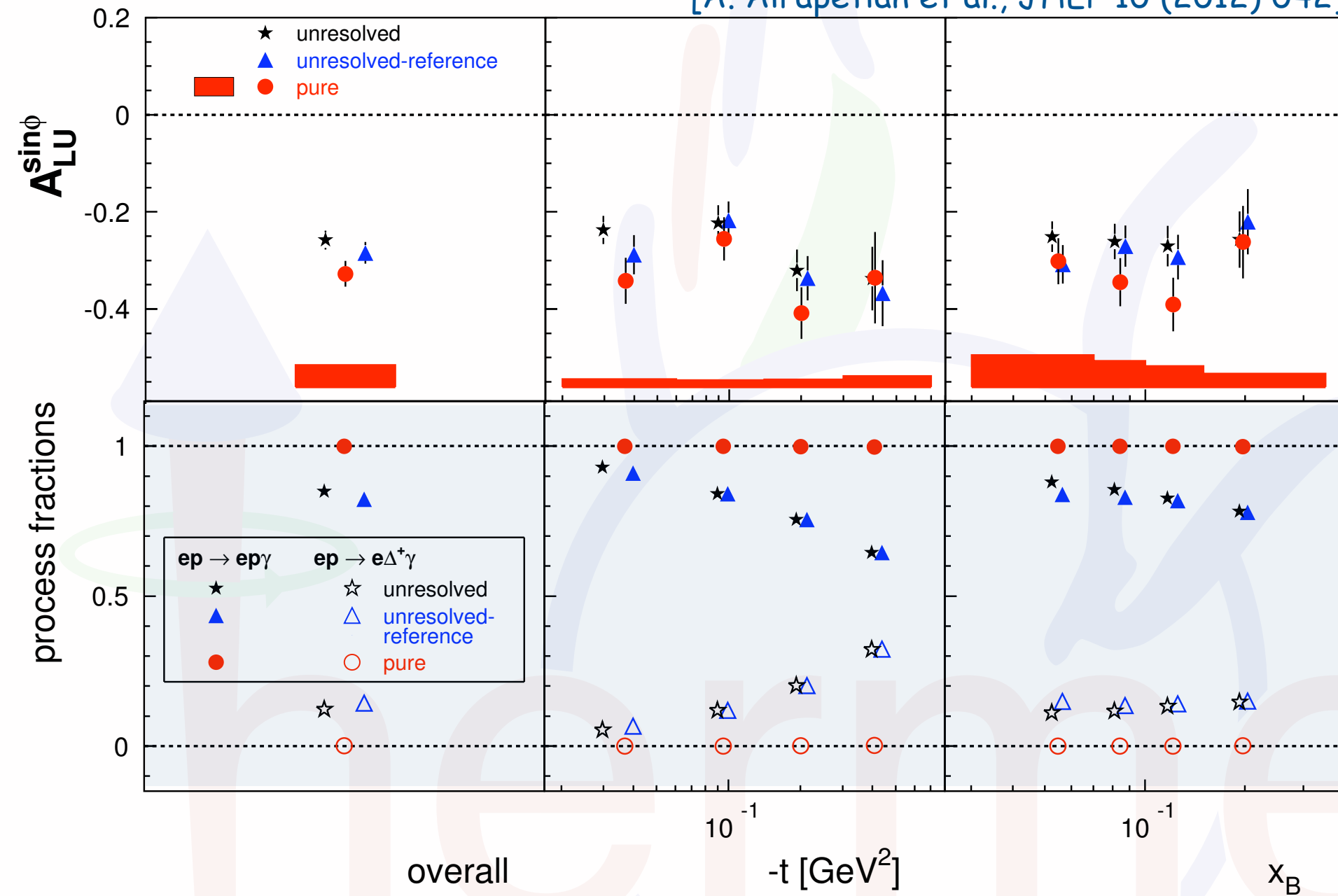
Missing mass:

$$M_x^2 = (k - k' + P_0 - P_\gamma)^2 = M^2 + 2M(\nu - E_\gamma) + t$$



# Single-charge BSA with recoil proton

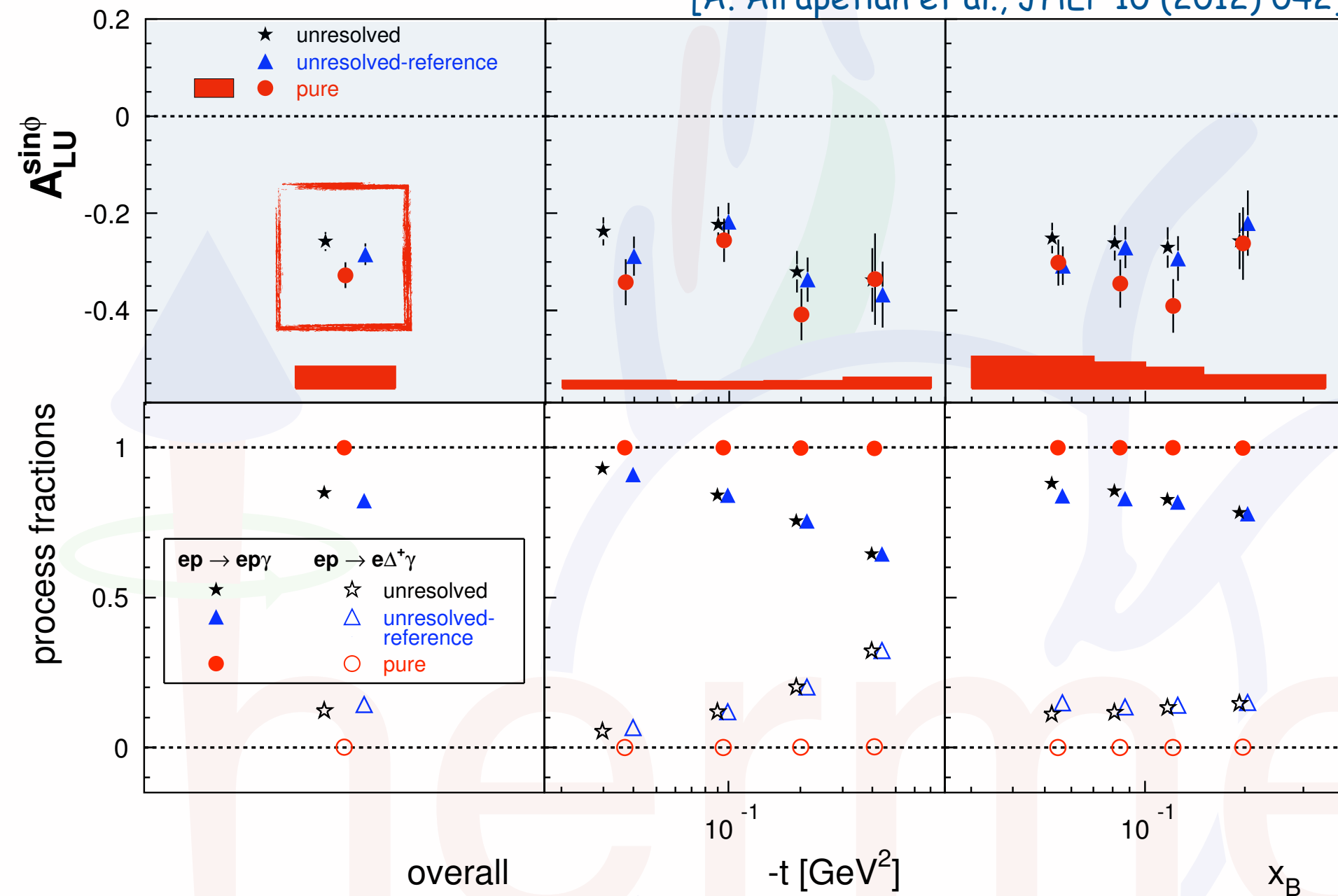
[A. Airapetian et al., JHEP 10 (2012) 042]



basically no  
contamination  
→ clear interpretation

# Single-charge BSA with recoil proton

[A. Airapetian et al., JHEP 10 (2012) 042]

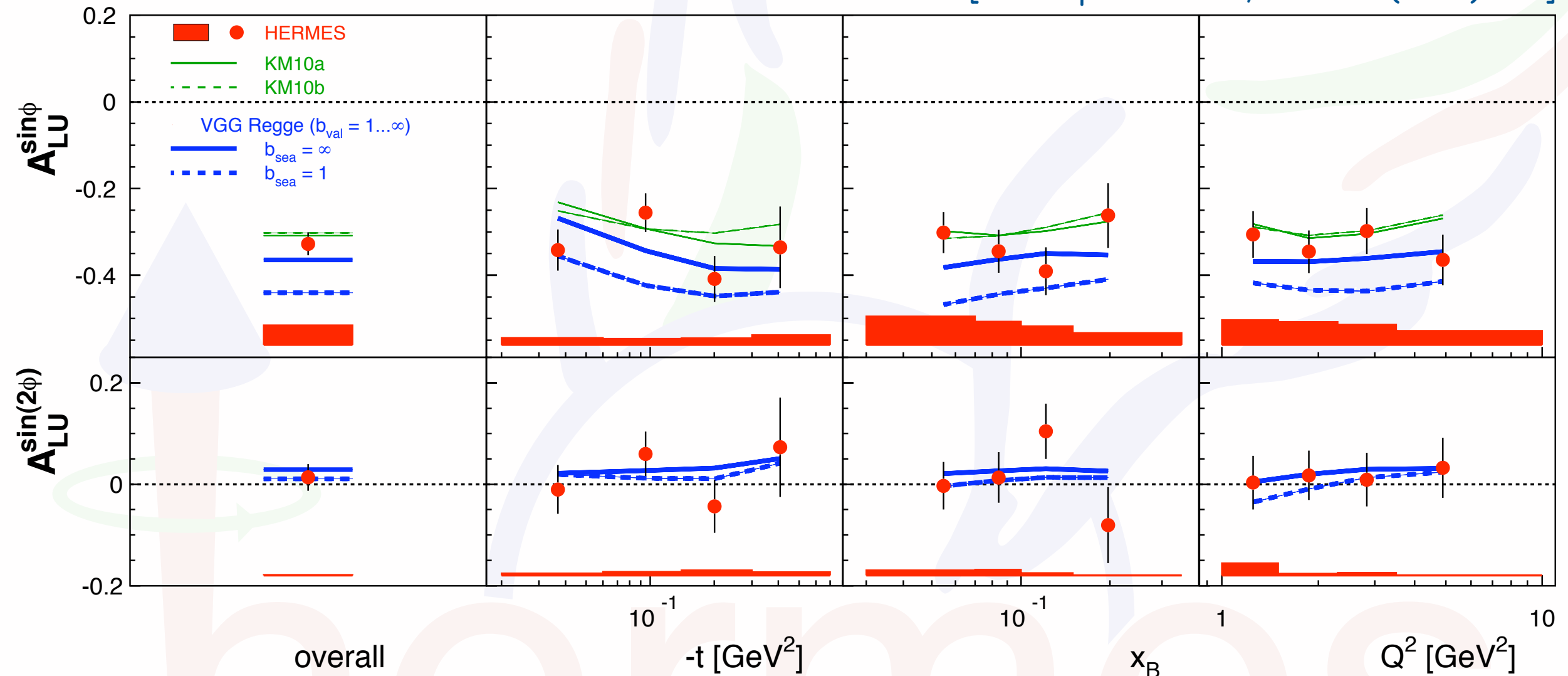


Magnitude of the leading asymmetry has increased by  $0.054 \pm 0.016$   
 (-> assoc. in traditional analysis mainly dilution)

basically no contamination  
 -> clear interpretation

# Single-charge BSA with recoil proton

[A. Airapetian et al., JHEP 10 (2012) 042]



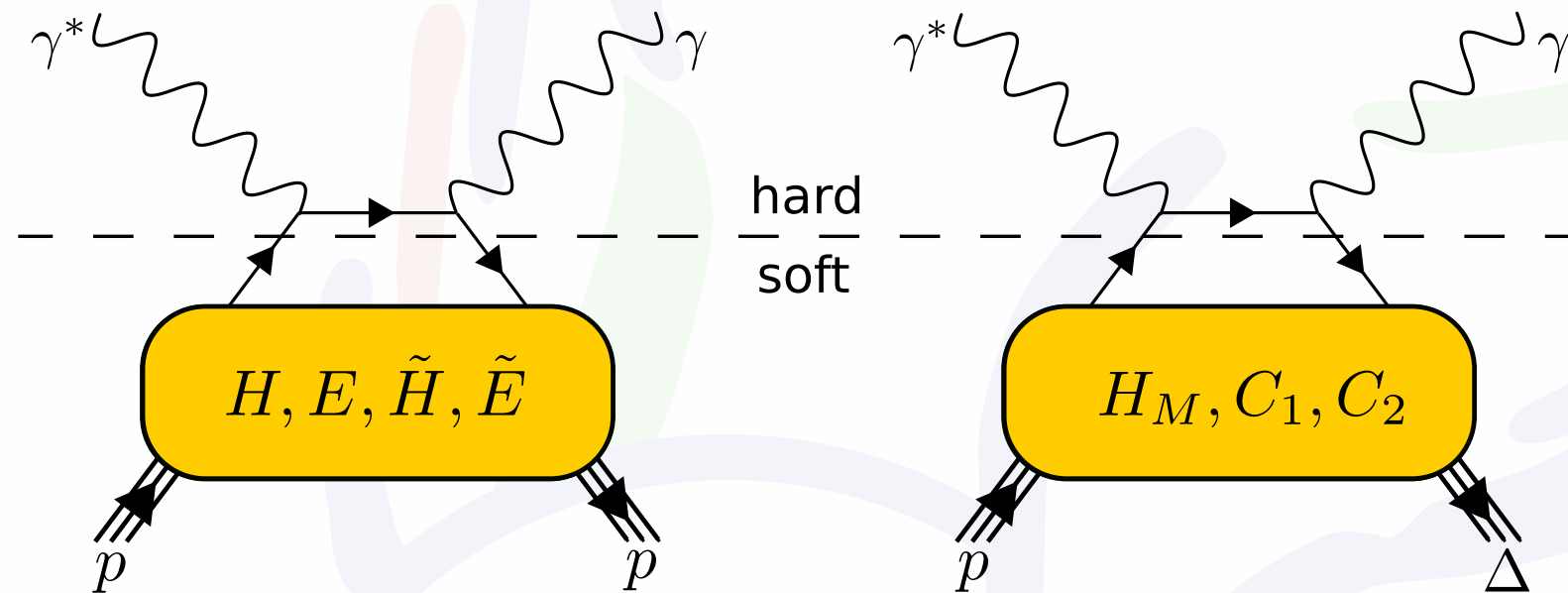
good agreement with models

KM10 - K. Kumericki and D. Müller, Nucl. Phys. B 841 (2010) 1

VGG - M. Vanderhaeghen et al., Phys. Rev. D 60 (1999) 094017

# Beam-spin asymmetries $ep \rightarrow e \gamma N \pi$

Besides a better understanding of the unresolved sample, associated DVCS in principle also allows further access to GPDs.

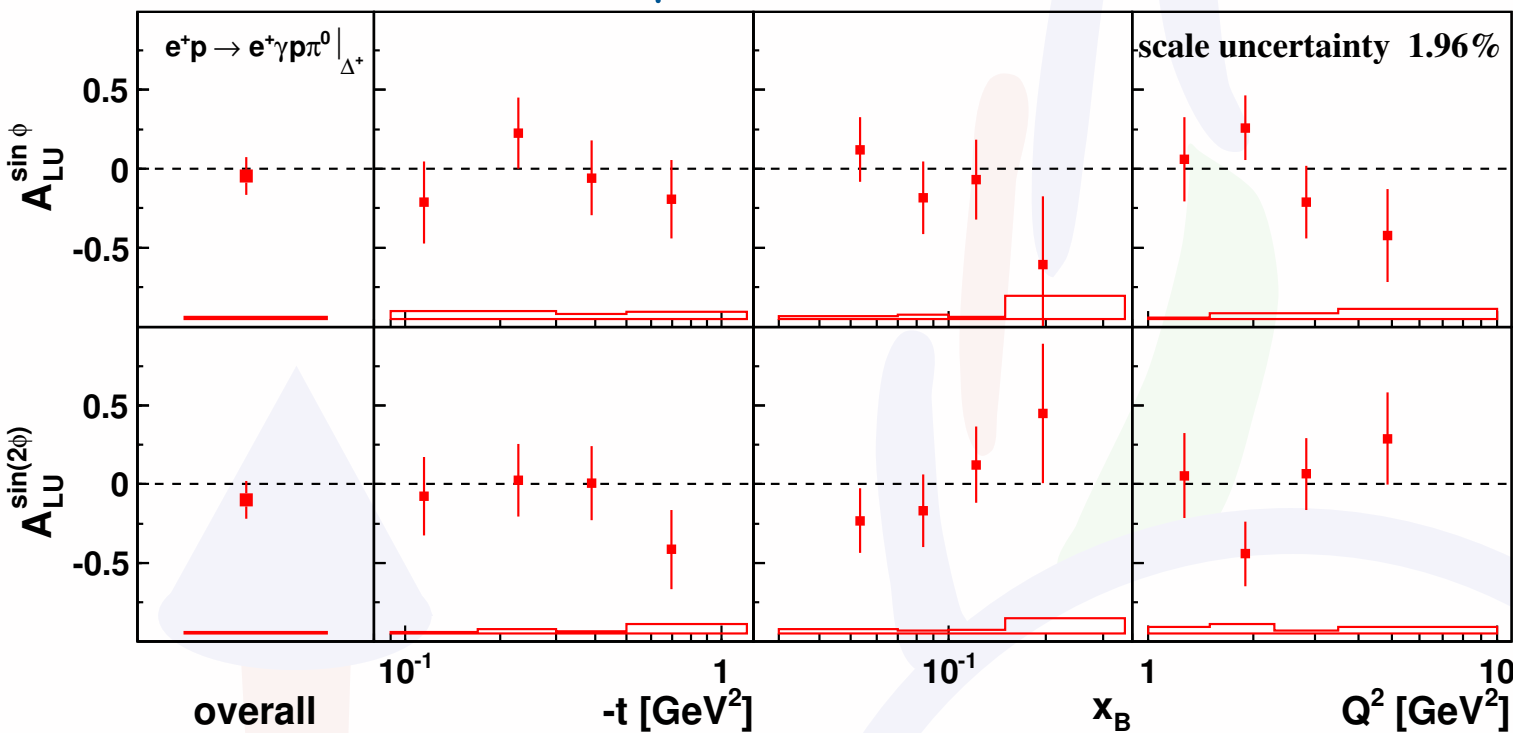


In the large- $N_c$  limit the remaining  $N \rightarrow \Delta$  GPDs can be related to the  $N \rightarrow N$  iso-vector GPDs:

$$\begin{aligned}
 H_M(x, \xi, t) &= \frac{2}{\sqrt{3}} \left[ E^u(x, \xi, t) - E^d(x, \xi, t) \right], \\
 C_1(x, \xi, t) &= \sqrt{3} \left[ \tilde{H}^u(x, \xi, t) - \tilde{H}^d(x, \xi, t) \right], \\
 C_2(x, \xi, t) &= \frac{\sqrt{3}}{4} \left[ \tilde{E}^u(x, \xi, t) - \tilde{E}^d(x, \xi, t) \right]
 \end{aligned}$$

# Beam-spin asymmetries $ep \rightarrow e \gamma p \pi^0$

[A. Airapetian et al., JHEP 01 (2014) 077]

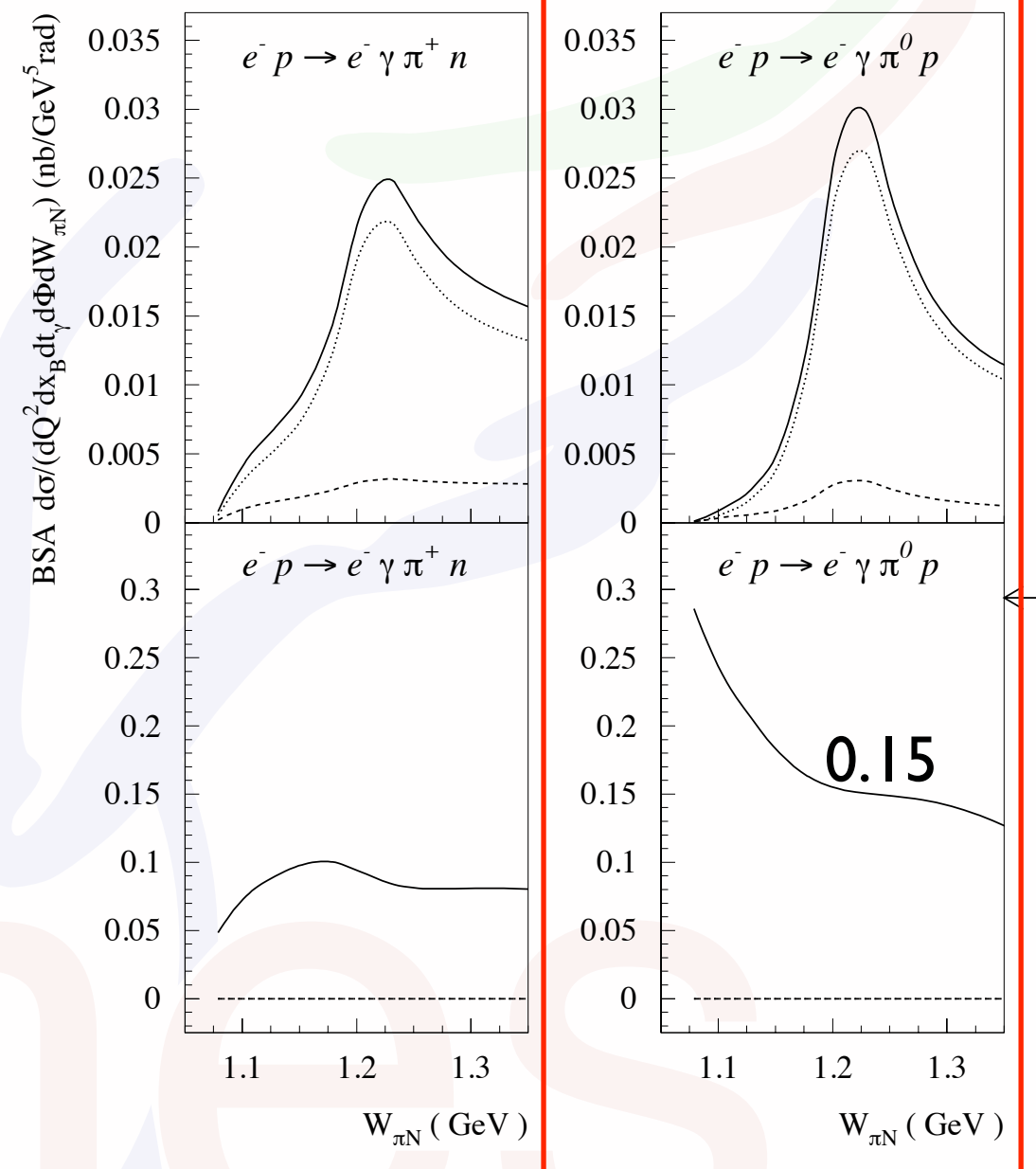


Shown amplitudes corrected for background  
(only overall fractions are listed here):

Associated DVCS/BH ( $ep \rightarrow e \gamma p \pi^0$ )	$85 \pm 1$
Elastic DVCS/BH ( $ep \rightarrow e \gamma p$ )	$4.6 \pm 0.1$
SIDIS ( $ep \rightarrow e X \pi^0$ )	$11 \pm 1$

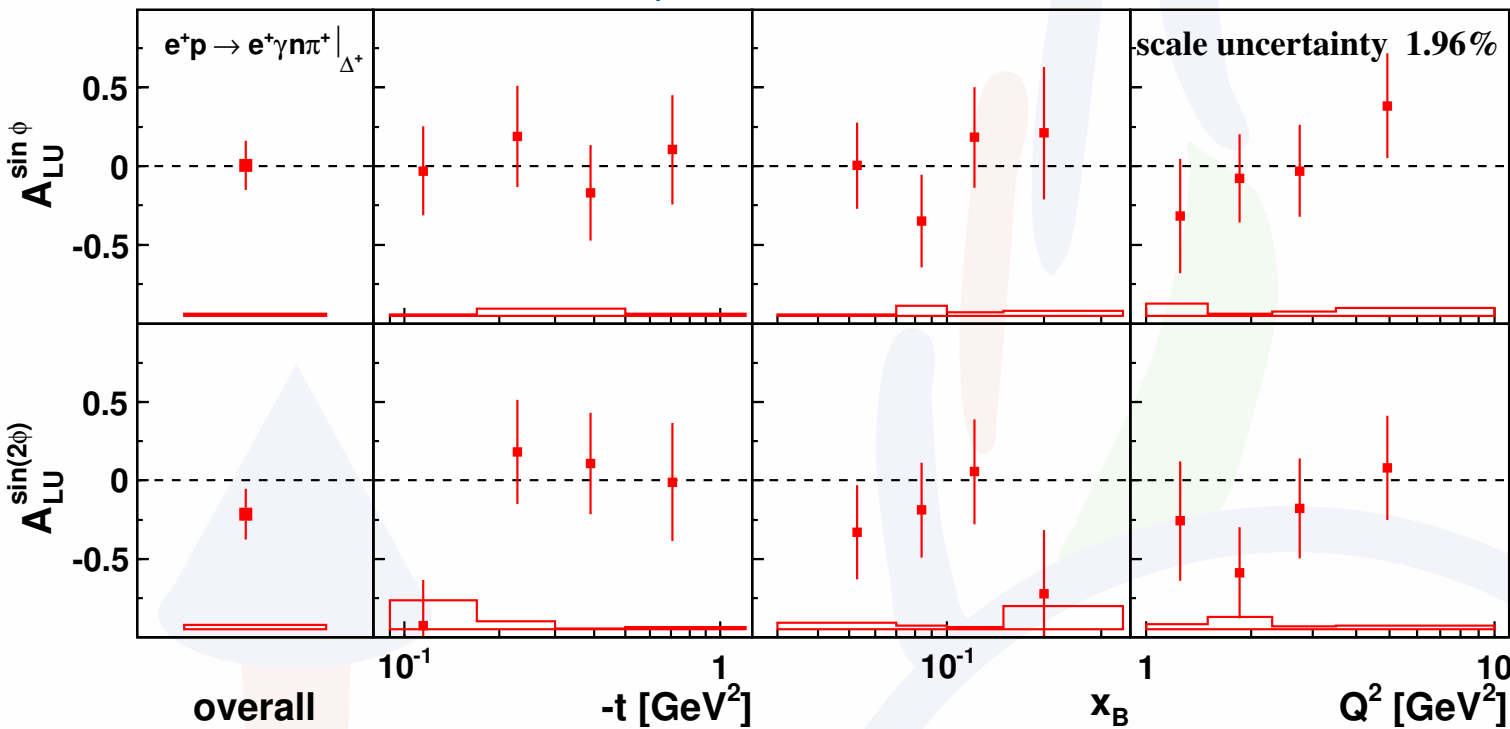
[Guichon et al., PRD 68 (2003) 034018]

$E_e = 27 \text{ GeV}$ ,  $Q^2 = 2.5 \text{ GeV}^2$ ,  $x_B = 0.15$ ,  $t_\gamma = -0.25 \text{ GeV}^2$ ,  $\Phi = 90^\circ$



# Beam-spin asymmetries $ep \rightarrow e \gamma n \pi^+$

[A. Airapetian et al., JHEP 01 (2014) 077]

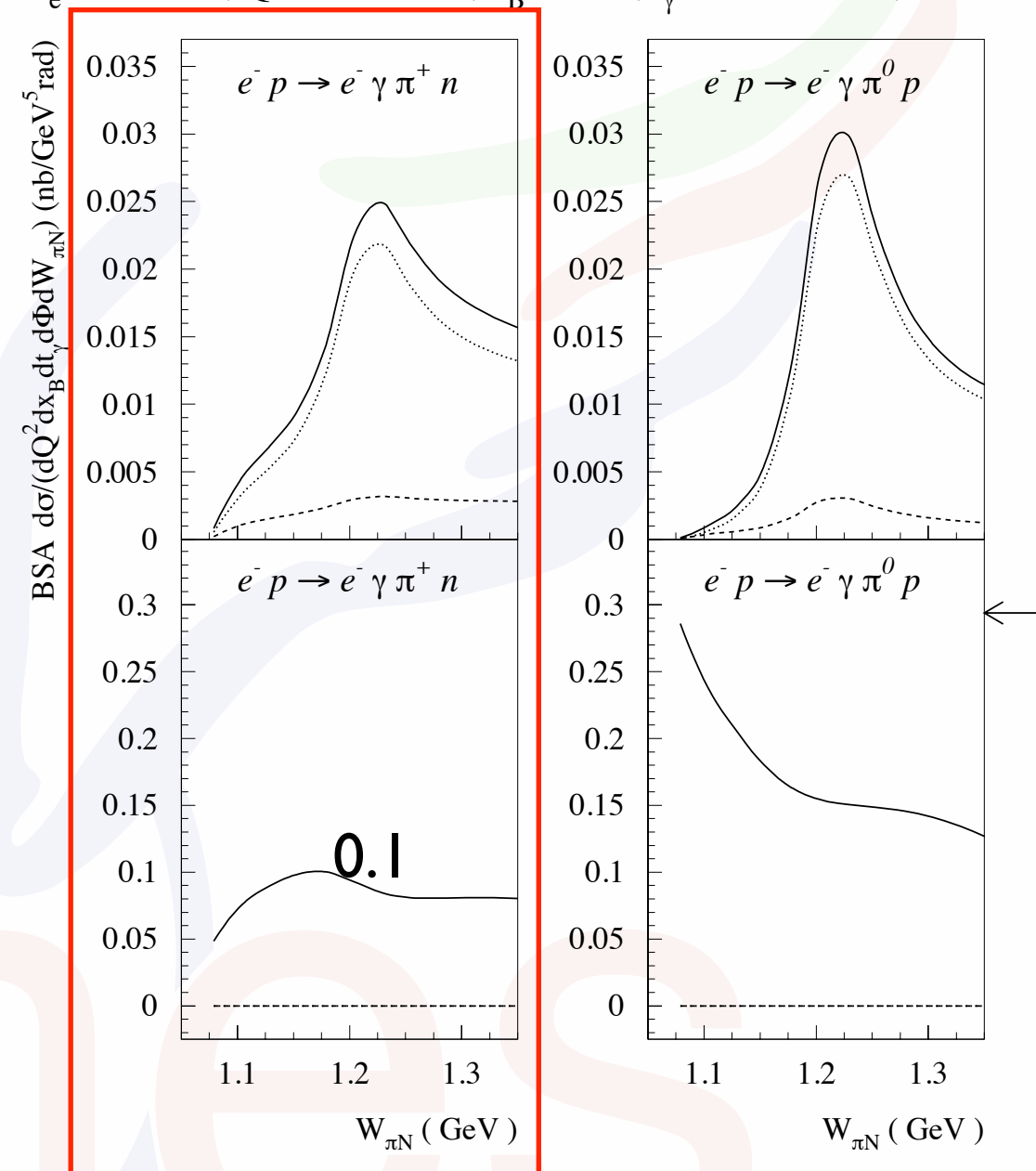


Shown amplitudes corrected for background  
(only overall fractions are listed here):

Associated DVCS/BH ( $ep \rightarrow e \gamma n \pi^+$ )	$77 \pm 2$
Elastic DVCS/BH ( $ep \rightarrow e \gamma p$ )	$0.2 \pm 0.1$
SIDIS ( $ep \rightarrow e X \pi^0$ )	$23 \pm 3$

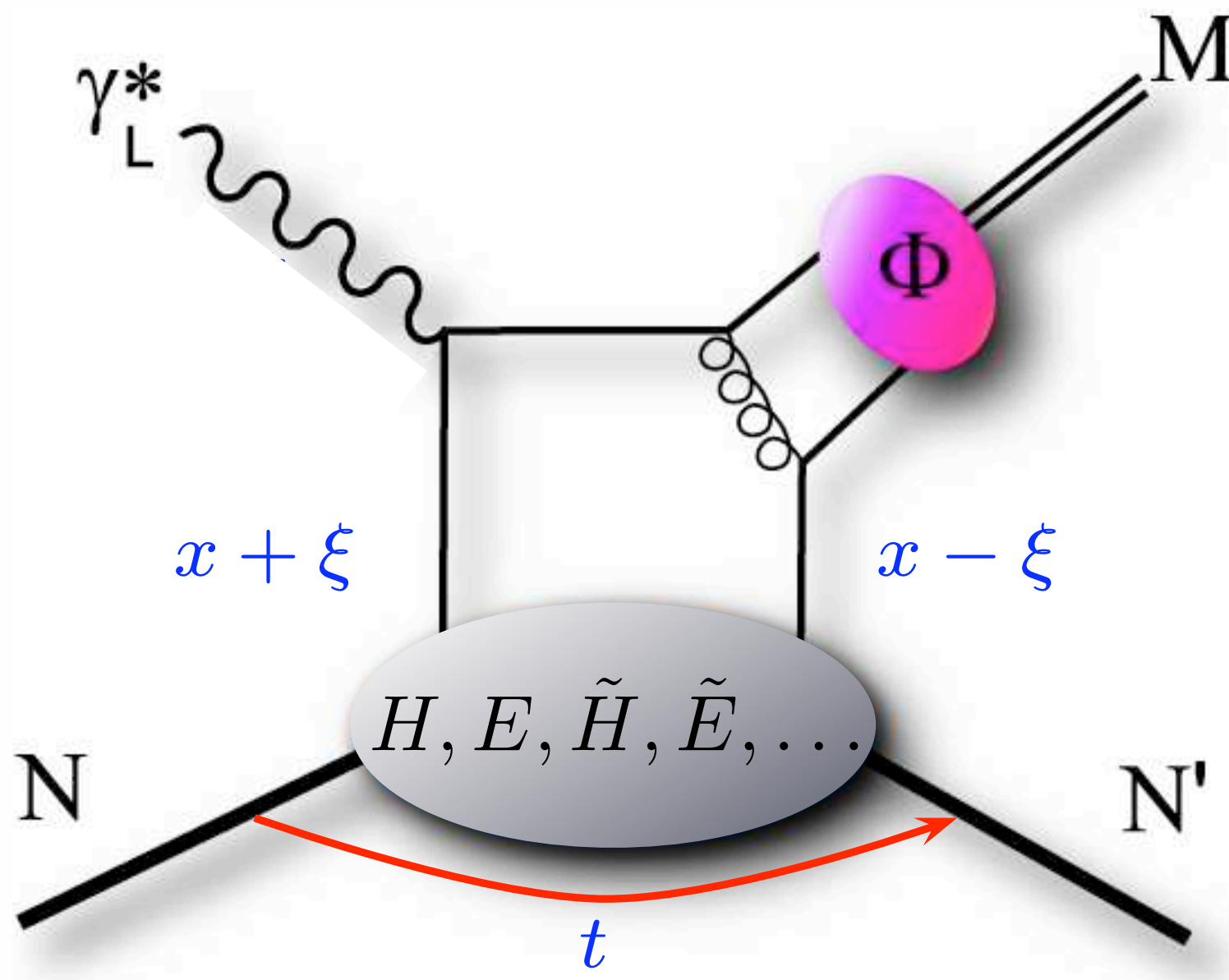
[Guichon et al., PRD 68 (2003) 034018]

$E_e = 27 \text{ GeV}$ ,  $Q^2 = 2.5 \text{ GeV}^2$ ,  $x_B = 0.15$ ,  $t_\gamma = -0.25 \text{ GeV}^2$ ,  $\Phi = 90^\circ$

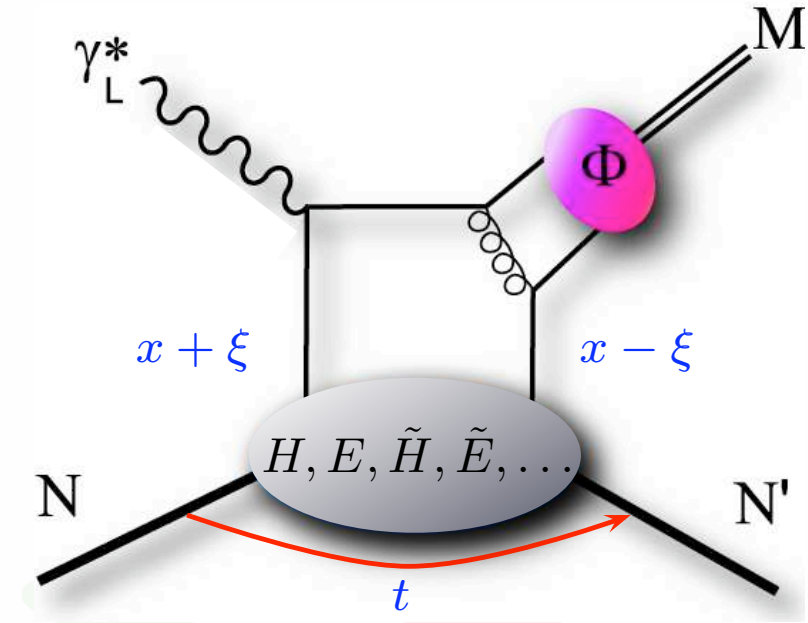




# Exclusive meson production



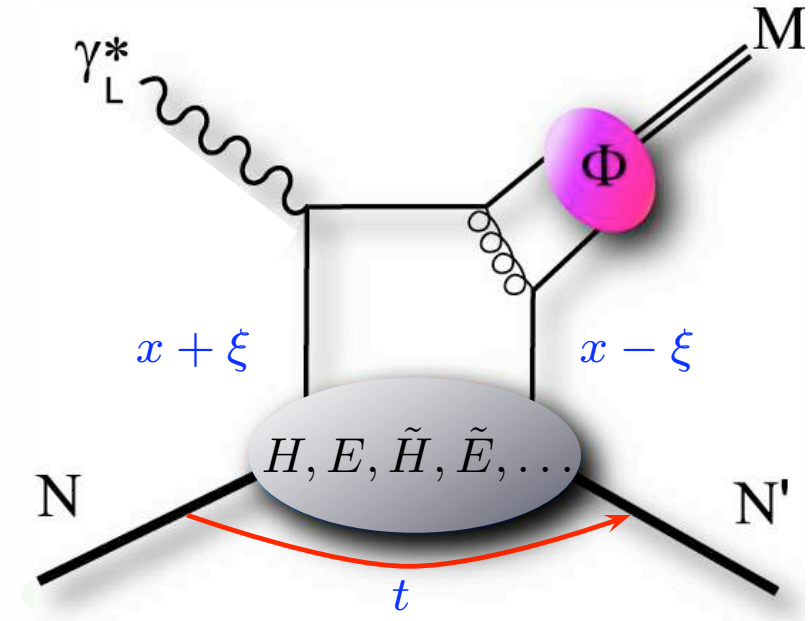
# Exclusive meson production



hermes

# Exclusive meson production

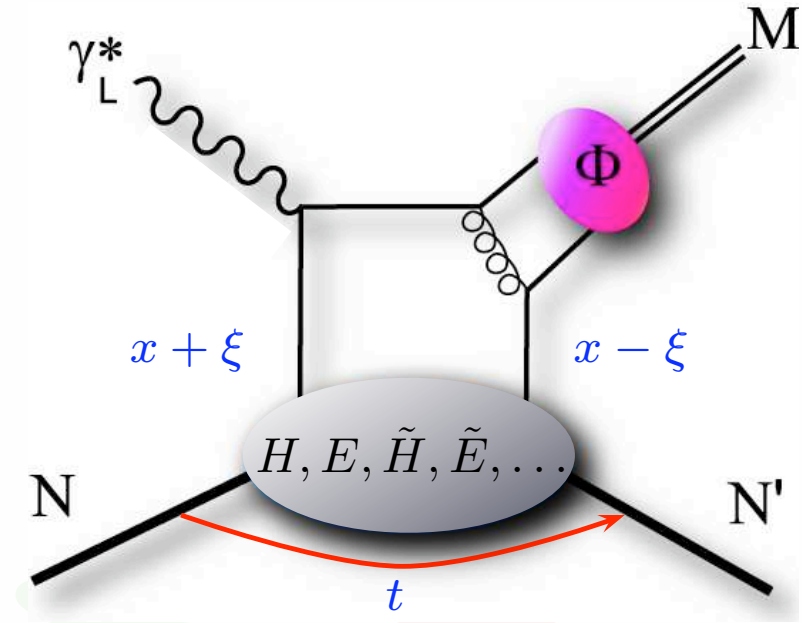
- GPDs convoluted with meson amplitude



hermes

# Exclusive meson production

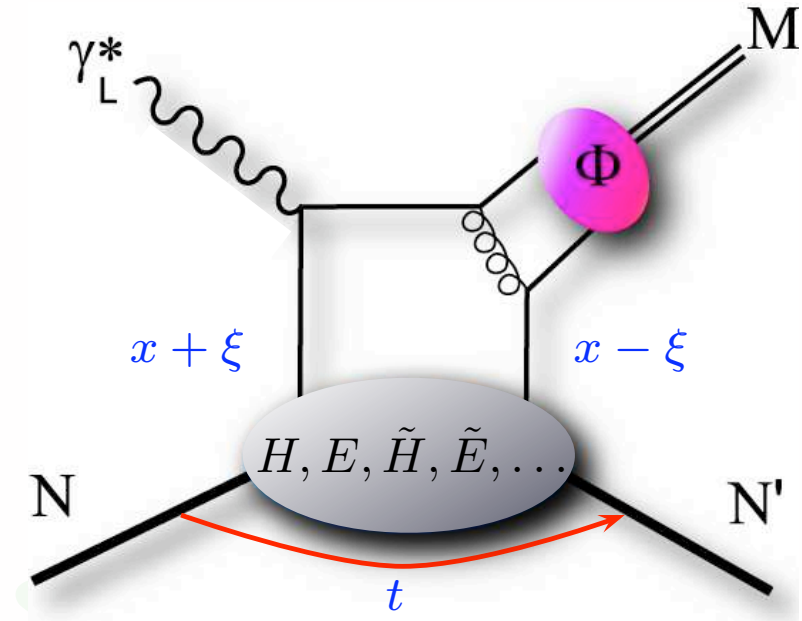
- GPDs convoluted with meson amplitude
- access to various quark-flavor combinations



$\pi^0$	$2\Delta u + \Delta d$
$\eta$	$2\Delta u - \Delta d$
$\rho^0$	$2u + d, 9g/4$
$\omega$	$2u - d, 3g/4$
$\phi$	$s, g$
$\rho^+$	$u - d$
$J/\psi$	$g$

# Exclusive meson production

- GPDs convoluted with meson amplitude
- access to various quark-flavor combinations
- factorization proven for longitudinal photons

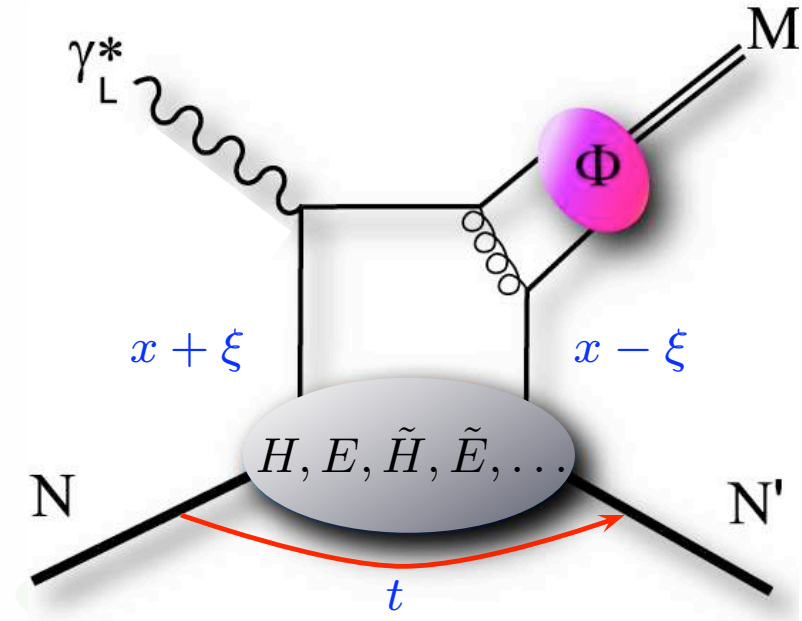


$\pi^0$	$2\Delta u + \Delta d$
$\eta$	$2\Delta u - \Delta d$
$\rho^0$	$2u + d, 9g/4$
$\omega$	$2u - d, 3g/4$
$\phi$	$s, g$
$\rho^+$	$u - d$
$J/\psi$	$g$

hermes

# Exclusive meson production

- GPDs convoluted with meson amplitude
- access to various quark-flavor combinations
- factorization proven for longitudinal photons
- generalized to transverse photons in GK model

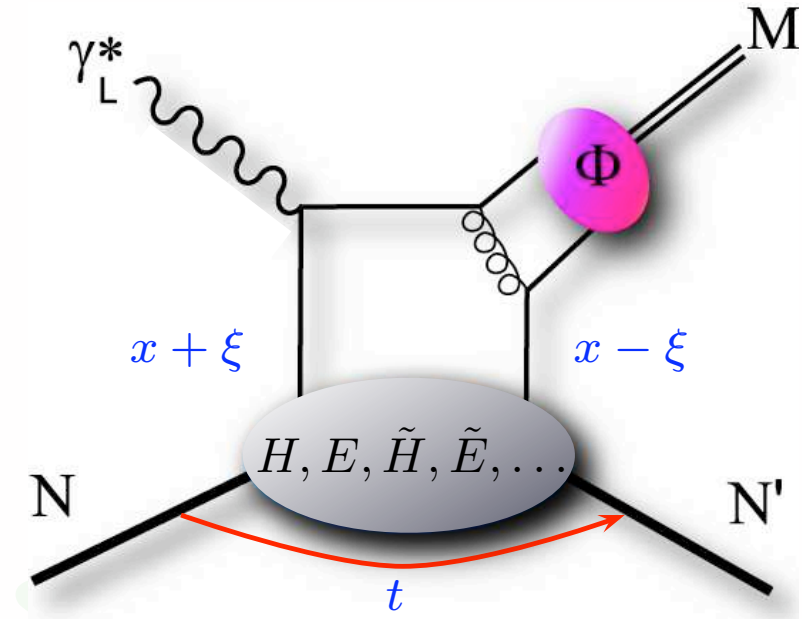


$\pi^0$	$2\Delta u + \Delta d$
$\eta$	$2\Delta u - \Delta d$
$\rho^0$	$2u + d, 9g/4$
$\omega$	$2u - d, 3g/4$
$\phi$	$s, g$
$\rho^+$	$u - d$
$J/\psi$	$g$



# Exclusive meson production

- GPDs convoluted with meson amplitude
- access to various quark-flavor combinations
- factorization proven for longitudinal photons
- generalized to transverse photons in GK model
- vector-meson cross section:



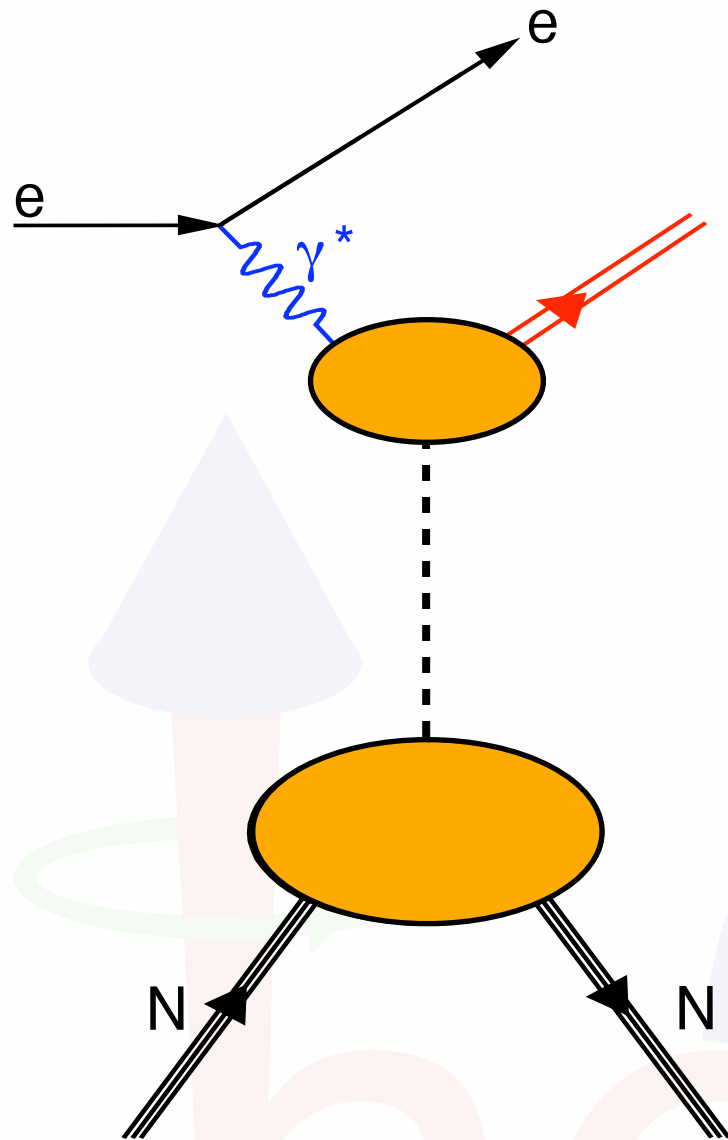
$\pi^0$	$2\Delta u + \Delta d$
$\eta$	$2\Delta u - \Delta d$
$\rho^0$	$2u + d, 9g/4$
$\omega$	$2u - d, 3g/4$
$\phi$	$s, g$
$\rho^+$	$u - d$
$J/\psi$	$g$

$$\frac{d\sigma}{dx_B dQ^2 dt d\phi_S d\phi d\cos\theta d\varphi} = \frac{d\sigma}{dx_B dQ^2 dt} W(x_B, Q^2, t, \phi_S, \phi, \cos\theta, \varphi)$$

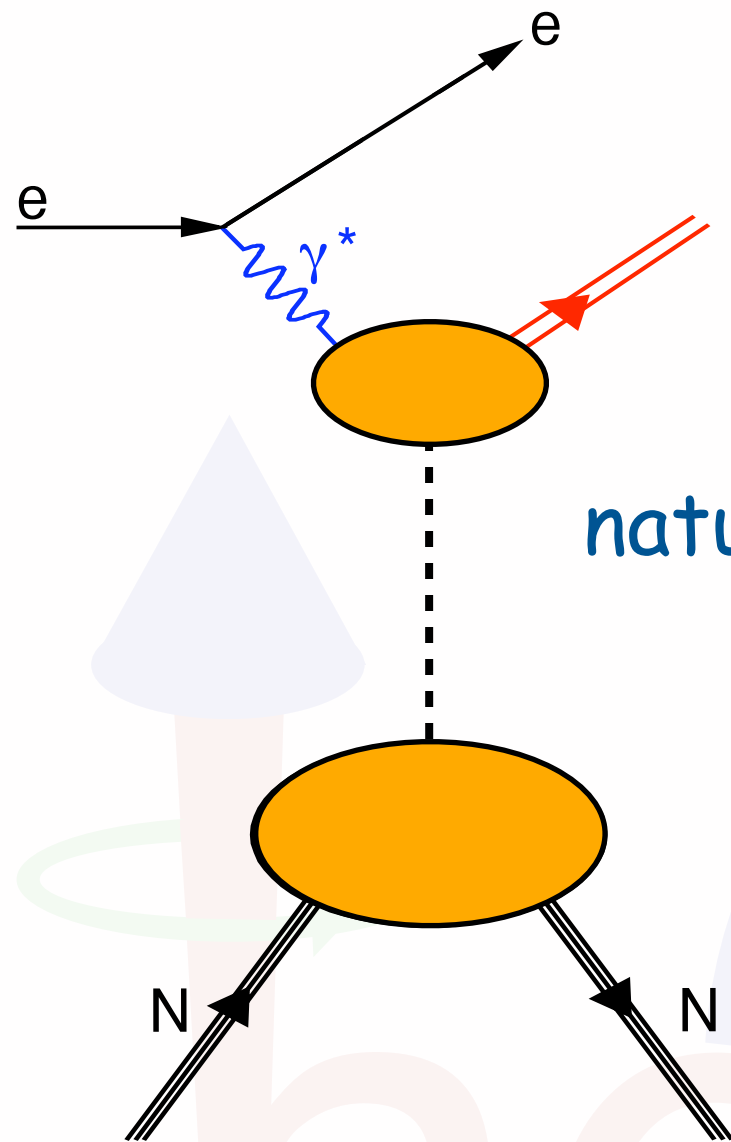
$$W = W_{UU} + P_B W_{LU} + S_L W_{UL} + P_B S_L W_{LL} + S_T W_{UT} + P_B S_T W_{LT}$$

look at various angular (decay) distributions to study helicity transitions ("spin-density matrix elements")

# "Regge phenomenology"

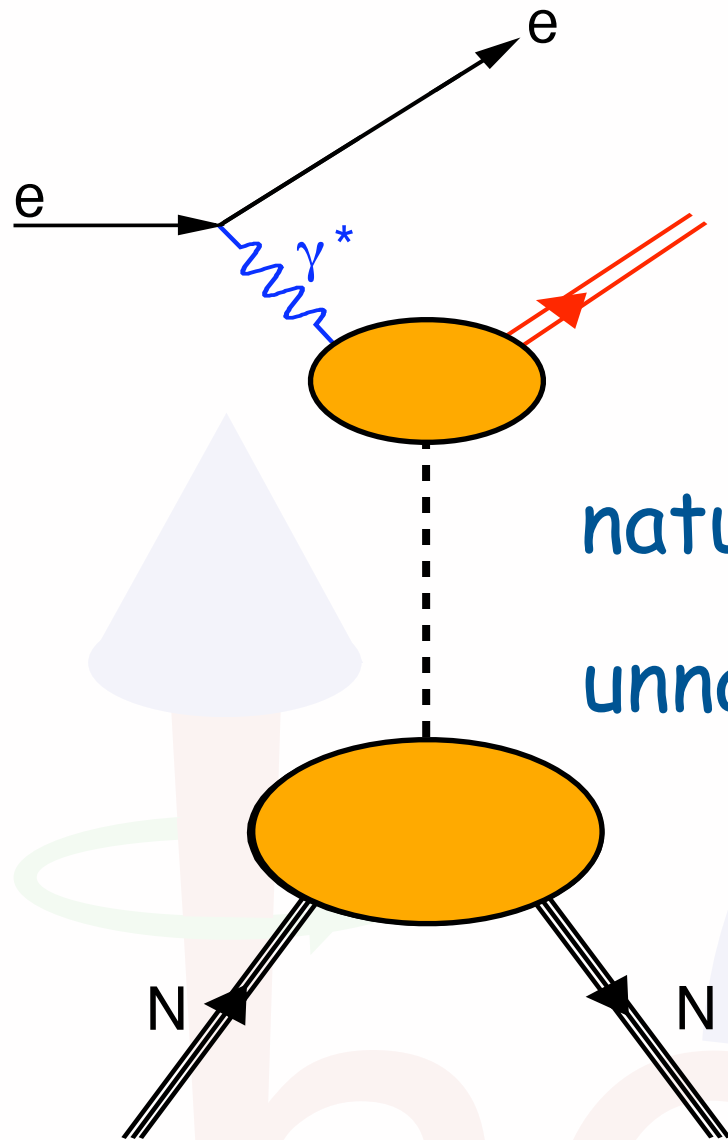


# "Regge phenomenology"



natural-parity exchange  $J^P = 0^+, 1^-, \dots$  GPDs H&E

# "Regge phenomenology"

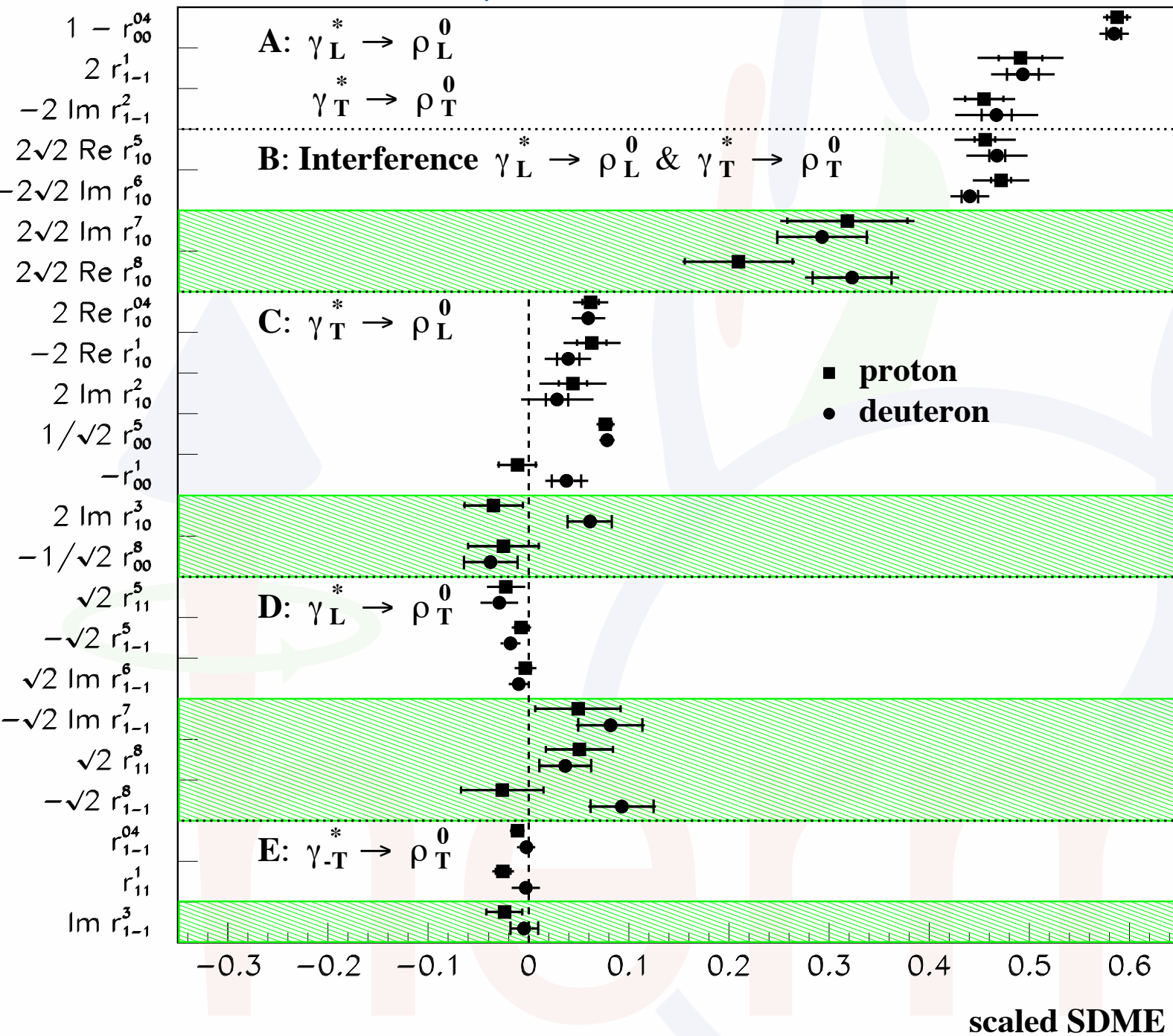


natural-parity exchange  $J^P = 0^+, 1^-, \dots$  GPDs H&E

unnatural-parity exchange  $J^P = 0^-, 1^+, \dots$  GPDs  $\tilde{H}$ & $\tilde{E}$

# $\rho^0$ SDMEs from HERMES

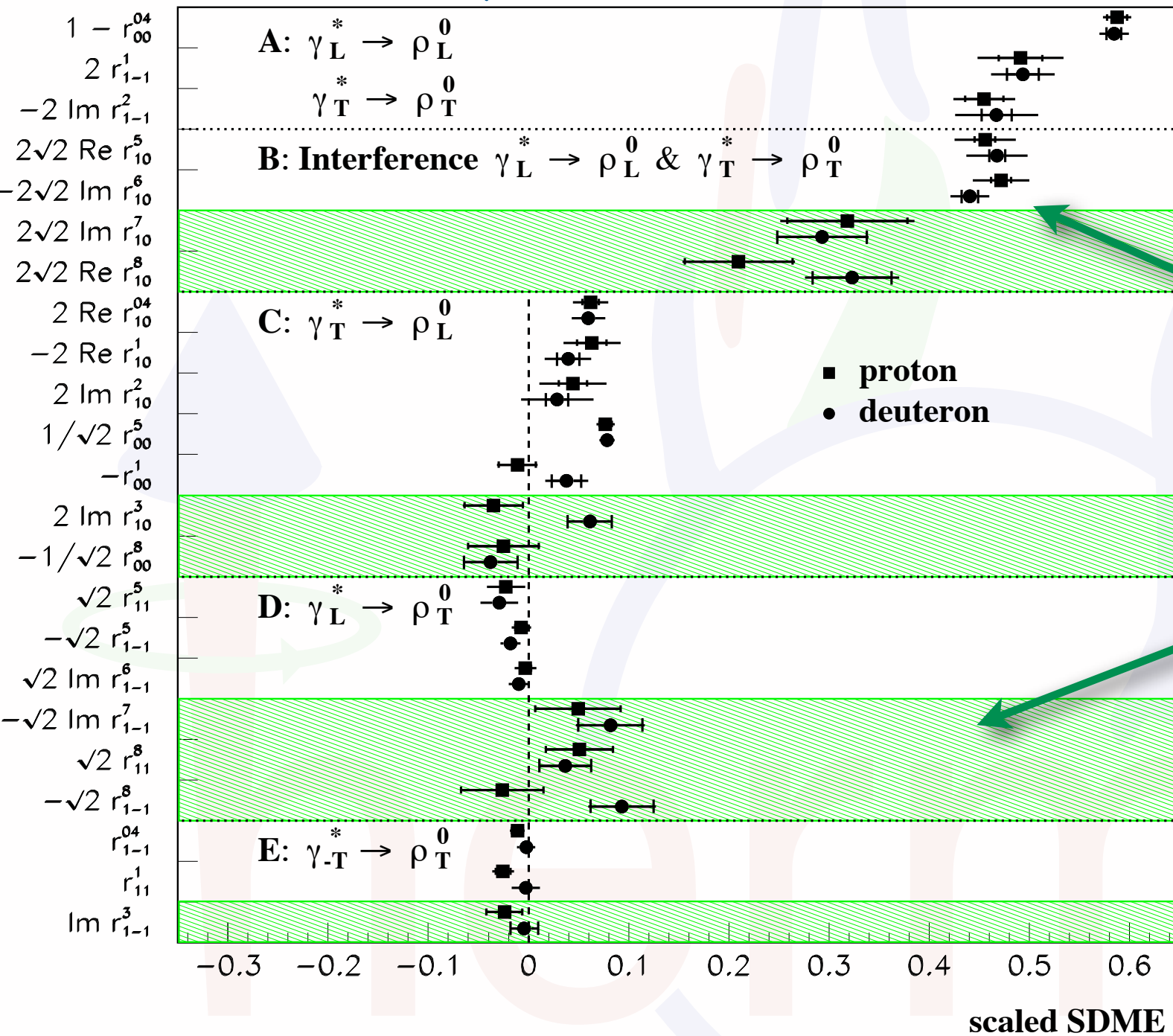
[A. Airapetian et al., EPJ C62 (2009) 659]



target-polarization independent SDMEs

# $\rho^0$ SDMEs from HERMES

[A. Airapetian et al., EPJ C62 (2009) 659]



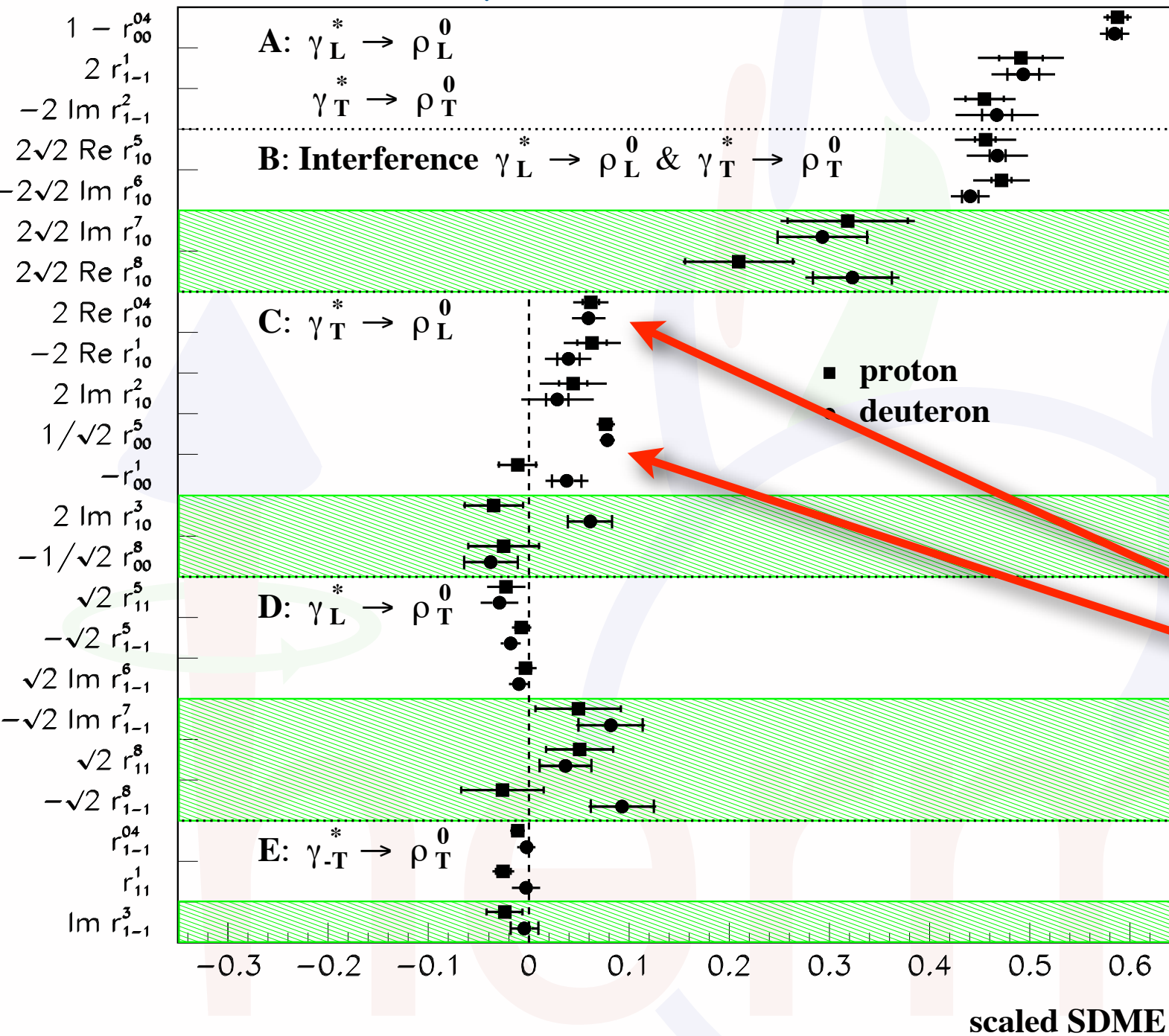
helicity non-flip much larger than helicity-flip and double helicity-flip

target-polarization independent SDMEs



# $\rho^0$ SDMEs from HERMES

[A. Airapetian et al., EPJ C62 (2009) 659]



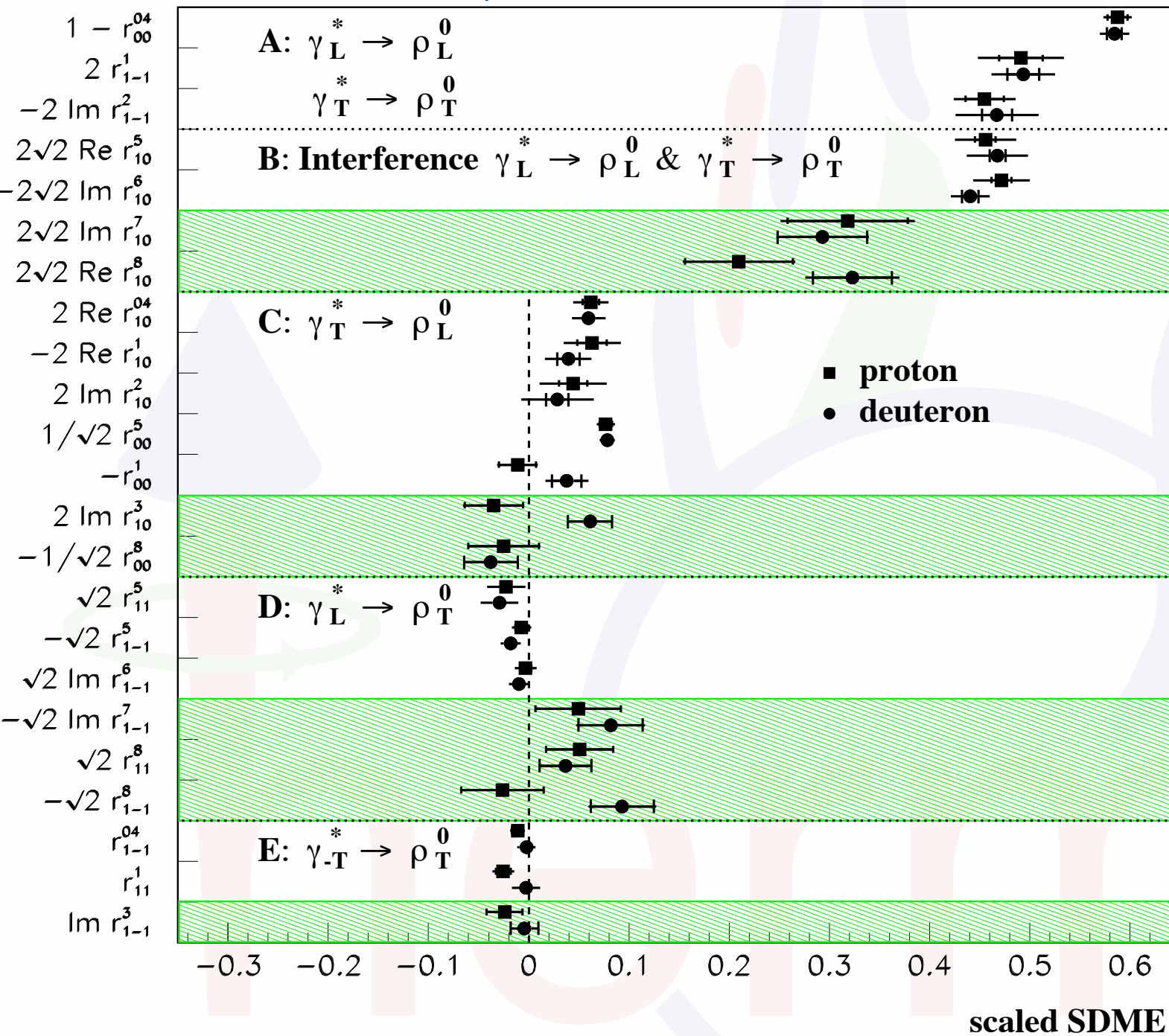
clear breaking of s-channel  
helicity conservation

target-polarization independent SDMEs

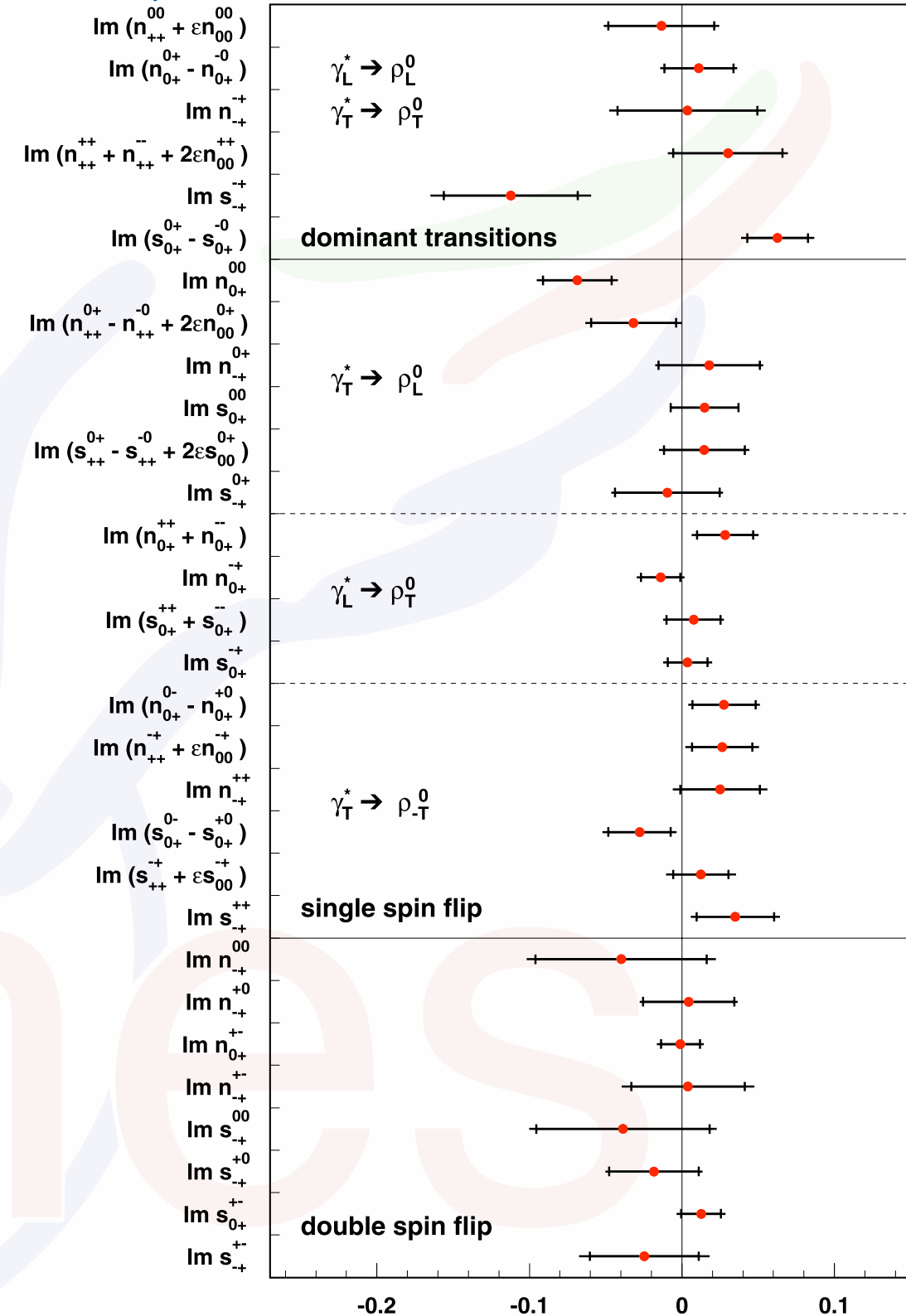
# $\rho^0$ SDMEs from HERMES

[A. Airapetian et al., PLB 679 (2009) 100]

[A. Airapetian et al., EPJ C62 (2009) 659]



target-polarization independent SDMEs



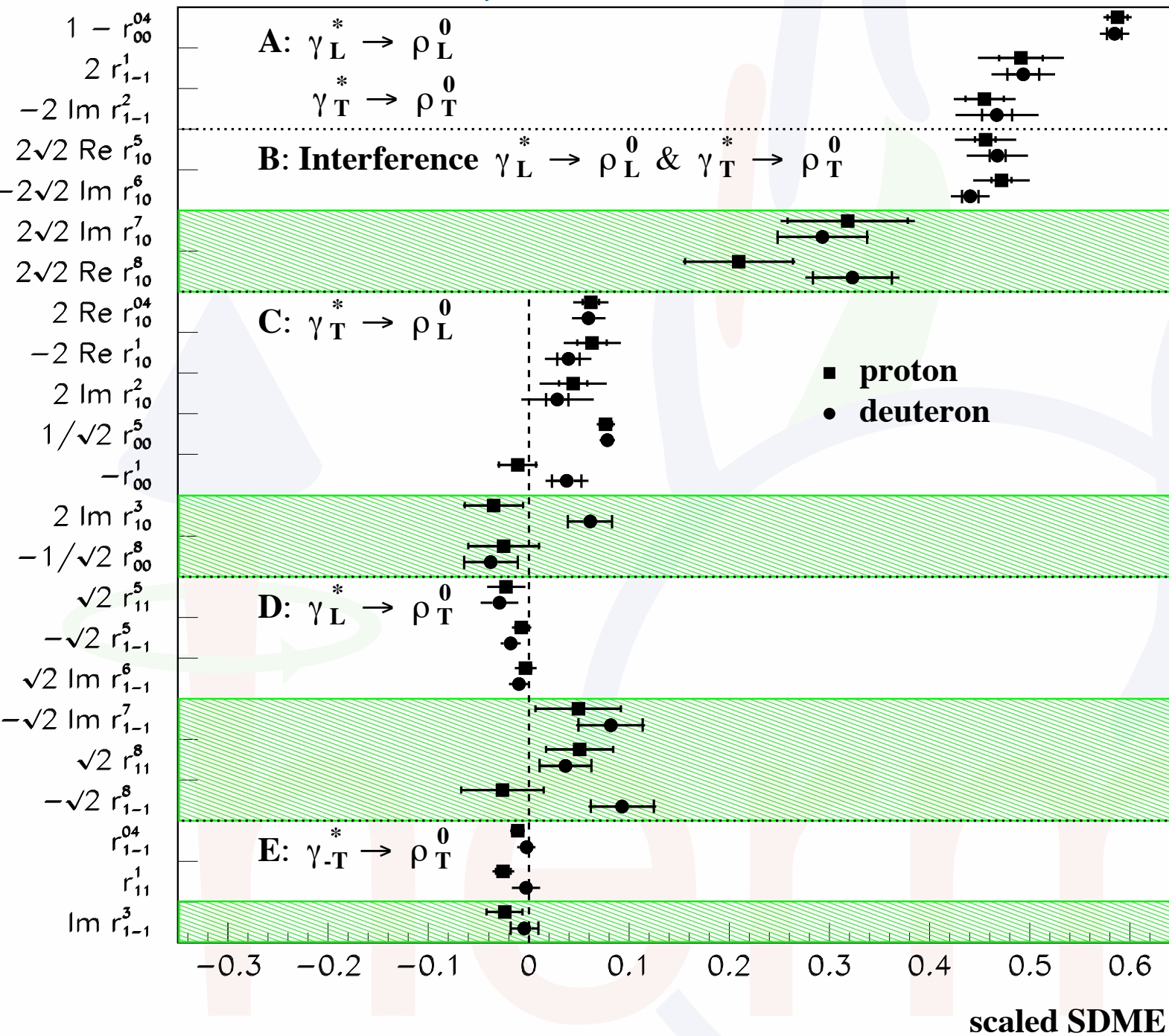
"transverse" SDMEs

PacSPIN 2015 - Taipei - Oct. 6<sup>th</sup>, 2015

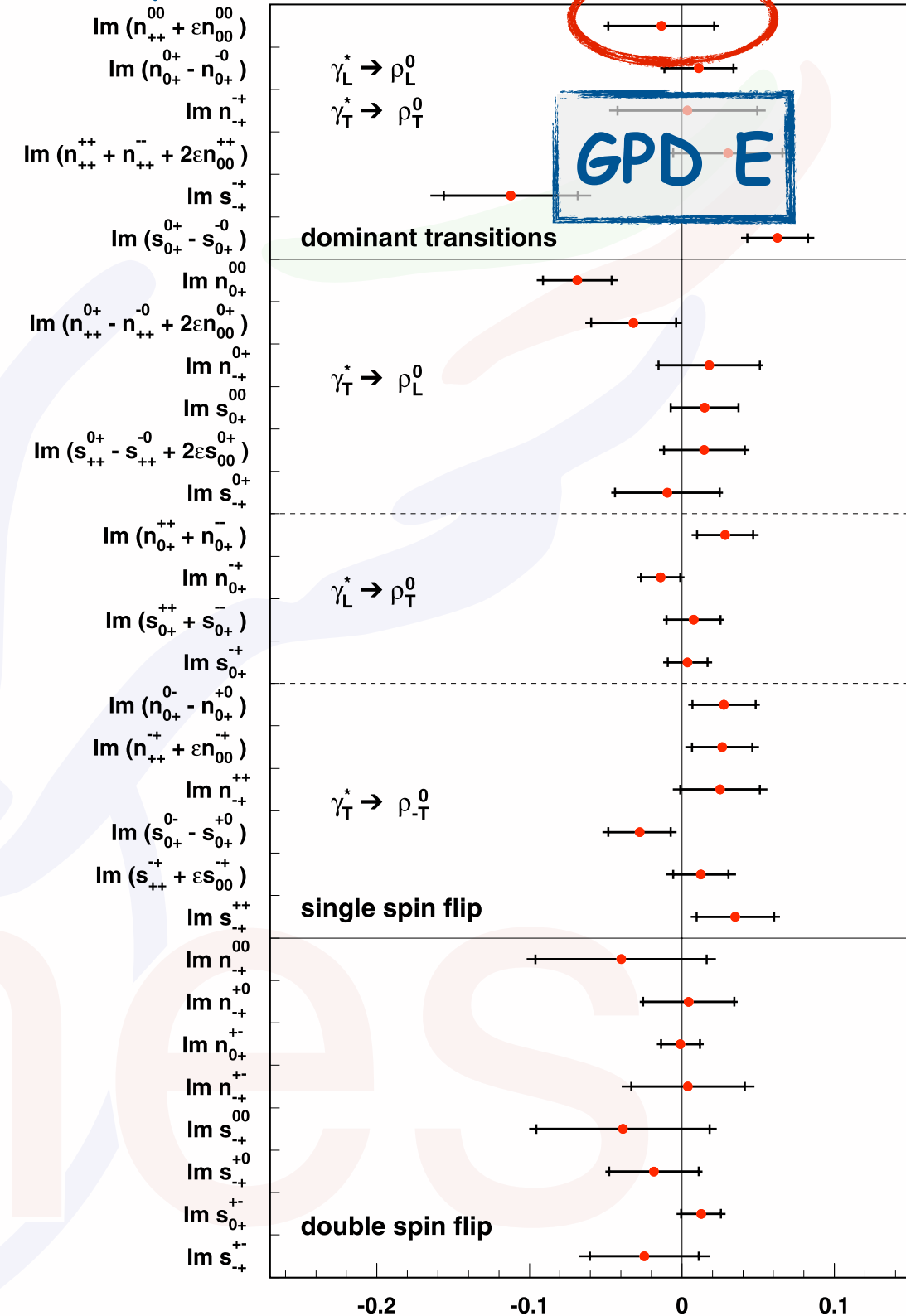
# $\rho^0$ SDMEs from HERMES

[A. Airapetian et al., PLB 679 (2009) 100]

[A. Airapetian et al., EPJ C62 (2009) 659]



target-polarization independent SDMEs

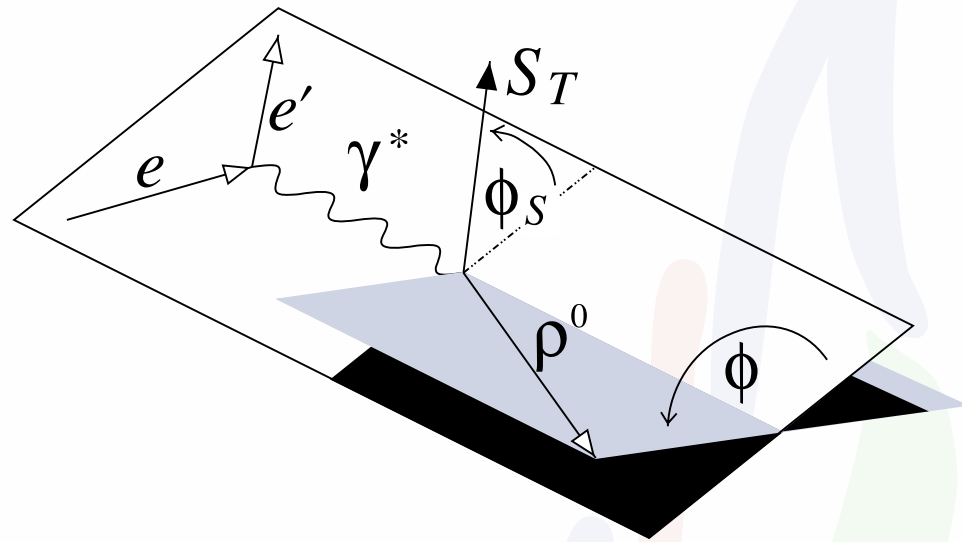


"transverse" SDMEs

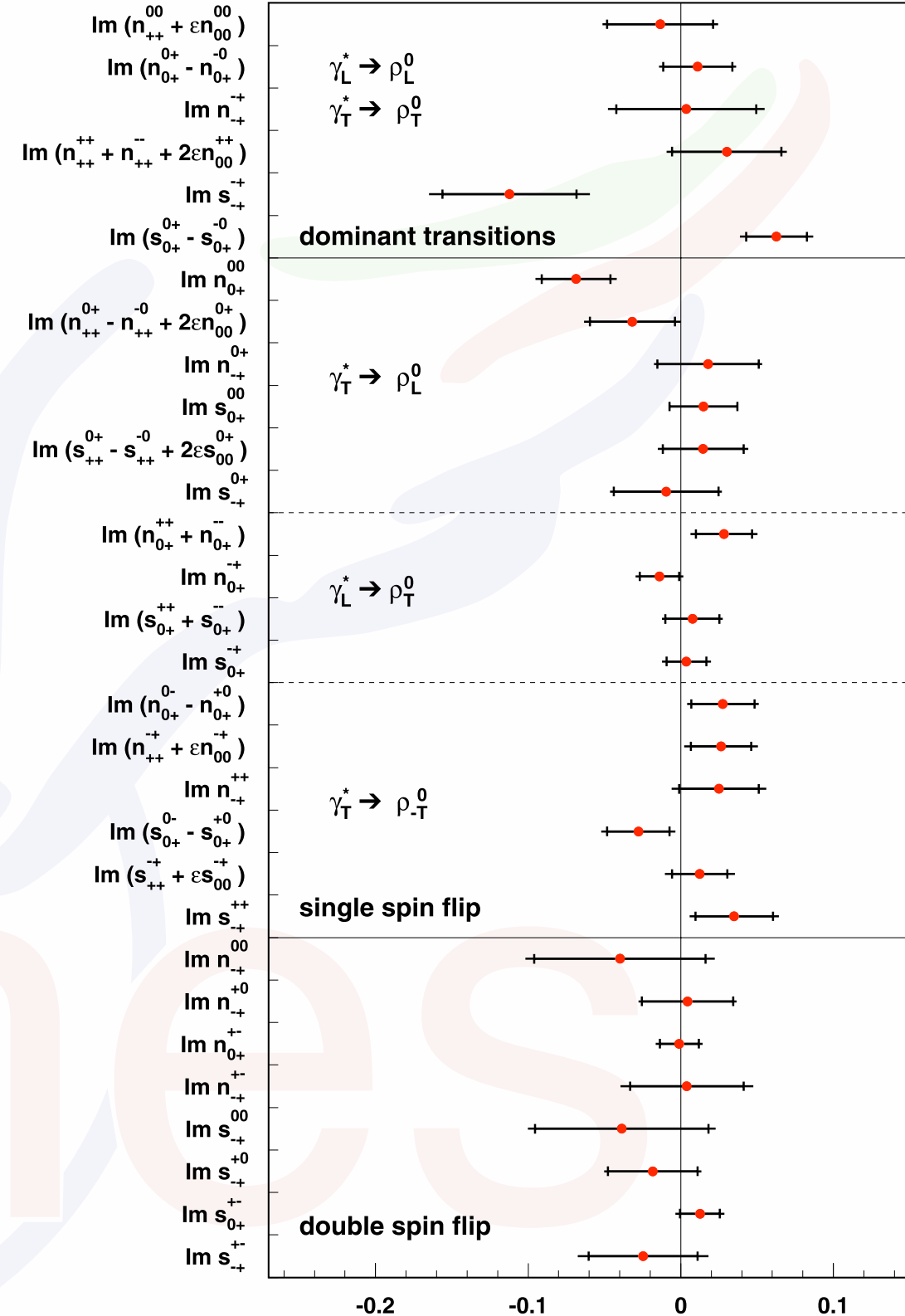
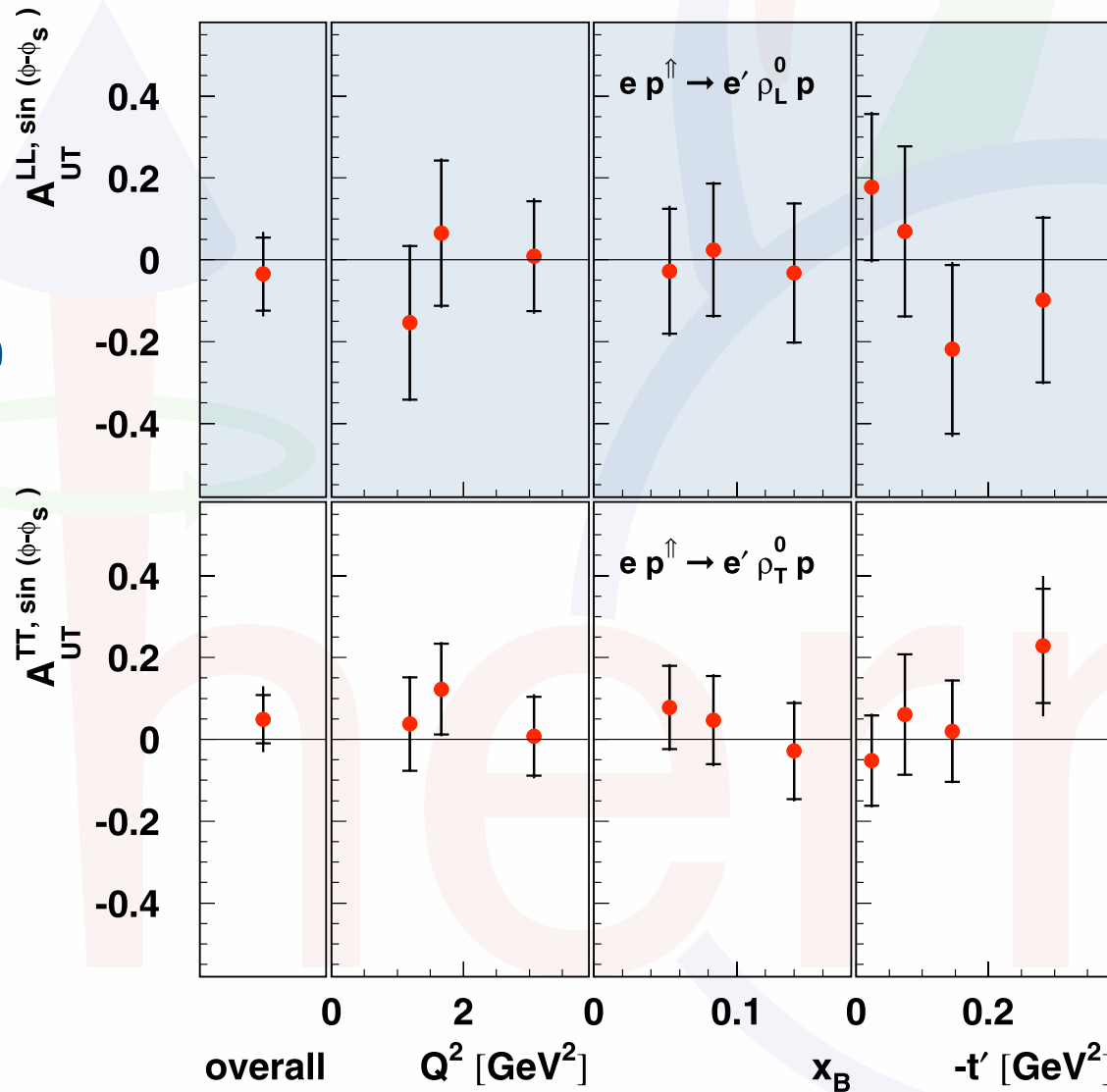
PacSPIN 2015 - Taipei - Oct. 6<sup>th</sup>, 2015

# $\rho^0$ SDMEs from HERMES

[A. Airapetian et al., PLB 679 (2009) 100]



transverse  $\rho^0$  longitudinal  $\rho^0$



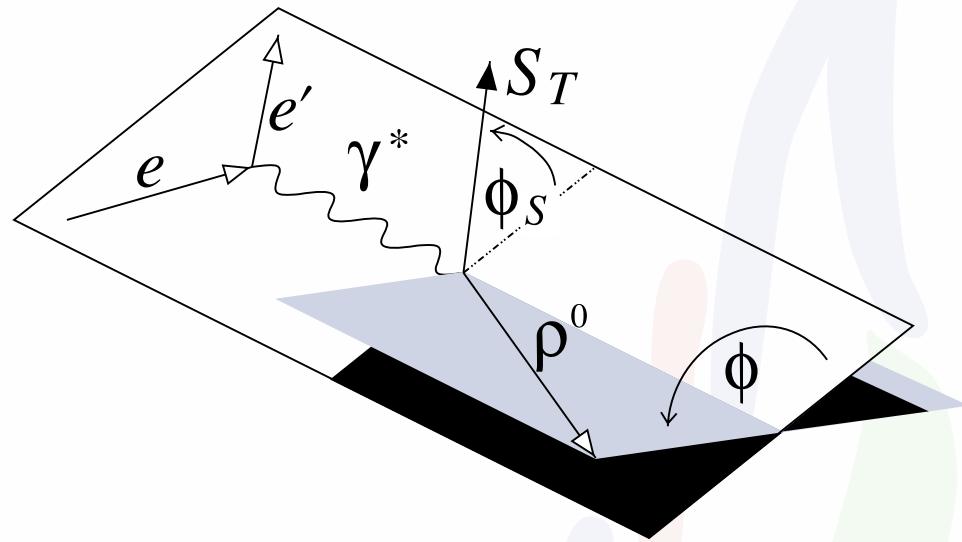
"transverse" SDMEs SDME values

PacSPIN 2015 - Taipei - Oct. 6<sup>th</sup>, 2015

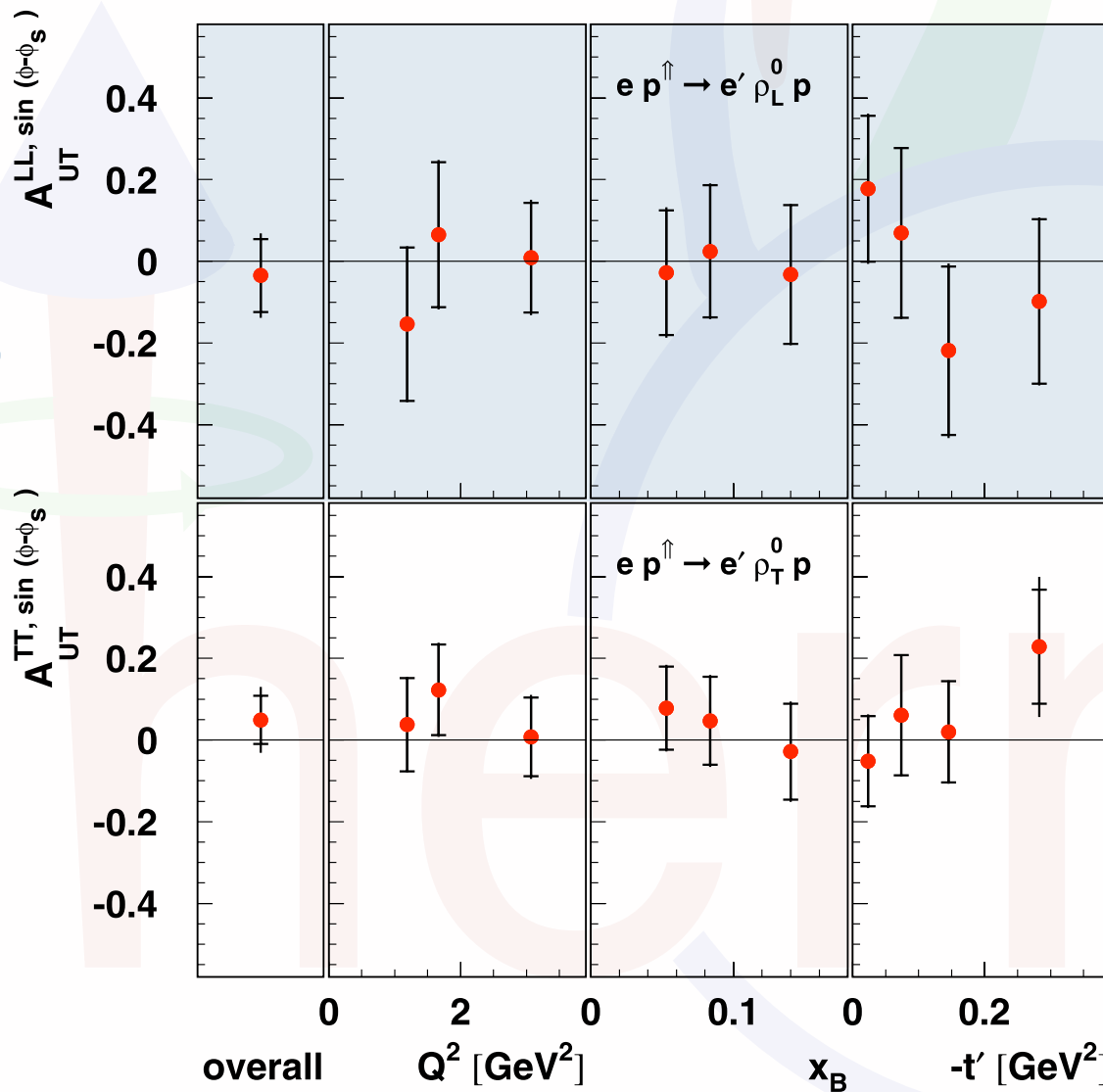


# $\rho^0$ SDMEs from HERMES

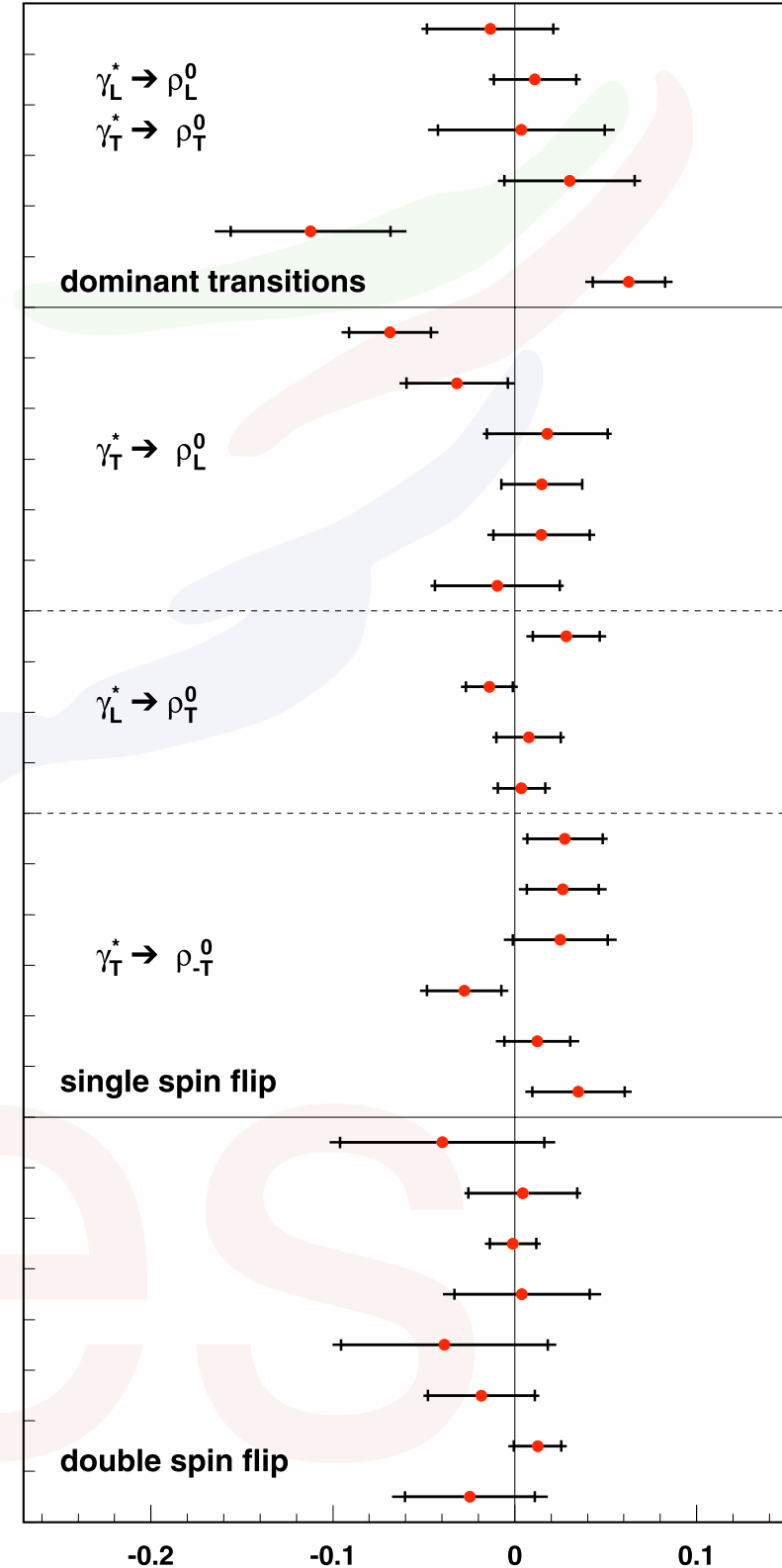
[A. Airapetian et al., PLB 679 (2009) 100]



transverse  $\rho^0$  longitudinal  $\rho^0$



$\text{Im}(n_{++}^{00} + \epsilon n_{00}^{00})$   
 $\text{Im}(n_{0+}^{0+} - n_{0+}^{-0})$   
 $\text{Im} n_{-+}^{+-}$   
 $\text{Im}(n_{++}^{++} + n_{++}^{--} + 2\epsilon n_{00}^{++})$   
 $\text{Im} s_{-+}^{+-}$   
 $\text{Im}(s_{0+}^{0+} - s_{0+}^{-0})$   
 $\text{Im} n_{0+}^{00}$   
 $\text{Im}(n_{++}^{0+} - n_{++}^{-0} + 2\epsilon n_{00}^{0+})$   
 $\text{Im} n_{-+}^{0+}$   
 $\text{Im} s_{0+}^{0+}$   
 $\text{Im}(s_{++}^{0+} - s_{++}^{-0} + 2\epsilon s_{00}^{0+})$   
 $\text{Im} s_{-+}^{0+}$   
 $\text{Im}(n_{0+}^{++} + n_{0+}^{--})$   
 $\text{Im} n_{0+}^{+-}$   
 $\text{Im}(s_{0+}^{++} + s_{0+}^{--})$   
 $\text{Im} s_{0+}^{+-}$   
 $\text{Im}(n_{0+}^{-0} - n_{0+}^{+0})$   
 $\text{Im}(n_{++}^{+-} + \epsilon n_{00}^{+-})$   
 $\text{Im} n_{-+}^{++}$   
 $\text{Im}(s_{0+}^{-0} - s_{0+}^{+0})$   
 $\text{Im}(s_{++}^{+-} + \epsilon s_{00}^{+-})$   
 $\text{Im} s_{-+}^{++}$   
 $\text{Im} n_{-+}^{00}$   
 $\text{Im} n_{-+}^{+0}$   
 $\text{Im} n_{0+}^{+-}$   
 $\text{Im} n_{-+}^{+-}$   
 $\text{Im} s_{-+}^{00}$   
 $\text{Im} s_{-+}^{+0}$   
 $\text{Im} s_{0+}^{+-}$   
 $\text{Im} s_{-+}^{+-}$

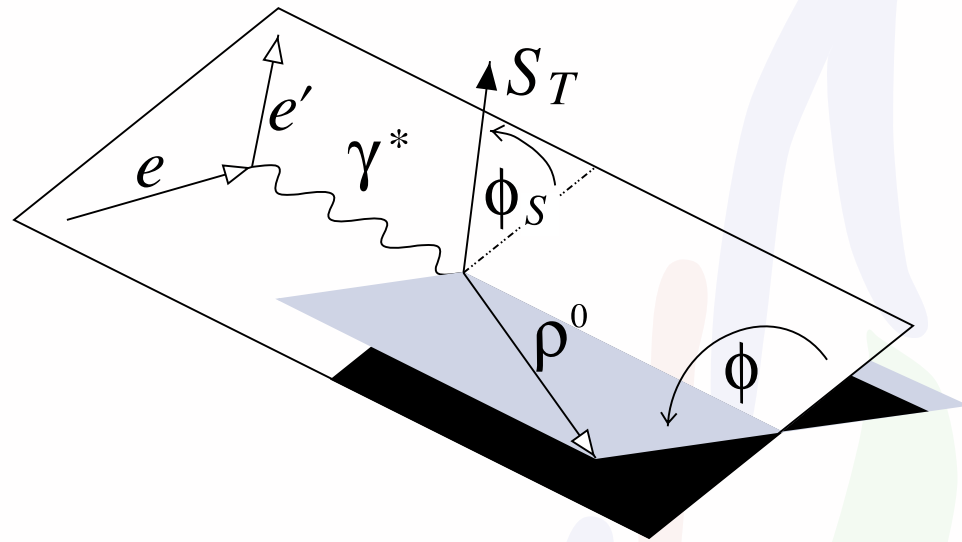


"transverse" SDMEs SDME values

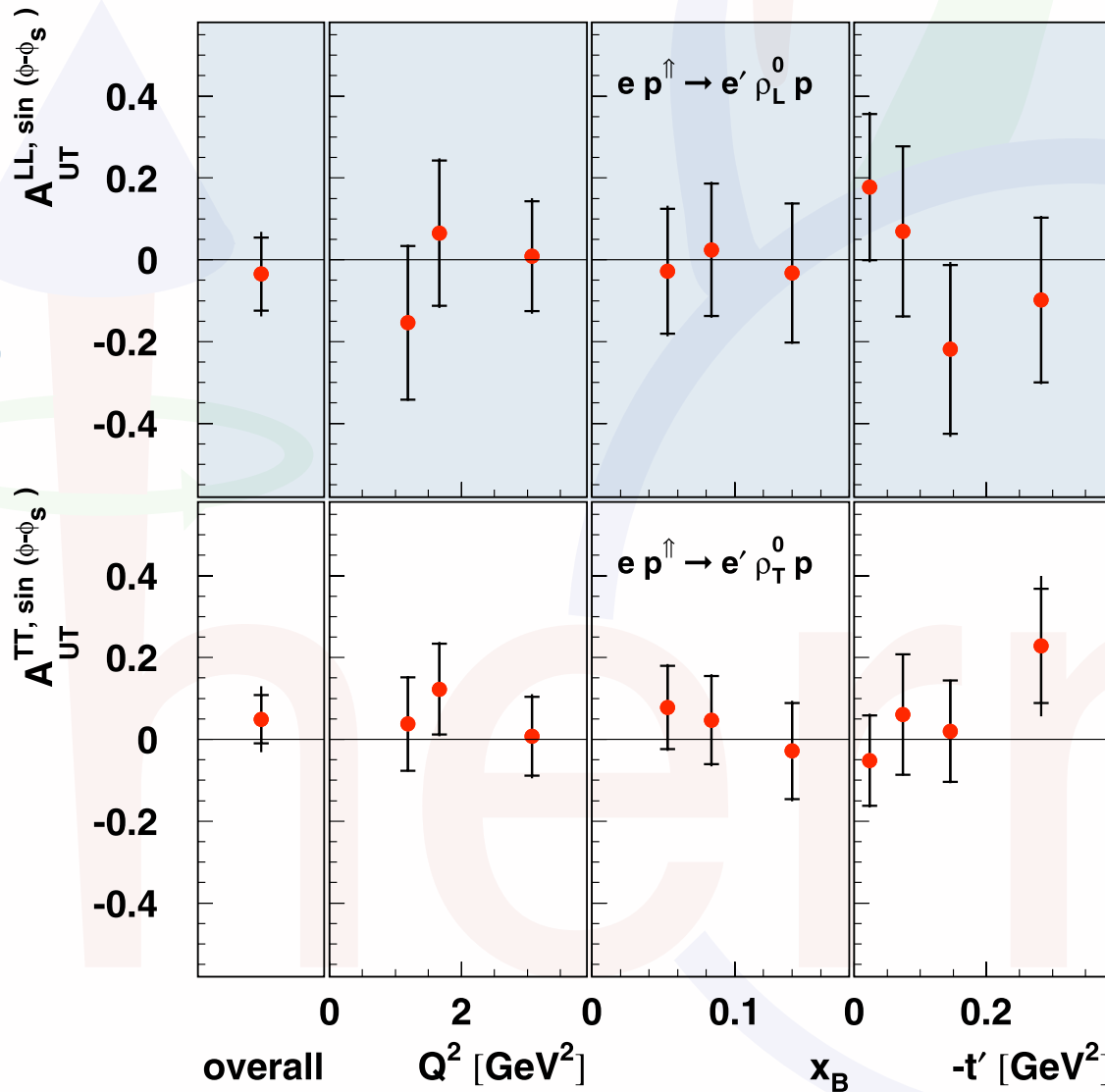
PacSPIN 2015 - Taipei - Oct. 6<sup>th</sup>, 2015

# $\rho^0$ SDMEs from HERMES

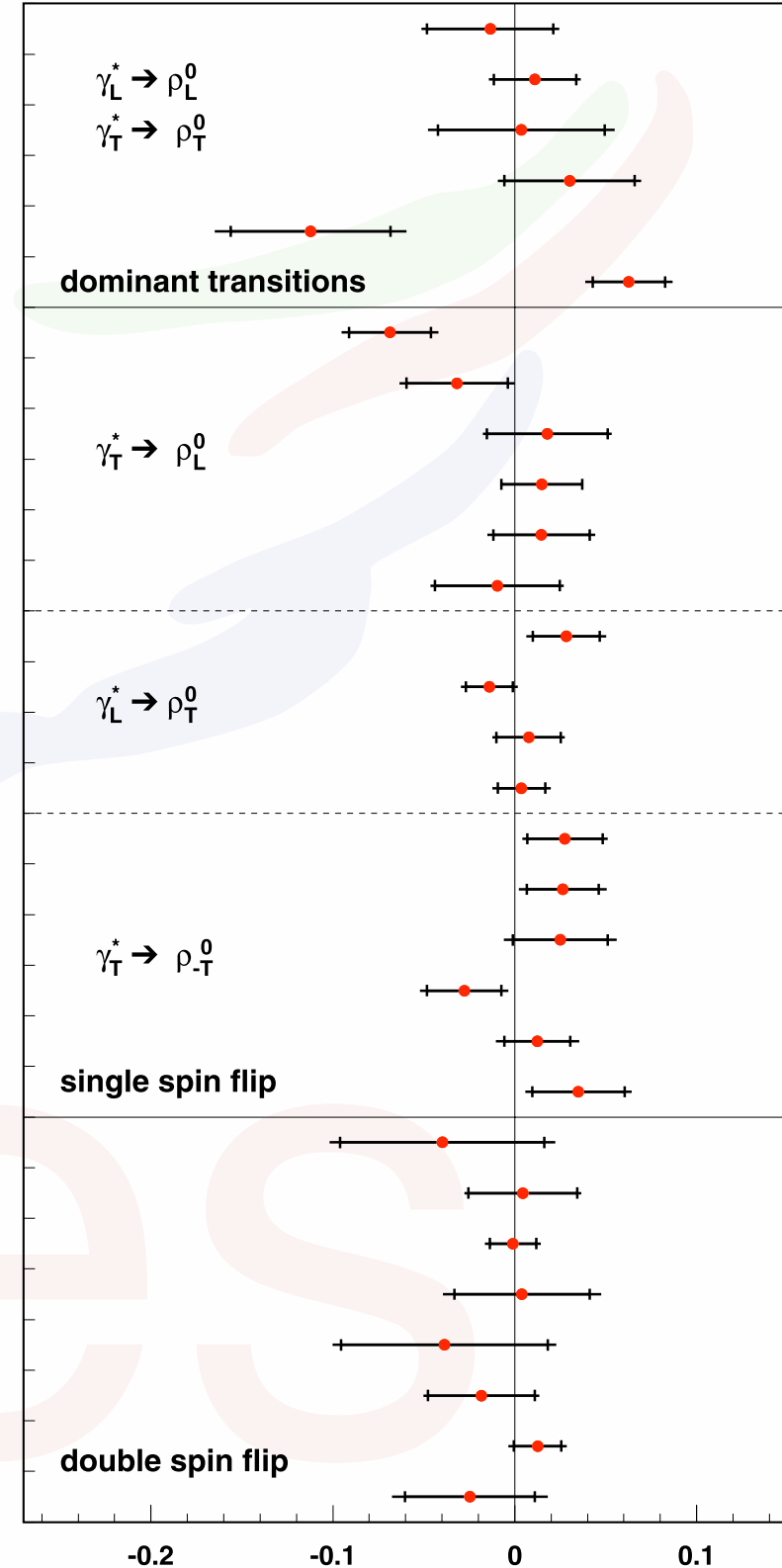
[A. Airapetian et al., PLB 679 (2009) 100]



transverse  $\rho^0$  longitudinal  $\rho^0$



$\text{Im}(n_{++}^{00} + \epsilon n_{00}^{00})$   
 $\text{Im}(n_{0+}^{0+} - n_{0+}^{-0})$   
 $\text{Im} n_{-+}^{+-}$   
 $\text{Im}(n_{++}^{++} + n_{++}^{--} + 2\epsilon n_{00}^{++})$   
 $\text{Im} s_{-+}^{+-}$   
 $\text{Im}(s_{0+}^{0+} - s_{0+}^{-0})$   
 $\text{Im} n_{0+}^{00}$   
 $\text{Im}(n_{++}^{0+} - n_{++}^{-0} + 2\epsilon n_{00}^{0+})$   
 $\text{Im} n_{-+}^{0+}$   
 $\text{Im} s_{0+}^{00}$   
 $\text{Im}(s_{++}^{0+} - s_{++}^{-0} + 2\epsilon s_{00}^{0+})$   
 $\text{Im} s_{-+}^{0+}$   
 $\text{Im}(n_{0+}^{++} + n_{0+}^{--})$   
 $\text{Im} n_{0+}^{+-}$   
 $\text{Im}(s_{0+}^{++} + s_{0+}^{--})$   
 $\text{Im} s_{0+}^{+-}$   
 $\text{Im}(n_{0+}^{-0} - n_{0+}^{+0})$   
 $\text{Im}(n_{++}^{+-} + \epsilon n_{00}^{+-})$   
 $\text{Im} n_{-+}^{++}$   
 $\text{Im}(s_{0+}^{-0} - s_{0+}^{+0})$   
 $\text{Im}(s_{++}^{+-} + \epsilon s_{00}^{+-})$   
 $\text{Im} s_{-+}^{++}$   
 $\text{Im} n_{-+}^{00}$   
 $\text{Im} n_{-+}^{+0}$   
 $\text{Im} n_{0+}^{+-}$   
 $\text{Im} n_{-+}^{+-}$   
 $\text{Im} s_{-+}^{00}$   
 $\text{Im} s_{-+}^{+0}$   
 $\text{Im} s_{0+}^{+-}$   
 $\text{Im} s_{-+}^{+-}$



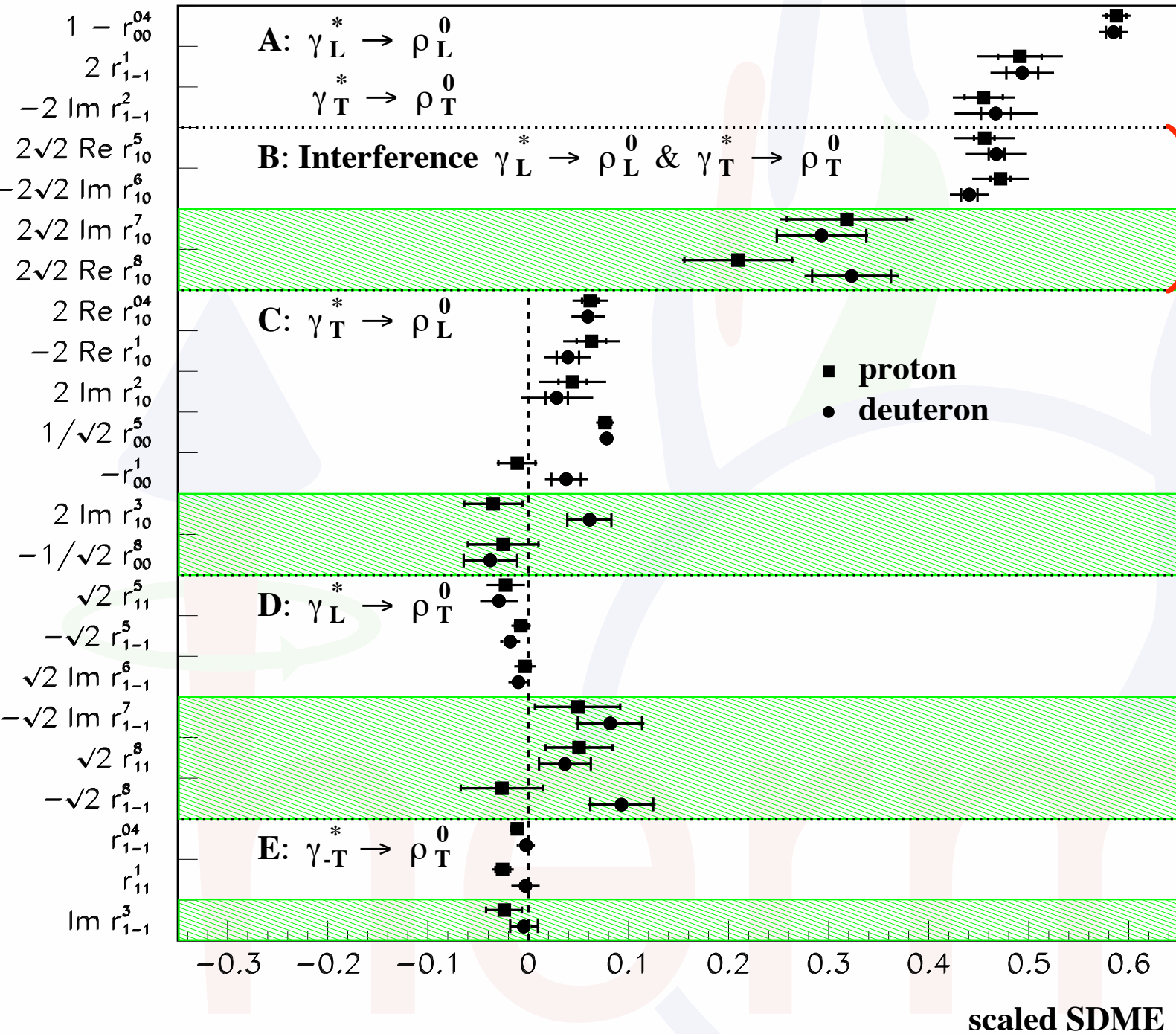
"transverse" SDMEs SDME values

PacSPIN 2015 - Taipei - Oct. 6<sup>th</sup>, 2015

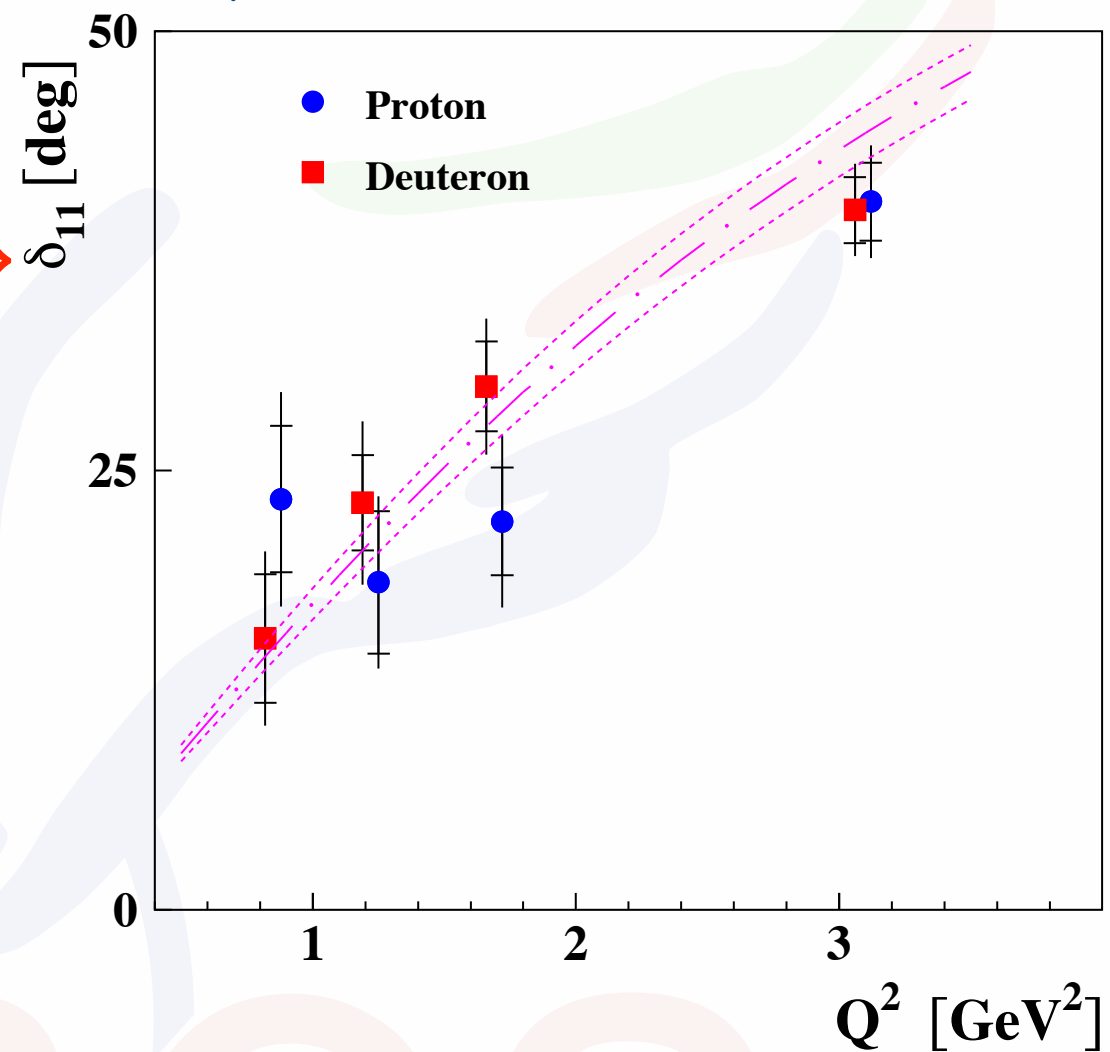


# $\rho^0$ SDMEs from HERMES: challenges

[A. Airapetian et al., EPJ C62 (2009) 659]



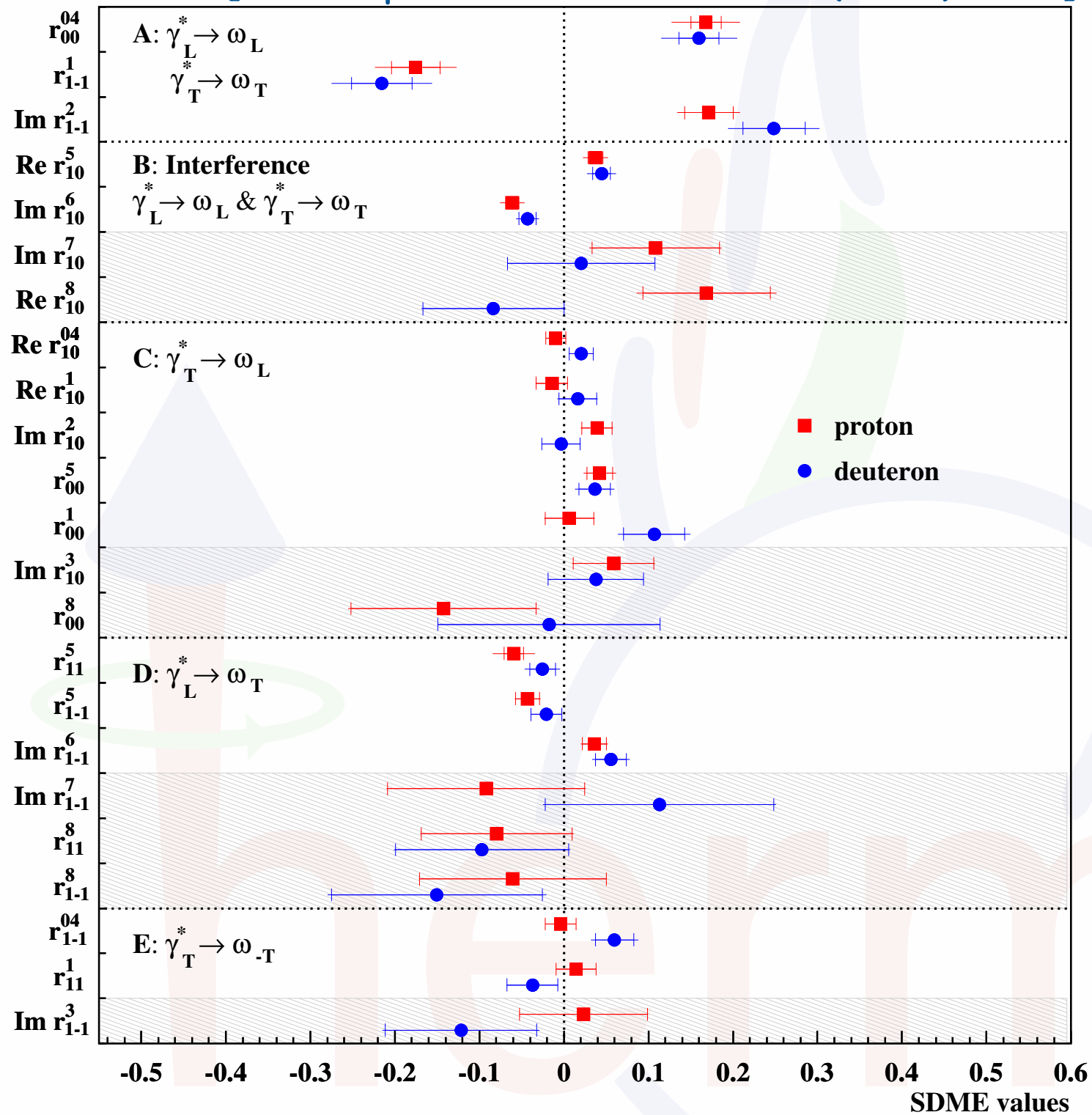
[A. Airapetian et al, EPJ C71 (2011) 1609]



Extraction of SDMEs and helicity amplitude ratios at HERMES for  $\rho$  mesons challenges GPD-based calculations (giving small values)

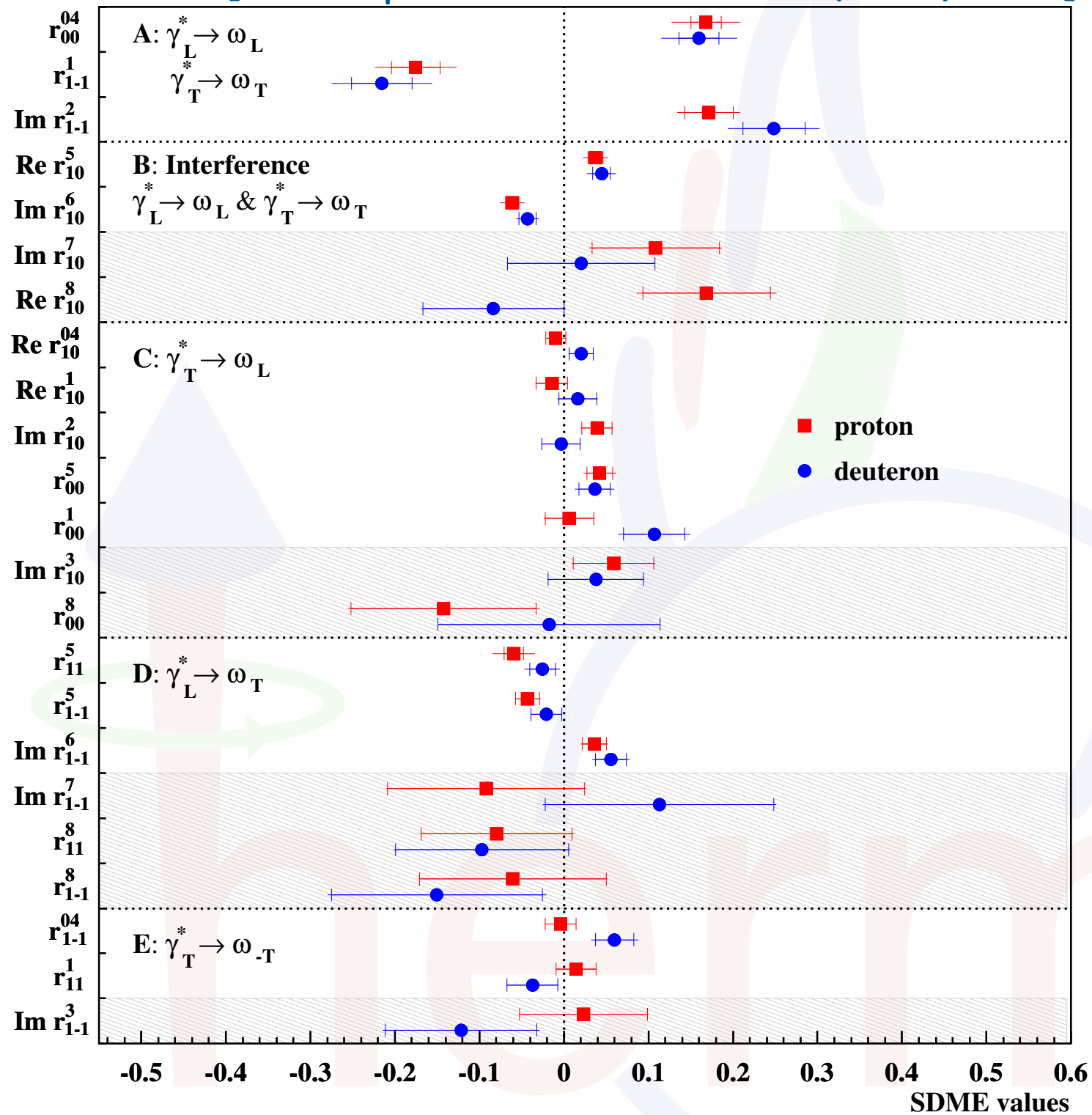
# ... $\omega$ production

[A. Airapetian et al., EPJ C74 (2014) 3110]



# ... $\omega$ production

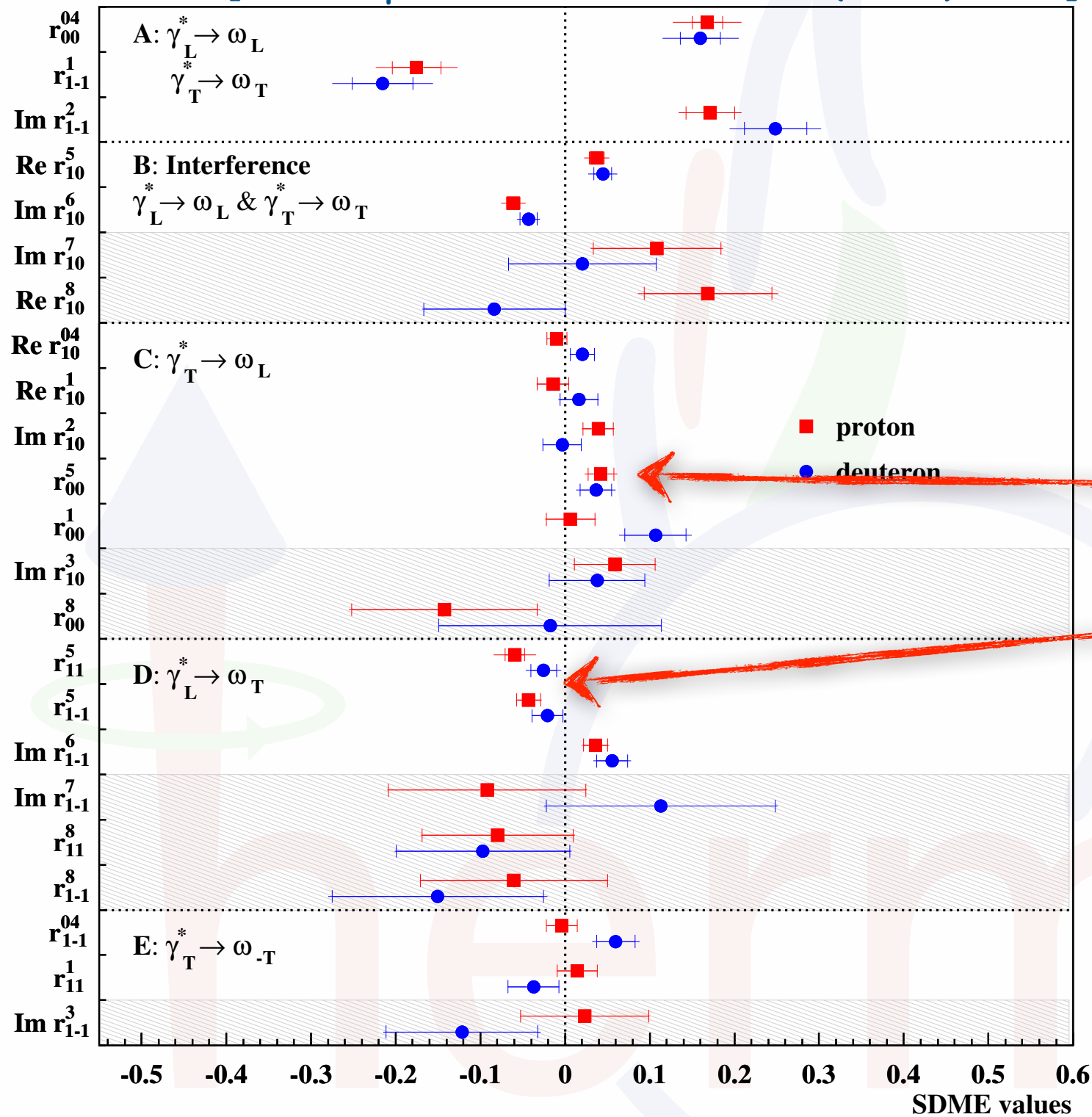
[A. Airapetian et al., EPJ C74 (2014) 3110]



- helicity-conserving SDMEs dominate

# ... $\omega$ production

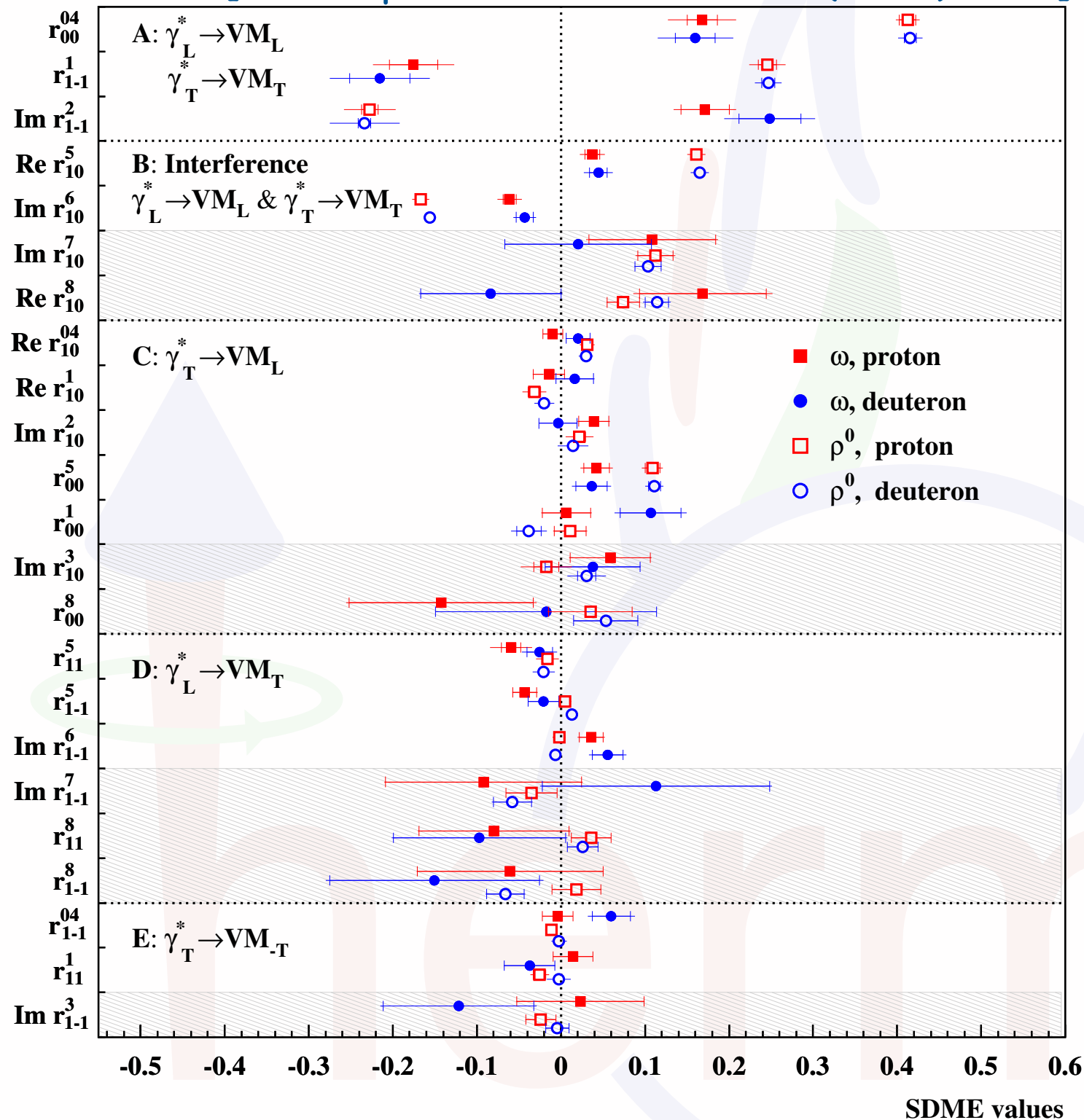
[A. Airapetian et al., EPJ C74 (2014) 3110]



- helicity-conserving SDMEs dominate
- hardly any violation of SCHC, except maybe for
  - $r_{00}^5$
  - $r_{11}^5 + r_{1-1}^5 - \Im r_{1-1}^6$

# ... $\omega$ production

[A. Airapetian et al., EPJ C74 (2014) 3110]

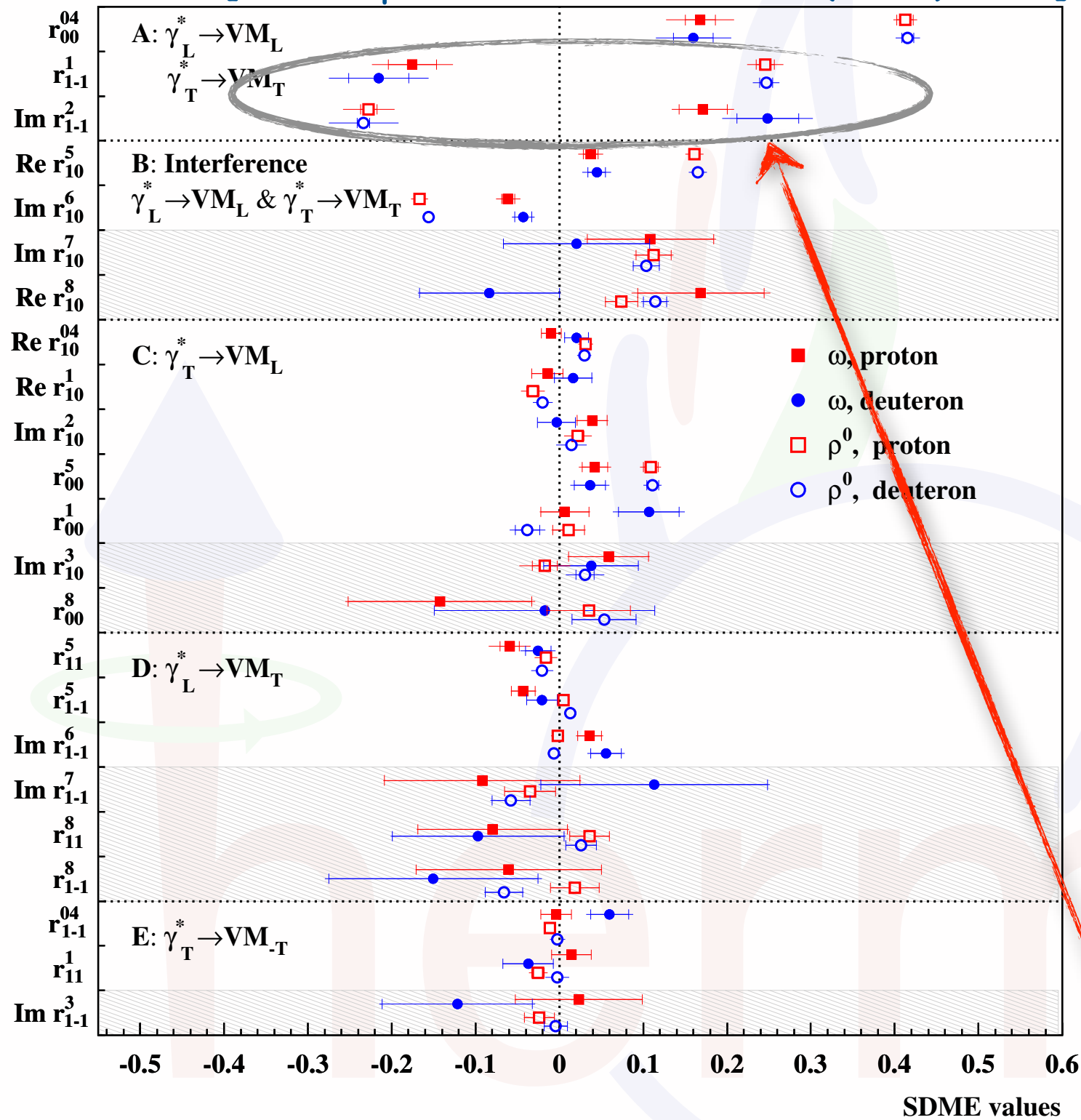


- helicity-conserving SDMEs dominate
- hardly any violation of SCHC, except maybe for
  - $r_{00}^5$
  - $r_{11}^5 + r_{1-1}^5 - \Im r_{1-1}^6$
- interference smaller than for  $\rho^0$  ...



# ... $\omega$ production

[A. Airapetian et al., EPJ C74 (2014) 3110]



- helicity-conserving SDMEs dominate
- hardly any violation of SCHC, except maybe for
  - $r_{00}^5$
  - $r_{11}^5 + r_{1-1}^5 - \Im r_{1-1}^6$
- interference smaller than for  $\rho^0$  ...
- ... and opposite signs for  $r_{1-1}^1$  &  $\Im r_{1-1}^2$



# (un)natural-parity exchange contributions

$$\Im r_{1-1}^2 - r_{1-1}^1 = \frac{1}{\mathcal{N}} \widetilde{\sum} (|U_{11}|^2 - |T_{11}|^2)$$

UPE contribution

NPE contribution

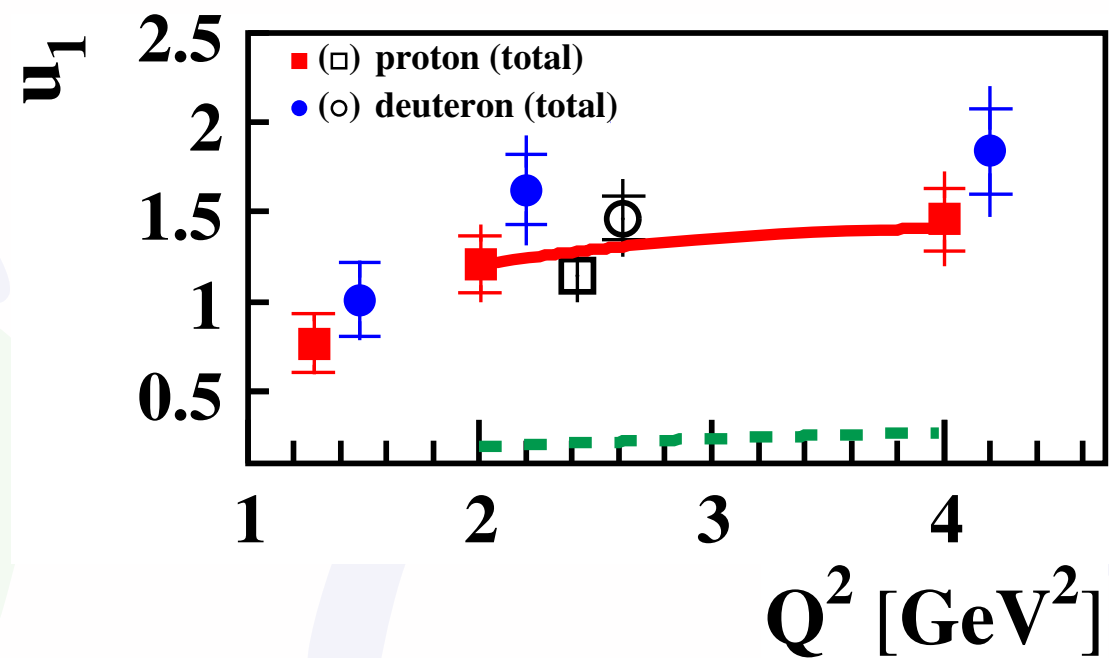
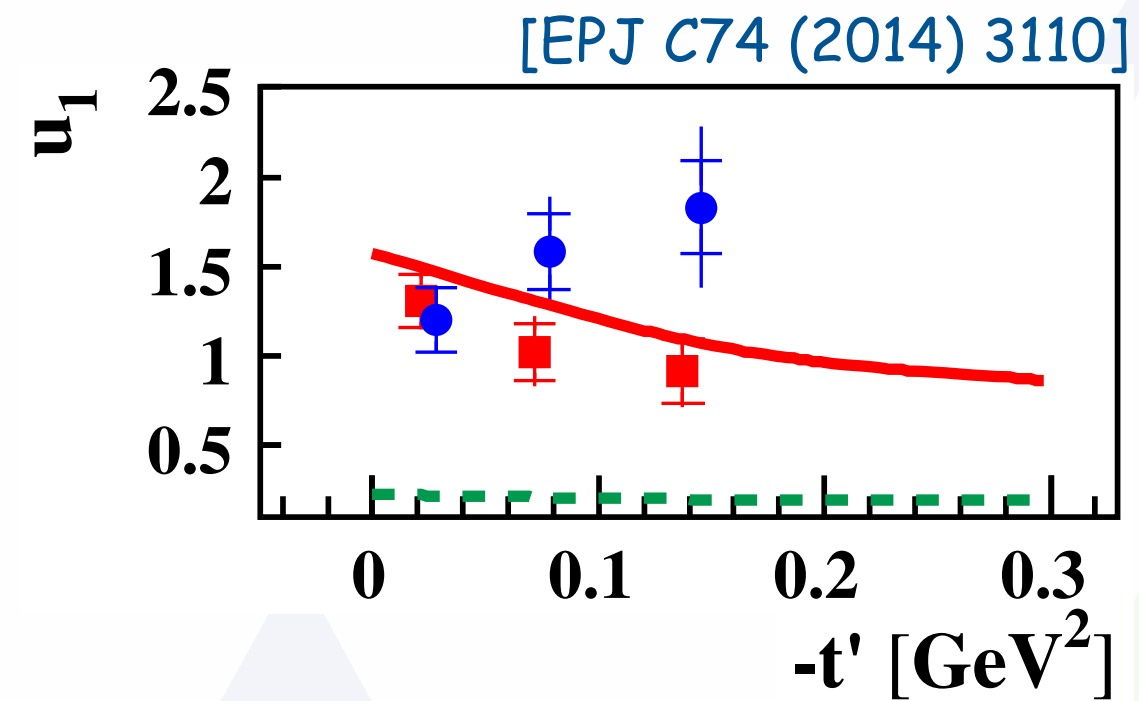
- positive for omega -> large UPE contributions (unlike for rho)
- can construct various UPE quantities:

$$u_1 = 1 - r_{00}^{04} + 2r_{1-1}^{04} - 2r_{11}^1 - 2r_{1-1}^1$$

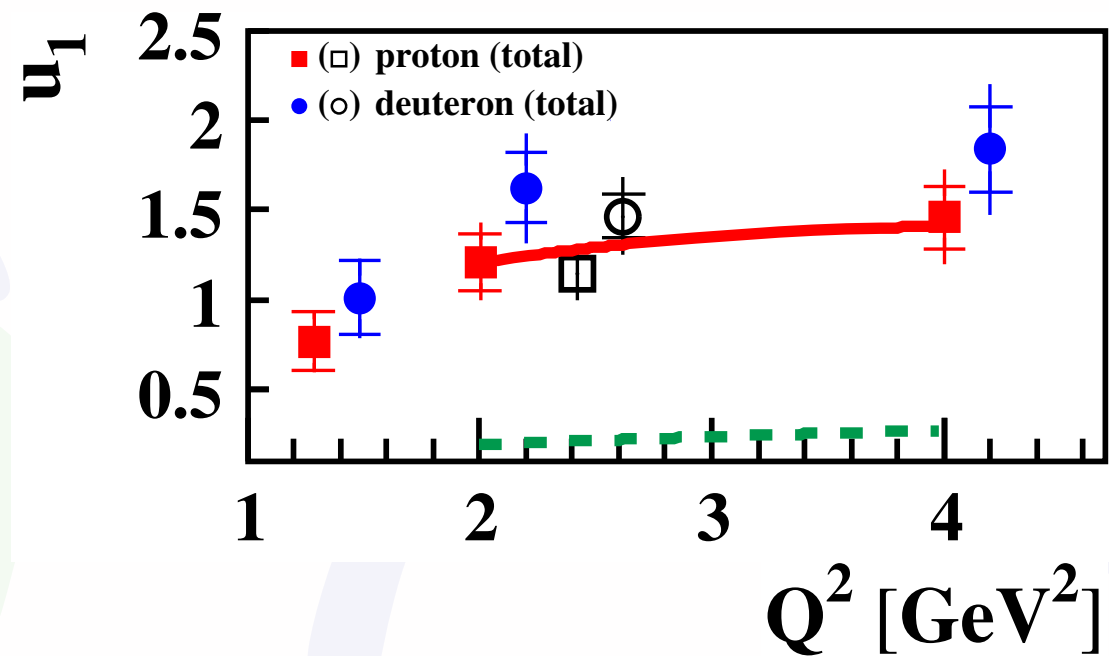
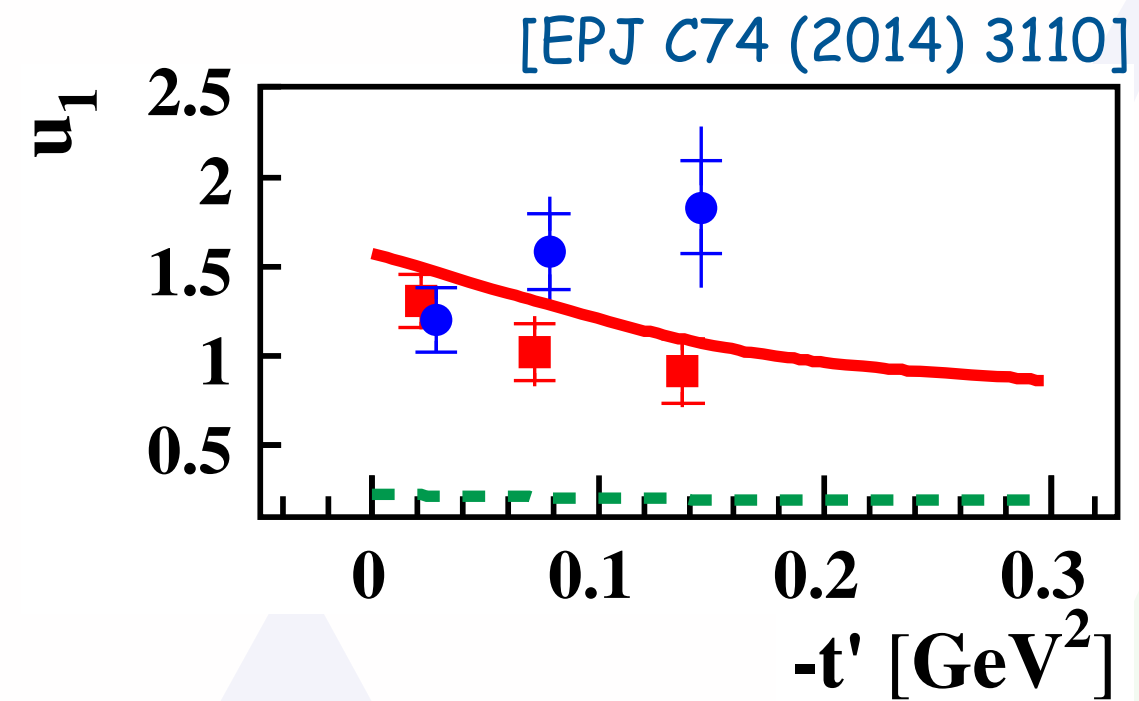
$$u_2 = r_{11}^5 + r_{1-1}^5$$

$$u_3 = r_{11}^8 + r_{1-1}^8$$

# test of UPE

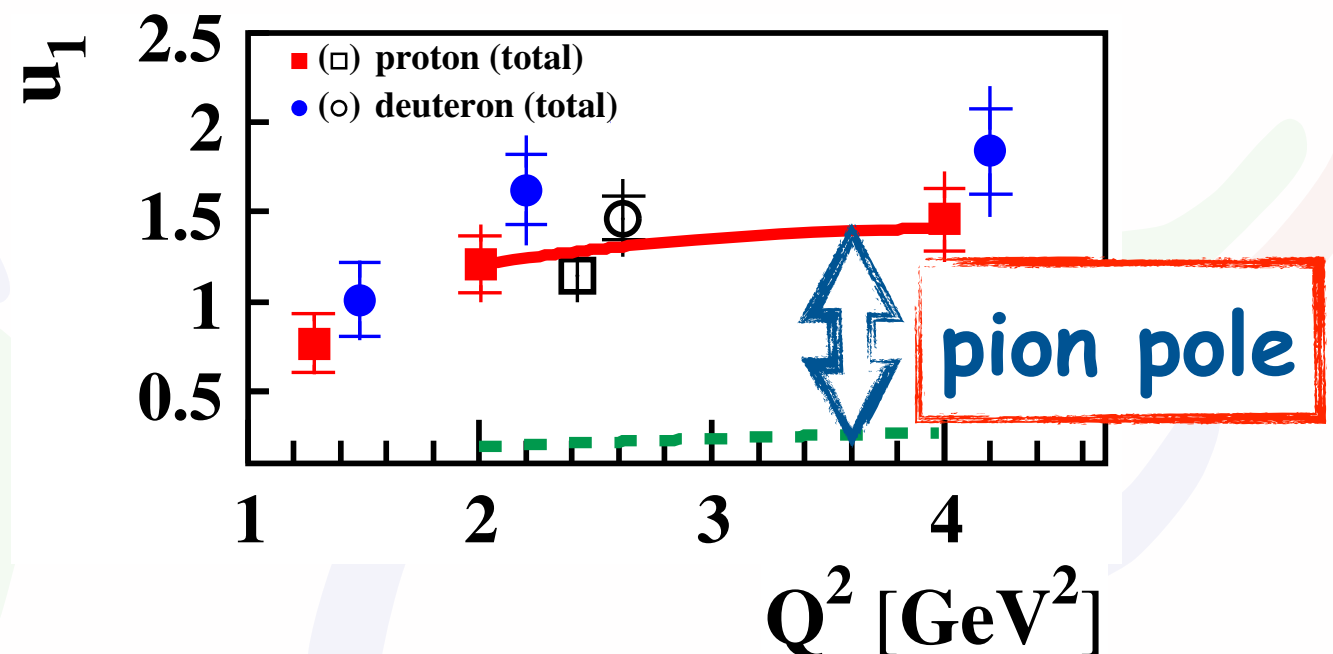
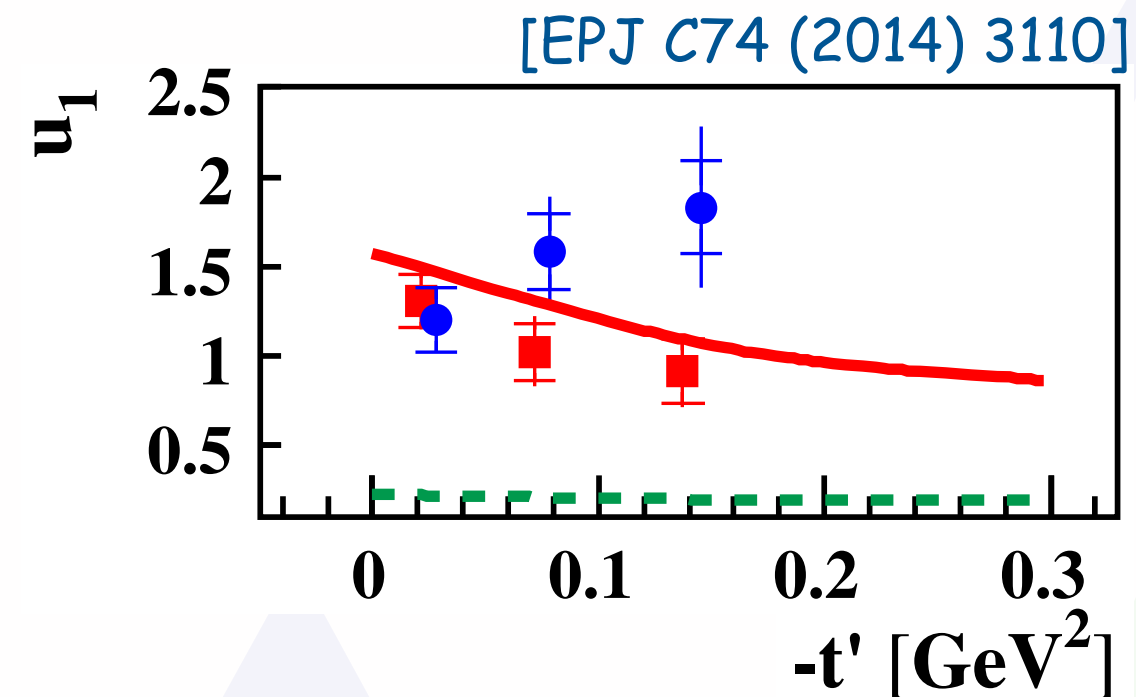


# test of UPE



- large UPE contributions

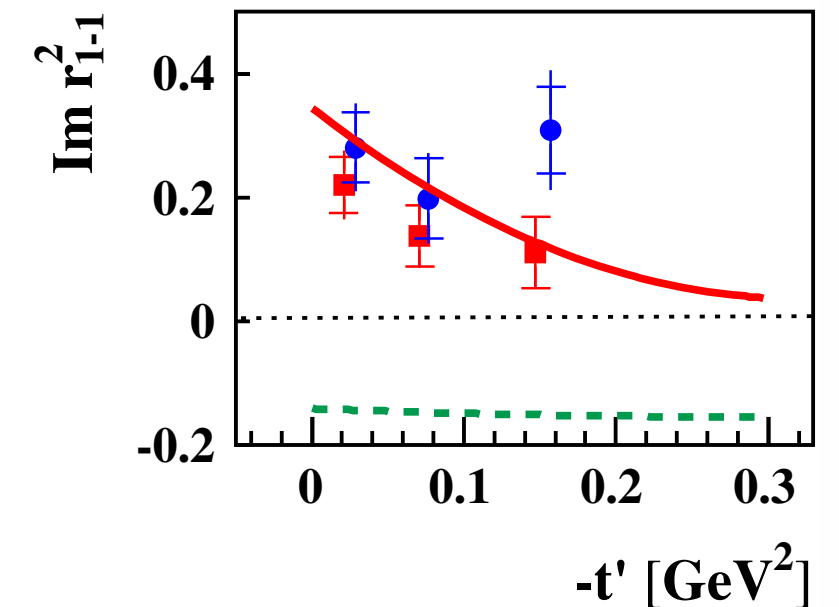
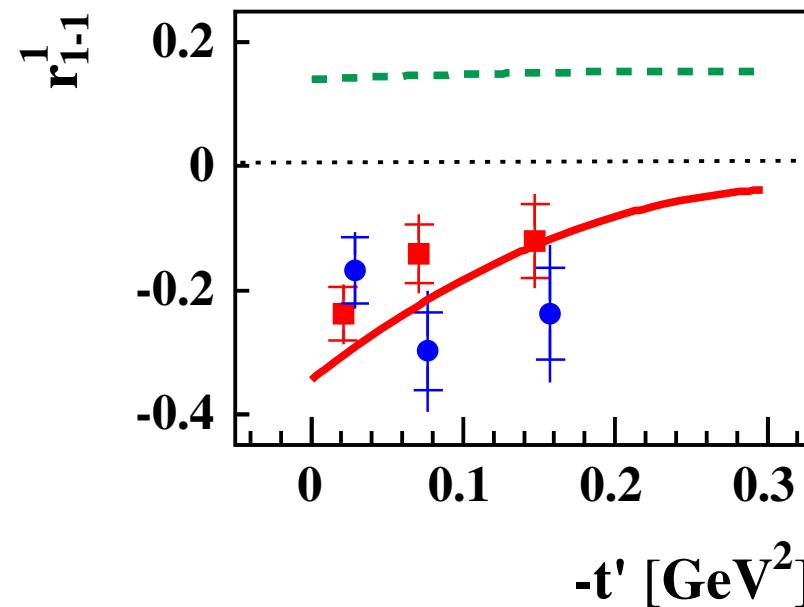
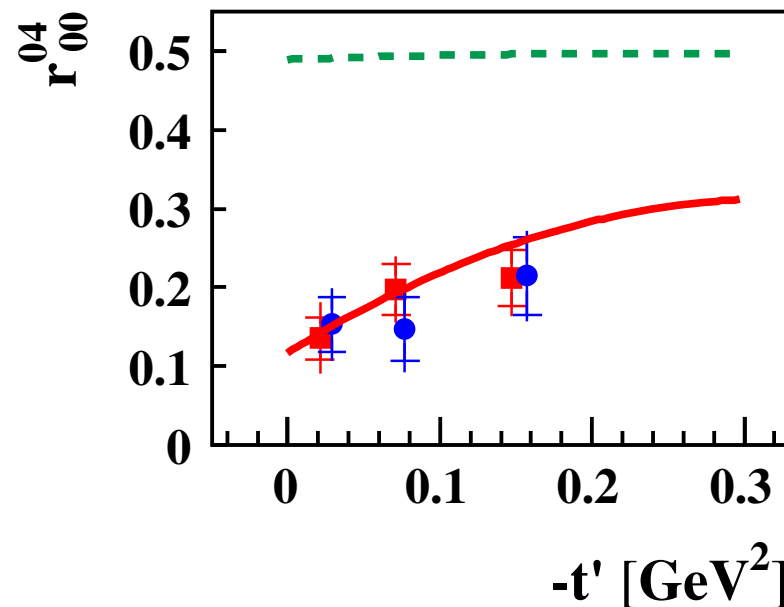
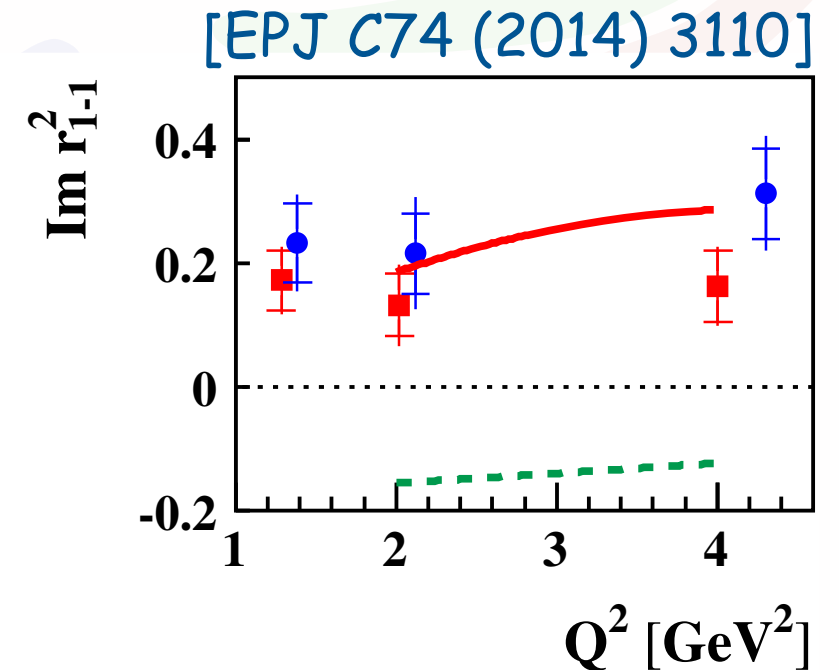
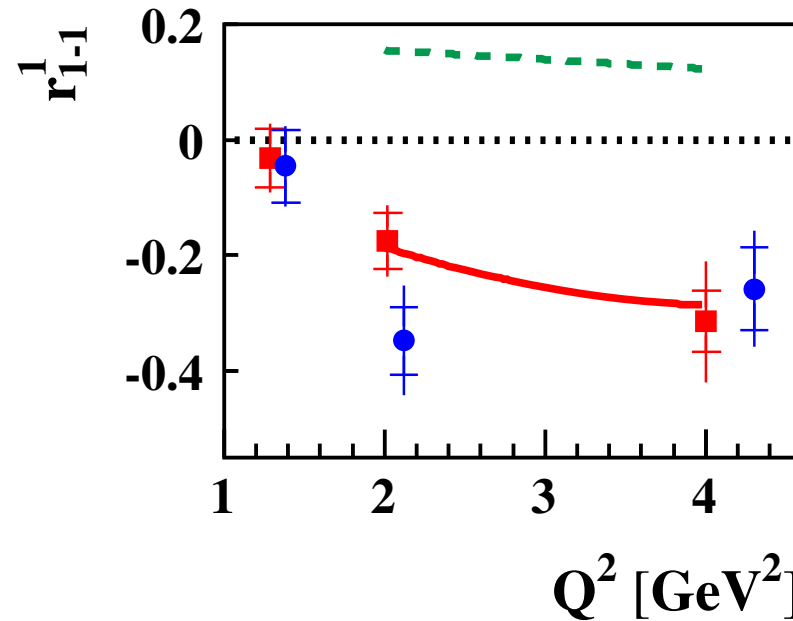
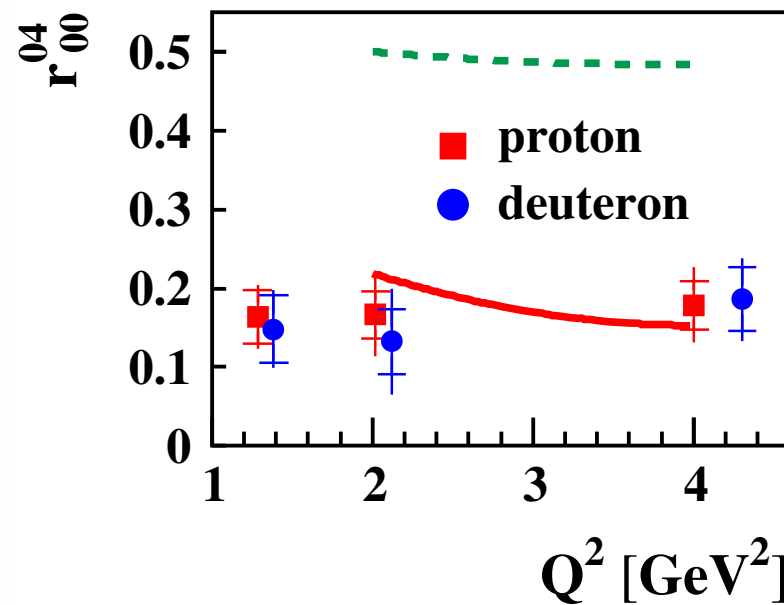
# test of UPE



- large UPE contributions
- modified GK model [EPJ A50 (2014) 146] can describe data when including
  - pion pole contribution (red curve)
  - corresponding  $\pi\omega$  transition form factor (fit to these data)

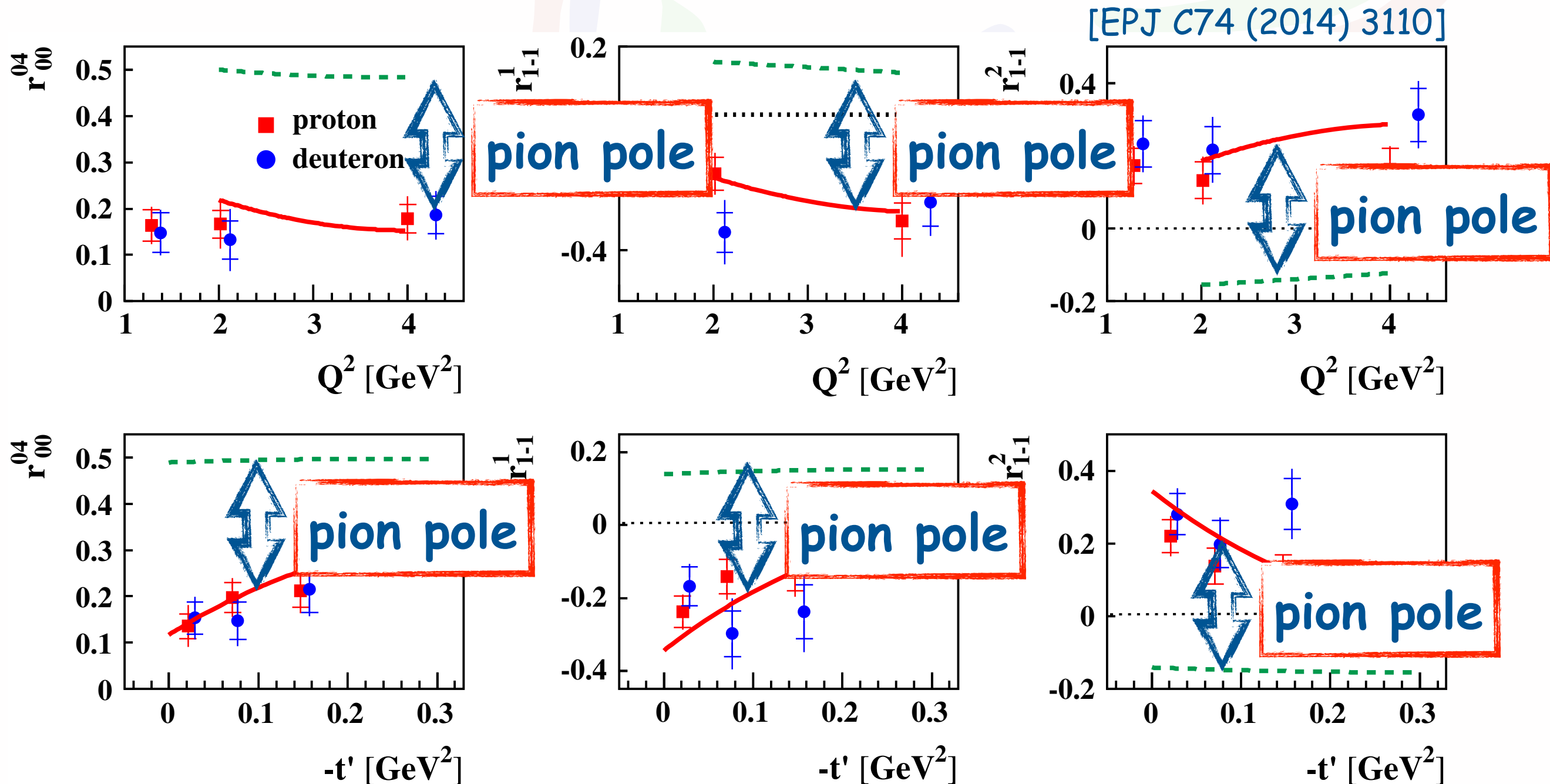
# impact of pion-pole contr. on SDMEs

- "class-A" - helicity-conserving transitions



# impact of pion-pole contr. on SDMEs

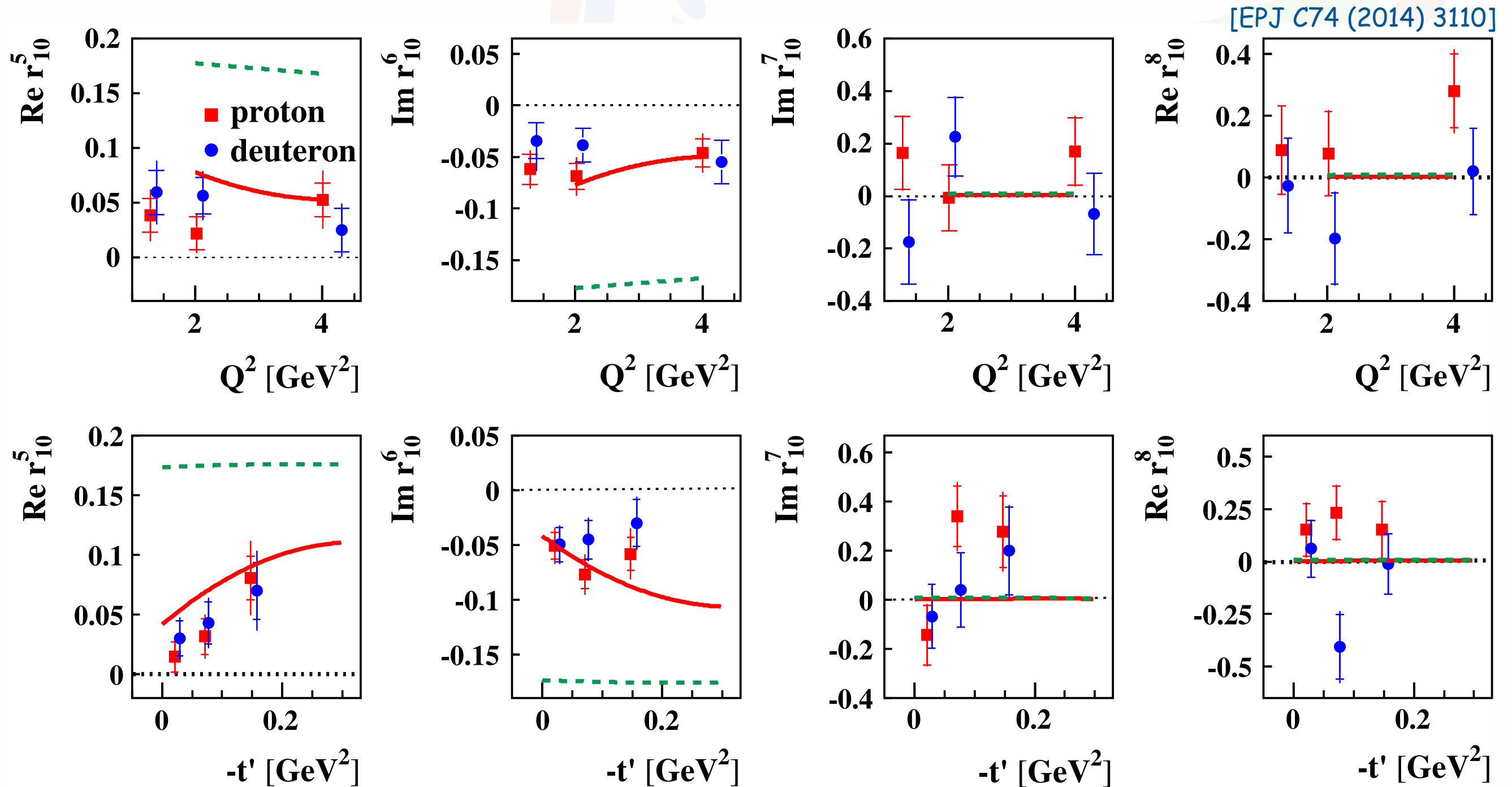
- "class-A" - helicity-conserving transitions





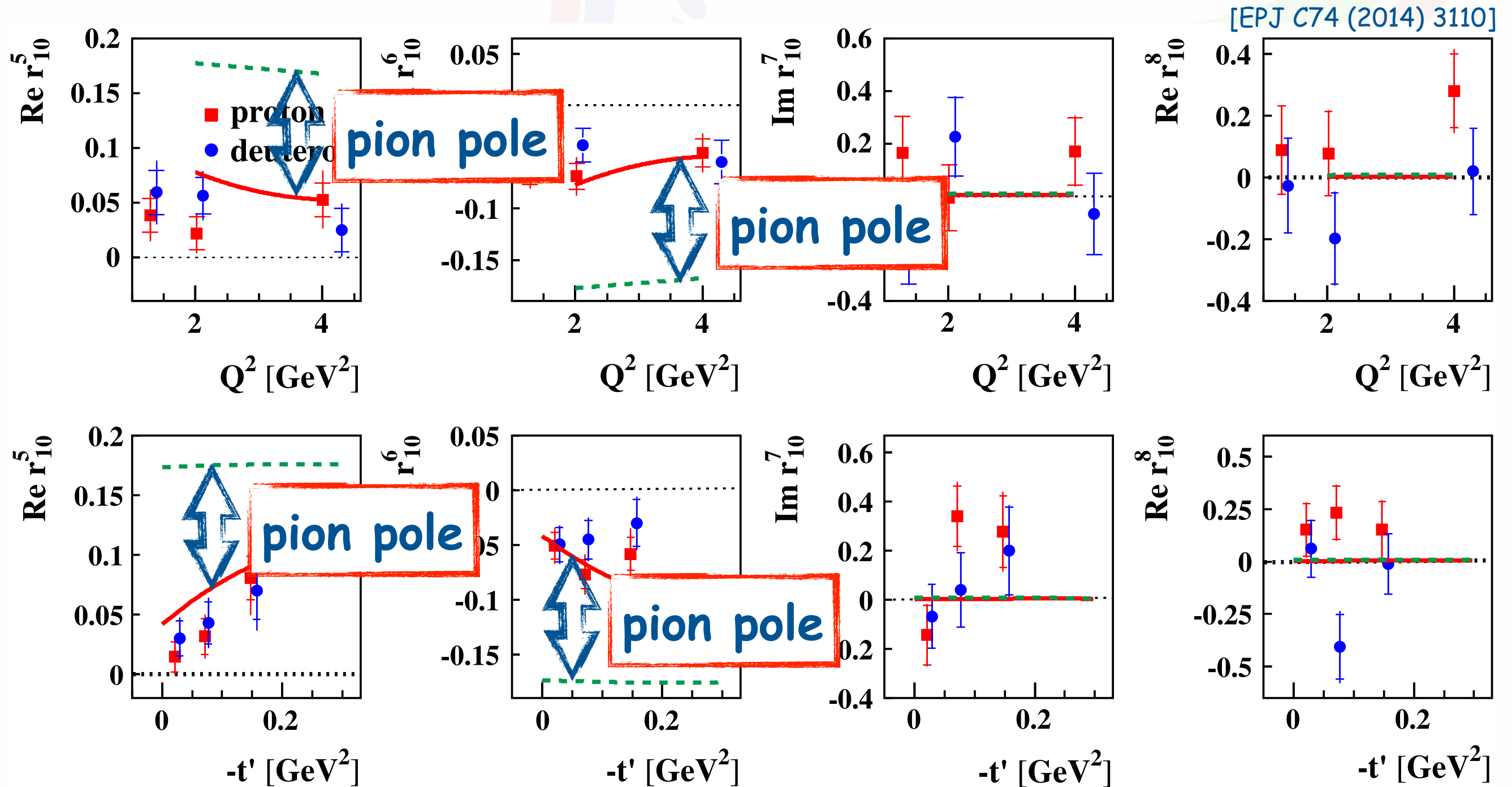
# impact of pion-pole contr. on SDMEs

- "class-B" - interference of helicity-conserving transitions



# impact of pion-pole contr. on SDMEs

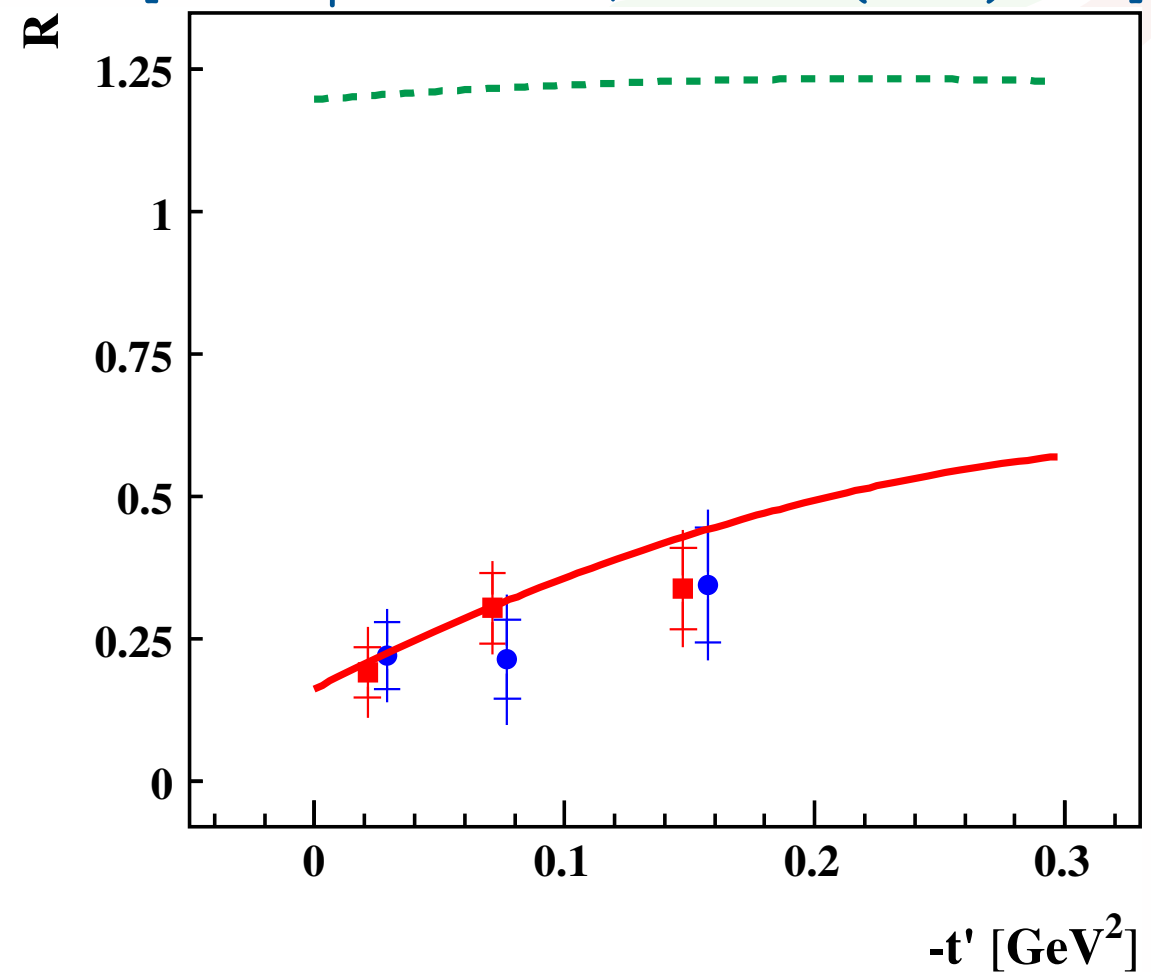
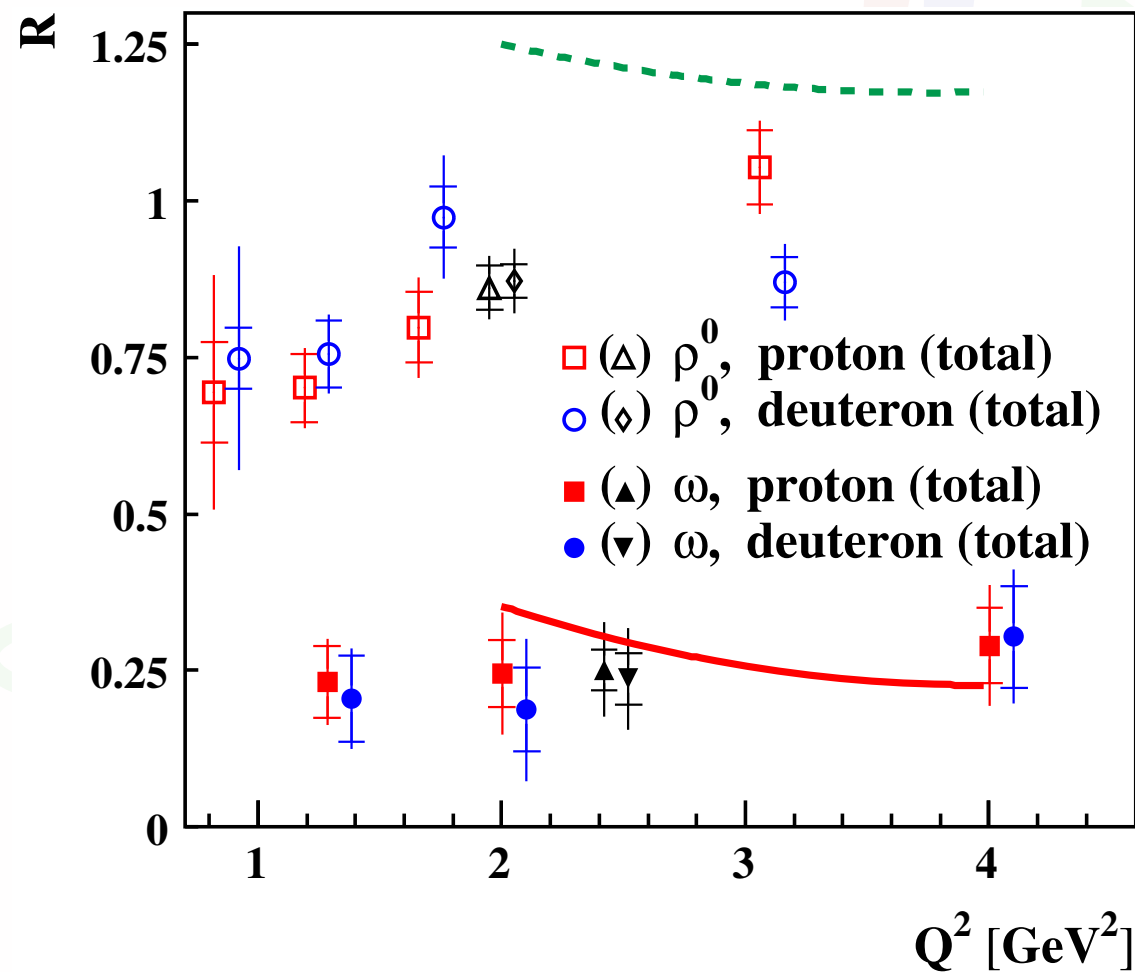
- "class-B" - interference of helicity-conserving transitions



# long.-to-transverse cross-section ratio

$$R = \frac{d\sigma(\gamma_L^* \rightarrow \omega)}{d\sigma(\gamma_T^* \rightarrow \omega)} \approx \frac{1}{\epsilon} \frac{r_{00}^{04}}{1 - r_{00}^{04}}$$

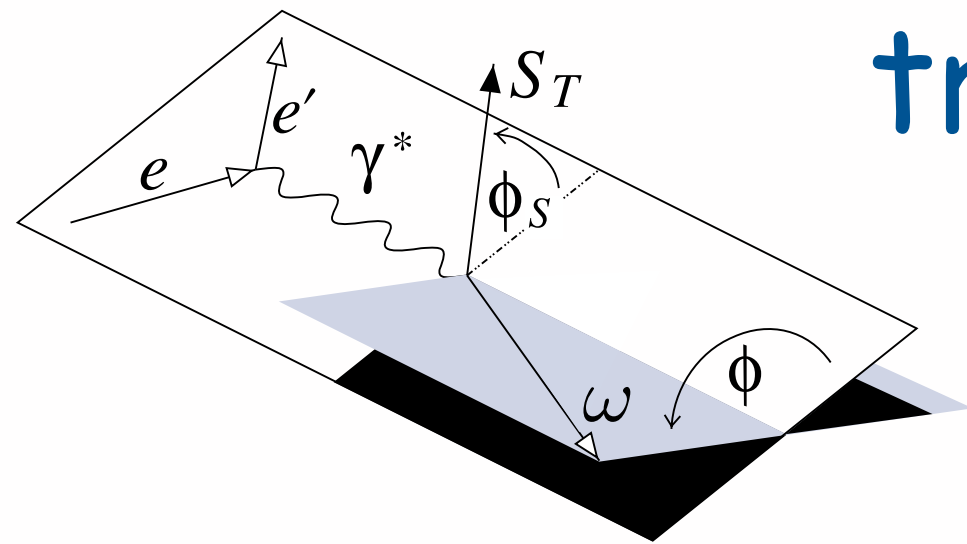
[A. Airapetian et al., EPJ C74 (2014) 3110]



- significantly smaller for  $\omega$  than for  $\rho$
- important contribution from pion pole

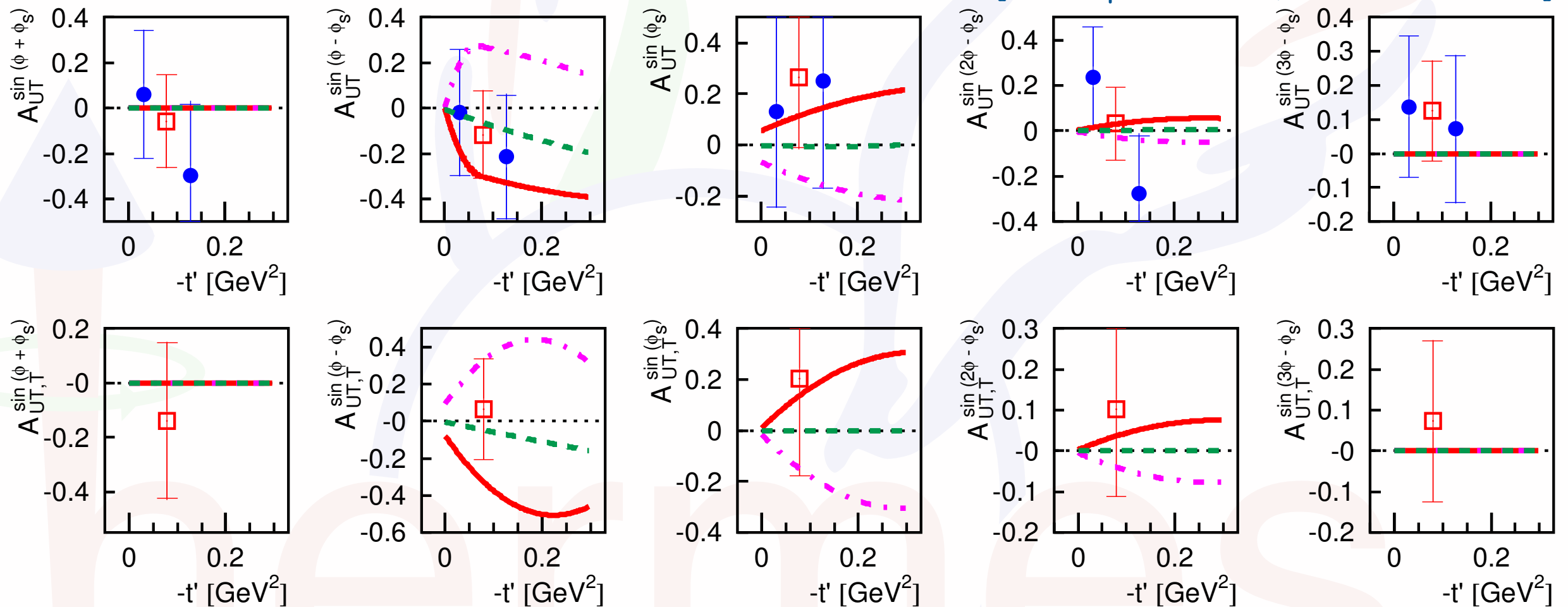
# transverse-spin asymmetry

sensitive, in principle, to sign of  $\pi\omega$  transition FF



[A. Airapetian et al., arXiv:1508.07612]

transverse  $\omega$



slight preference for positive  $\pi\omega$  transition FF (red/full line)  
vs. negative one (magenta/dash-dotted line)

summary

# DVCS @ HERMES

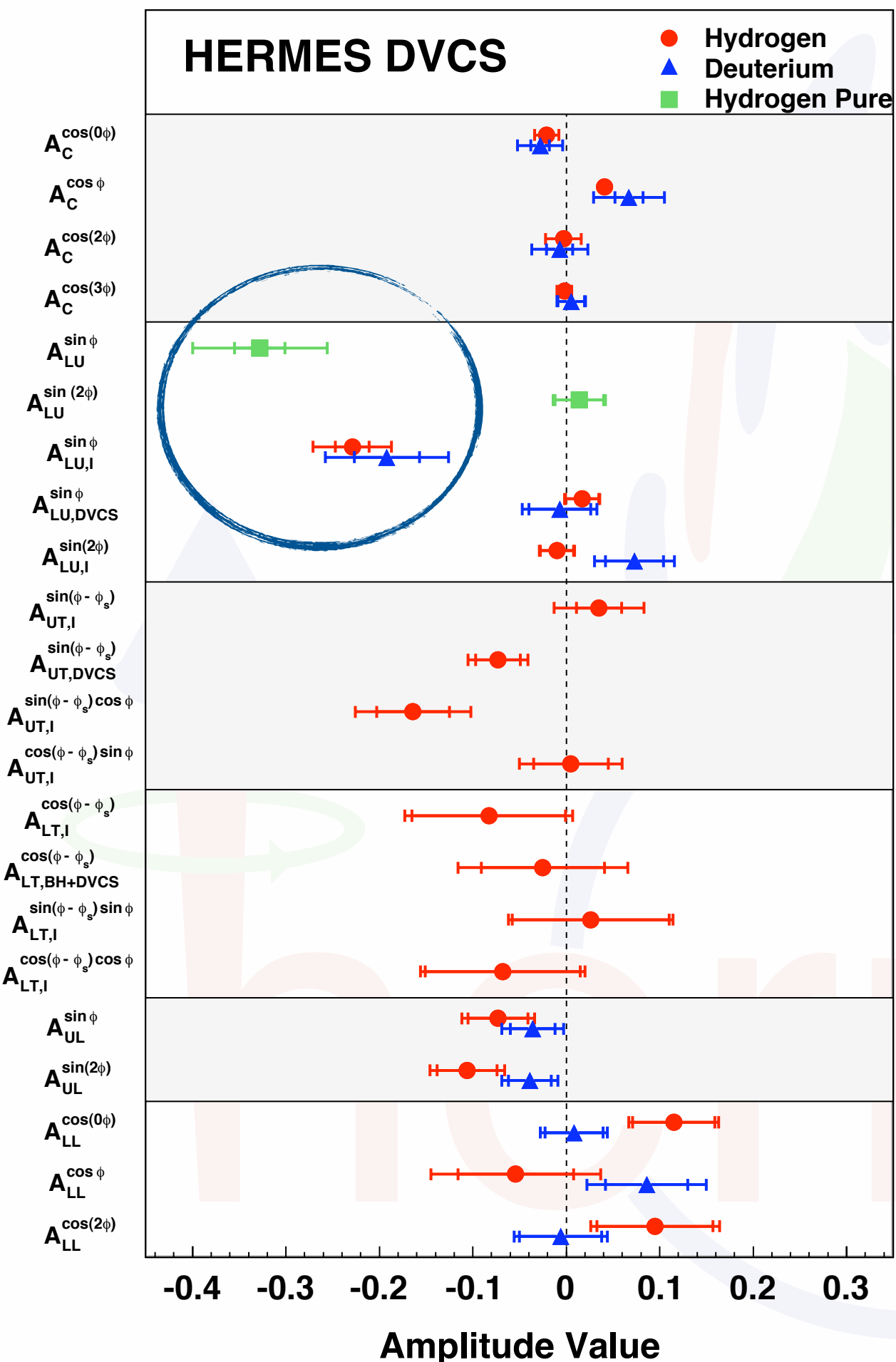
HERMES analyzed a wealth of DVCS-related asymmetries on nucleon and nuclear targets

data with recoil-proton detection allows clean interpretation

indication of larger amplitudes for pure sample

-> assoc. DVCS in "traditional" analysis mainly dilution, supported by recent results from HERMES  
[JHEP 01 (2014) 077]:

assoc. DVCS results consistent with zero but also with model prediction

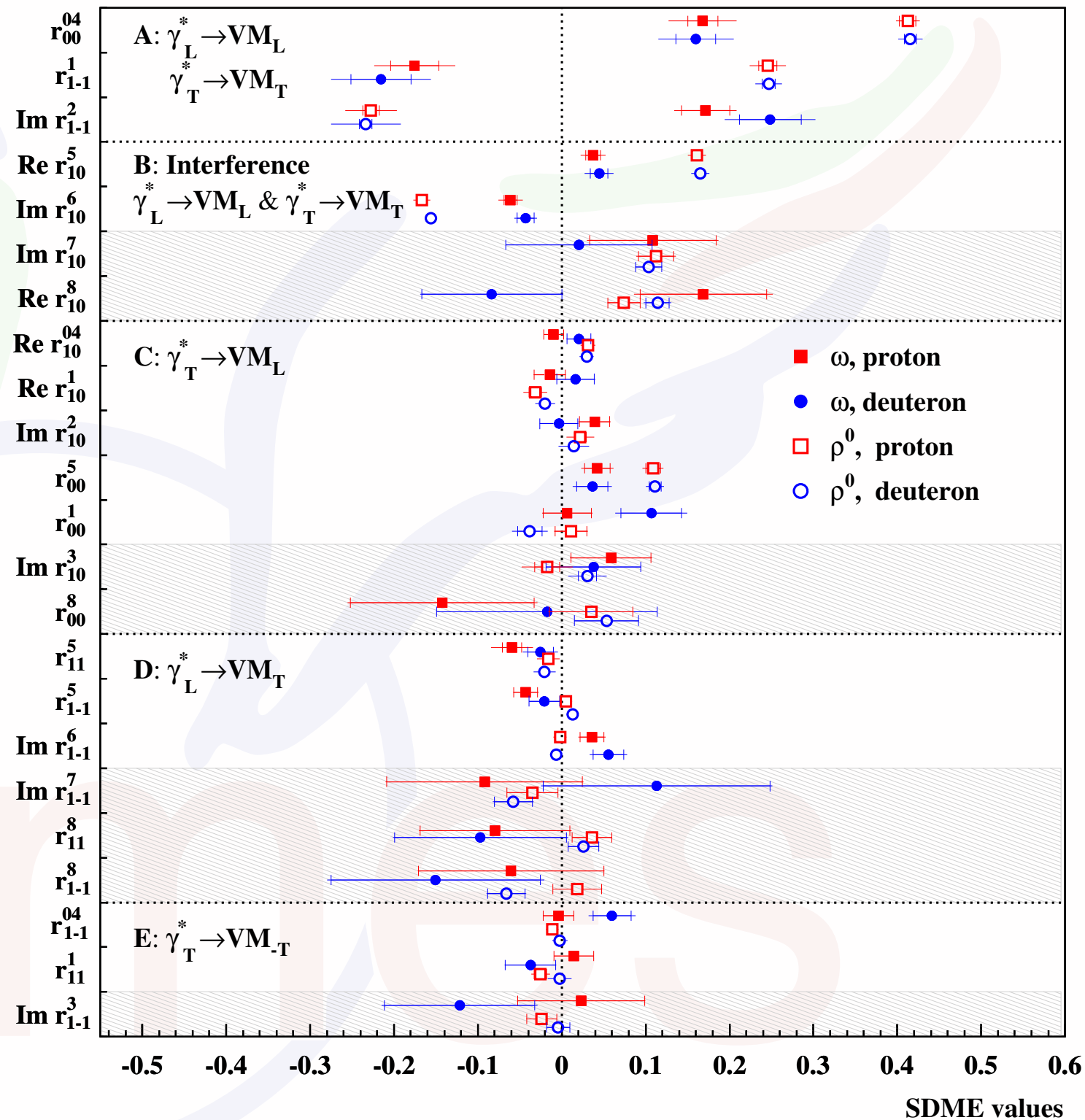




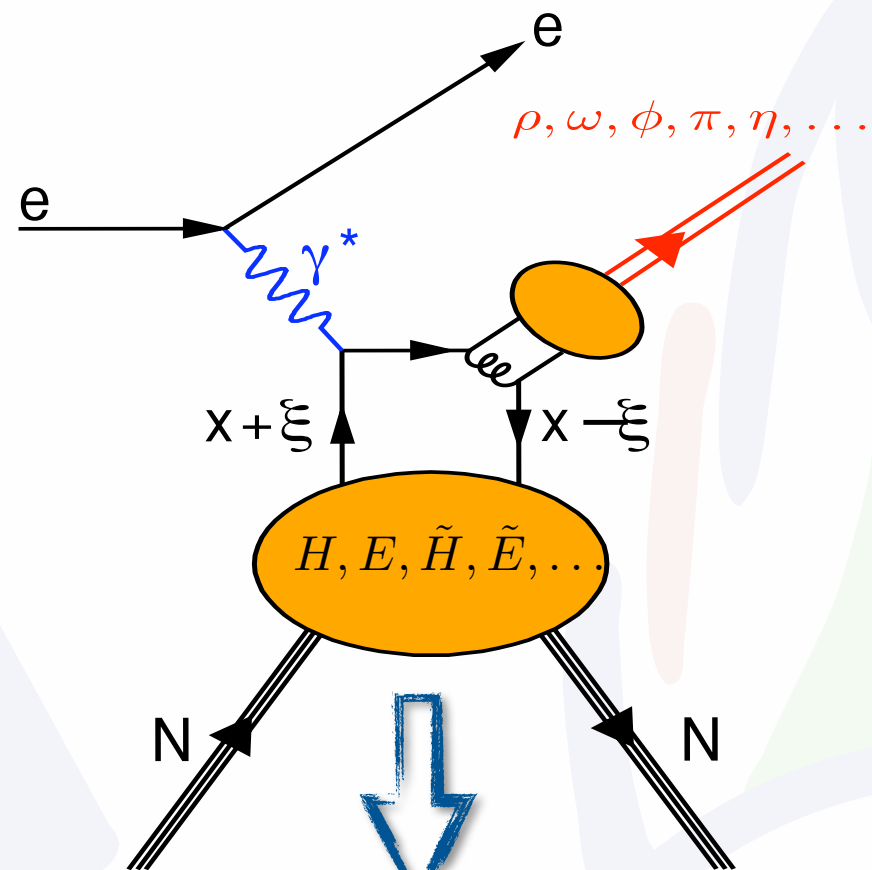
# HEMP @ HERMES

- extensive data set on unpolarized and polarized SDMEs in vector-meson production
- (not shown:) cross section and  $A_{UT}$  for excl.  $\pi^+$
- essential input in model building
- recent results on omega production require pion-pole contributions with a preference for positive  $\pi\omega$  transition FF

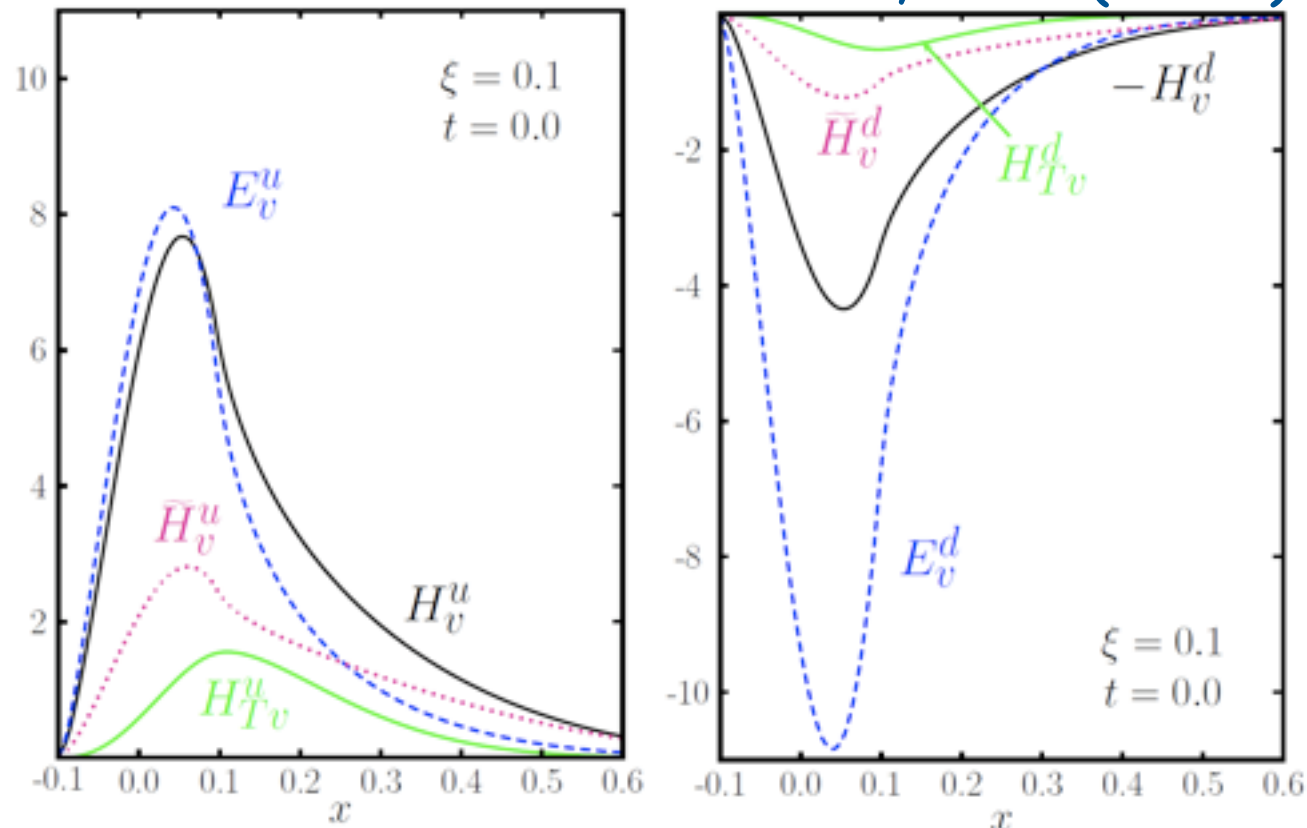
[A. Airapetian et al., EPJ C74 (2014) 3110, EPJ C62 (2009) 659]



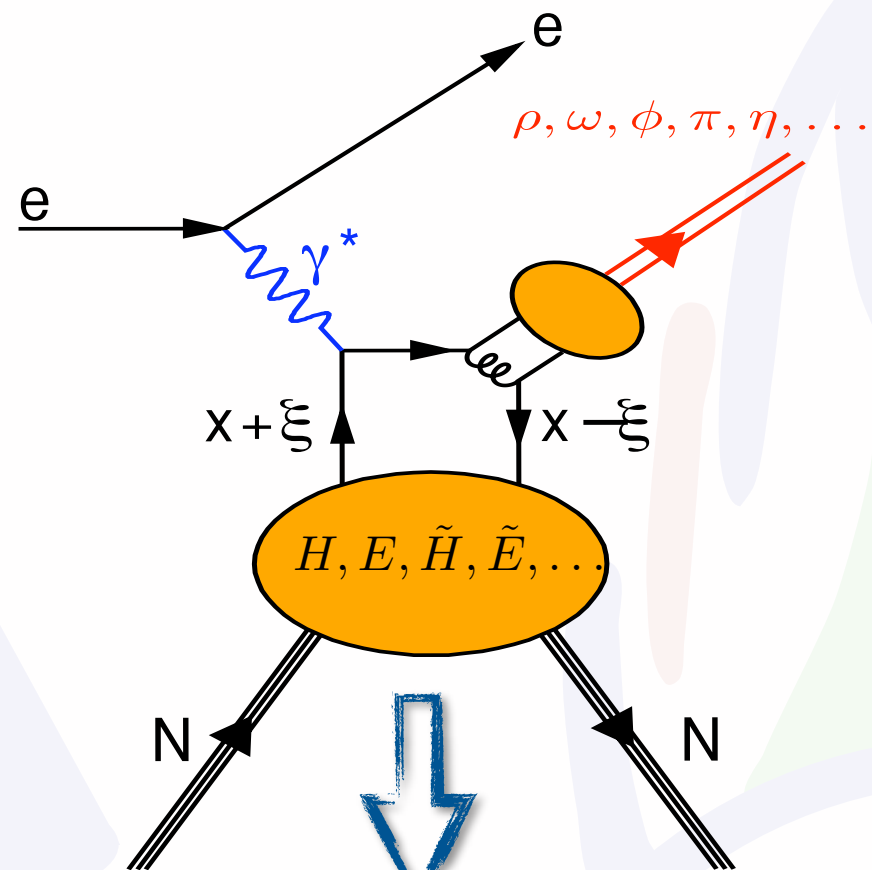
# GPDs - a nice success story!



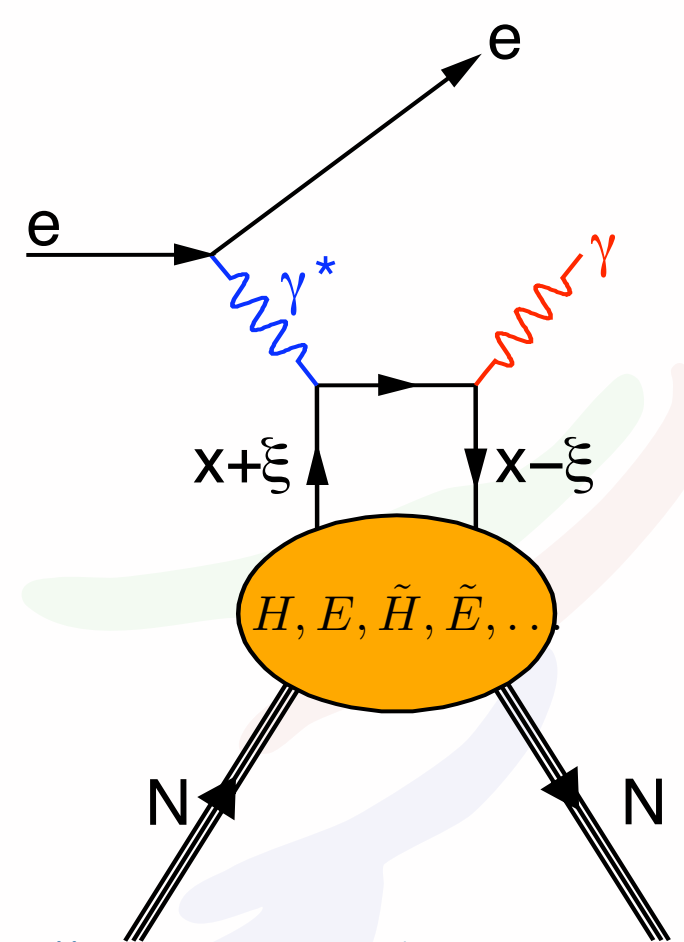
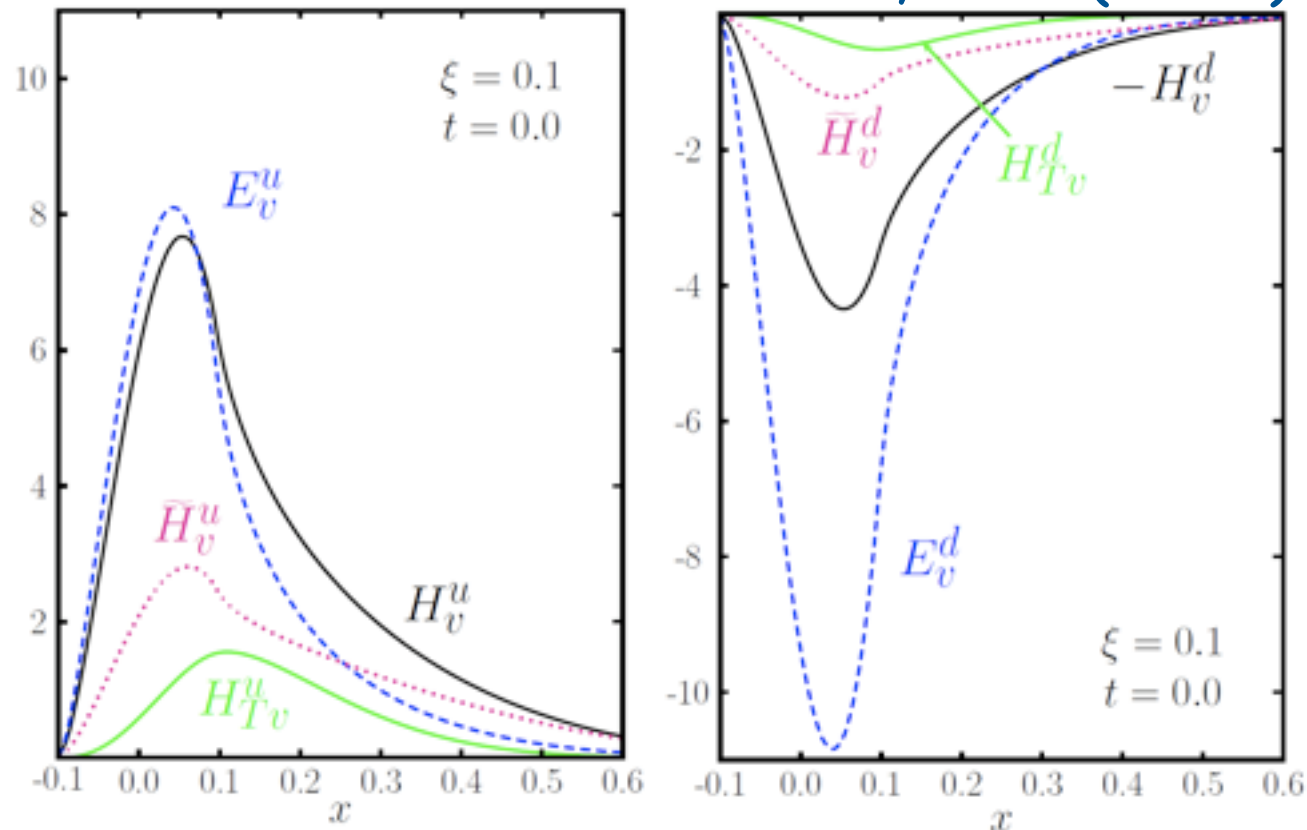
Goloskokov, Kroll (2007)



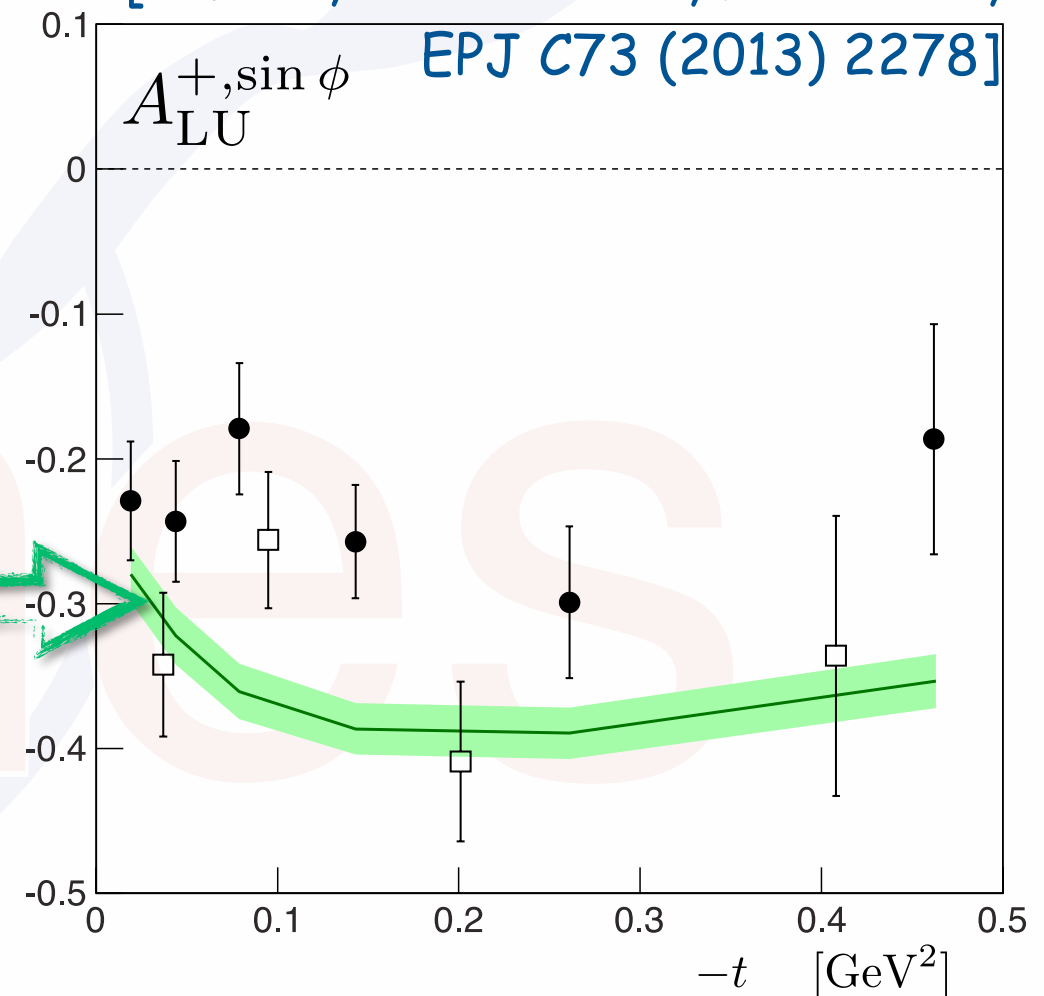
# GPDs - a nice success story!



Goloskokov, Kroll (2007)

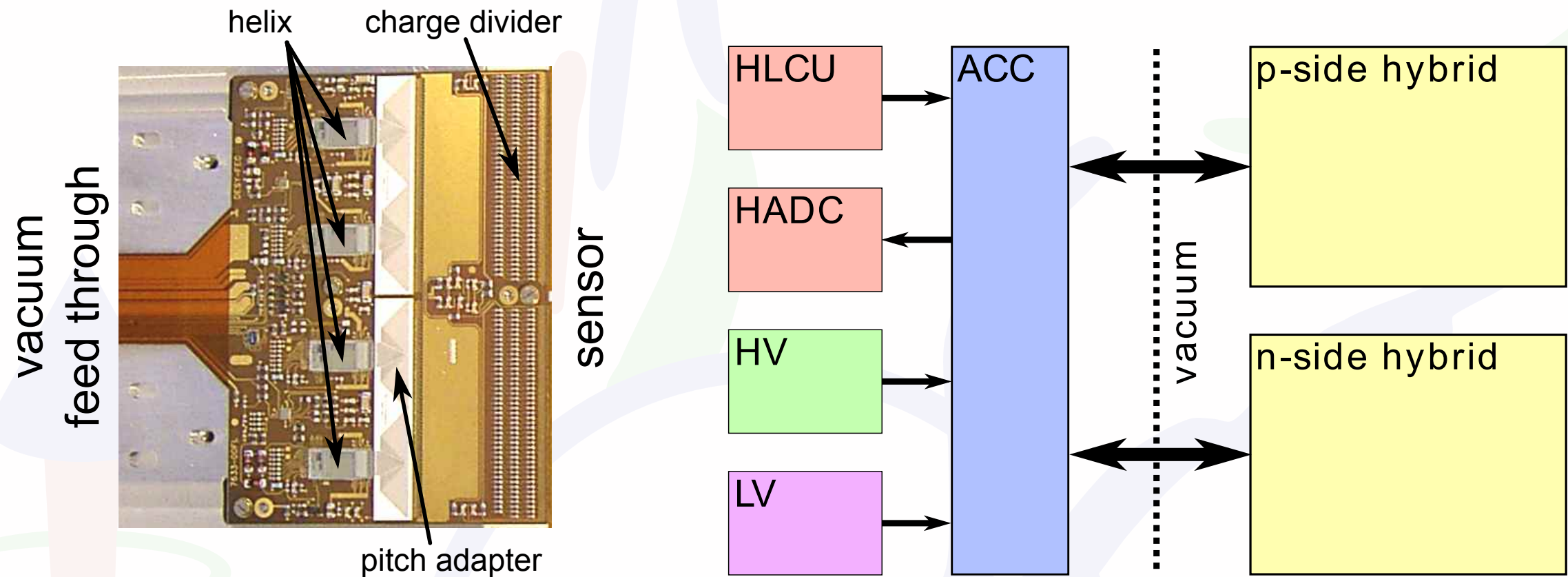


[P. Kroll, H. Moutarde, F. Sabatie, EPJ C73 (2013) 2278]



backup

# SSD (silicon strip detector)



5.8 cm away from lepton beam, 1.5 cm gap

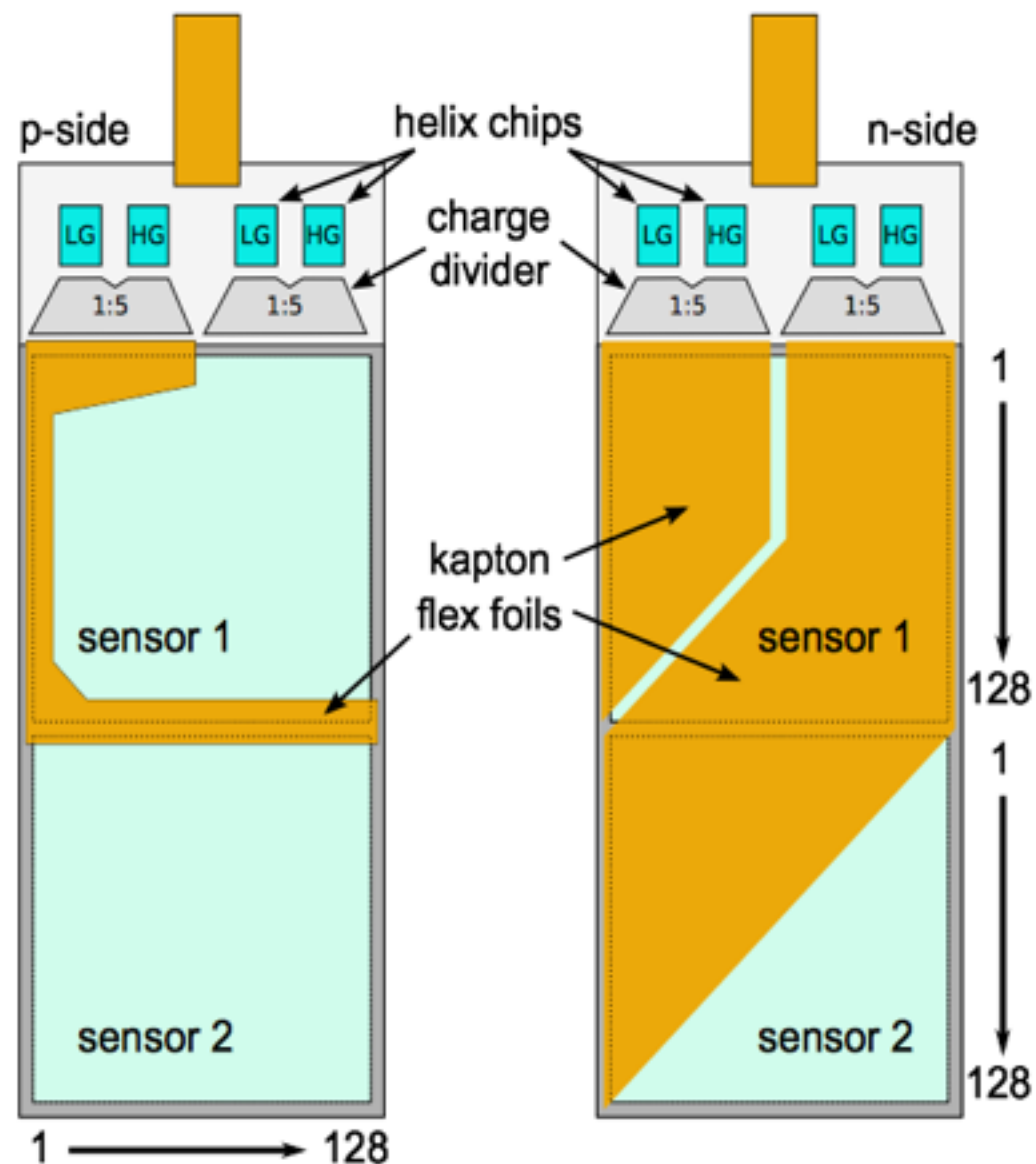
sensor thickness  $295\ \mu\text{m}$  -  $315\ \mu\text{m}$

thickness of target cell  $75\ \mu\text{m}$

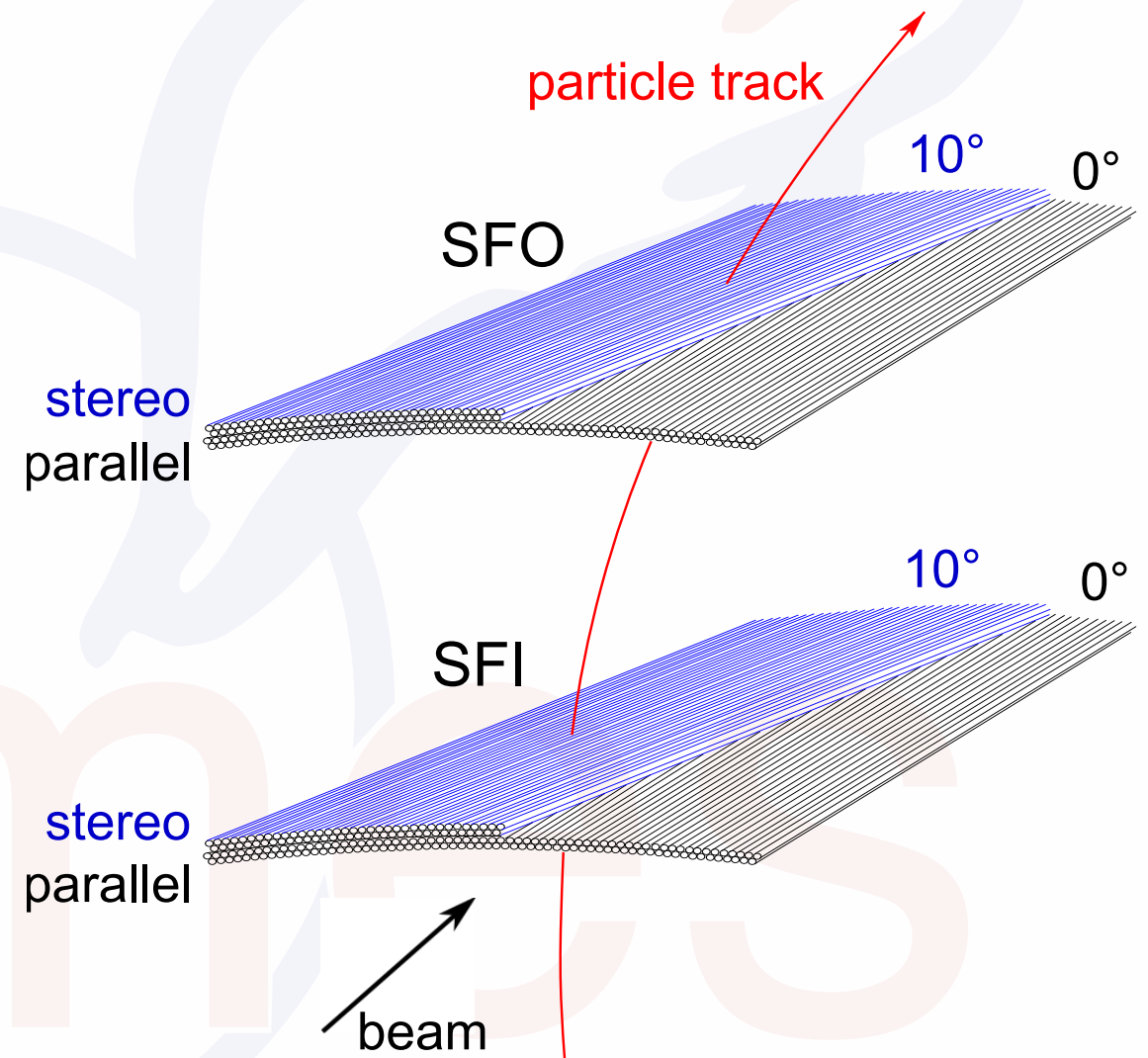


# The HERMES recoil detector

Sketch of front- and backside of a silicon strip detector module (SSD)



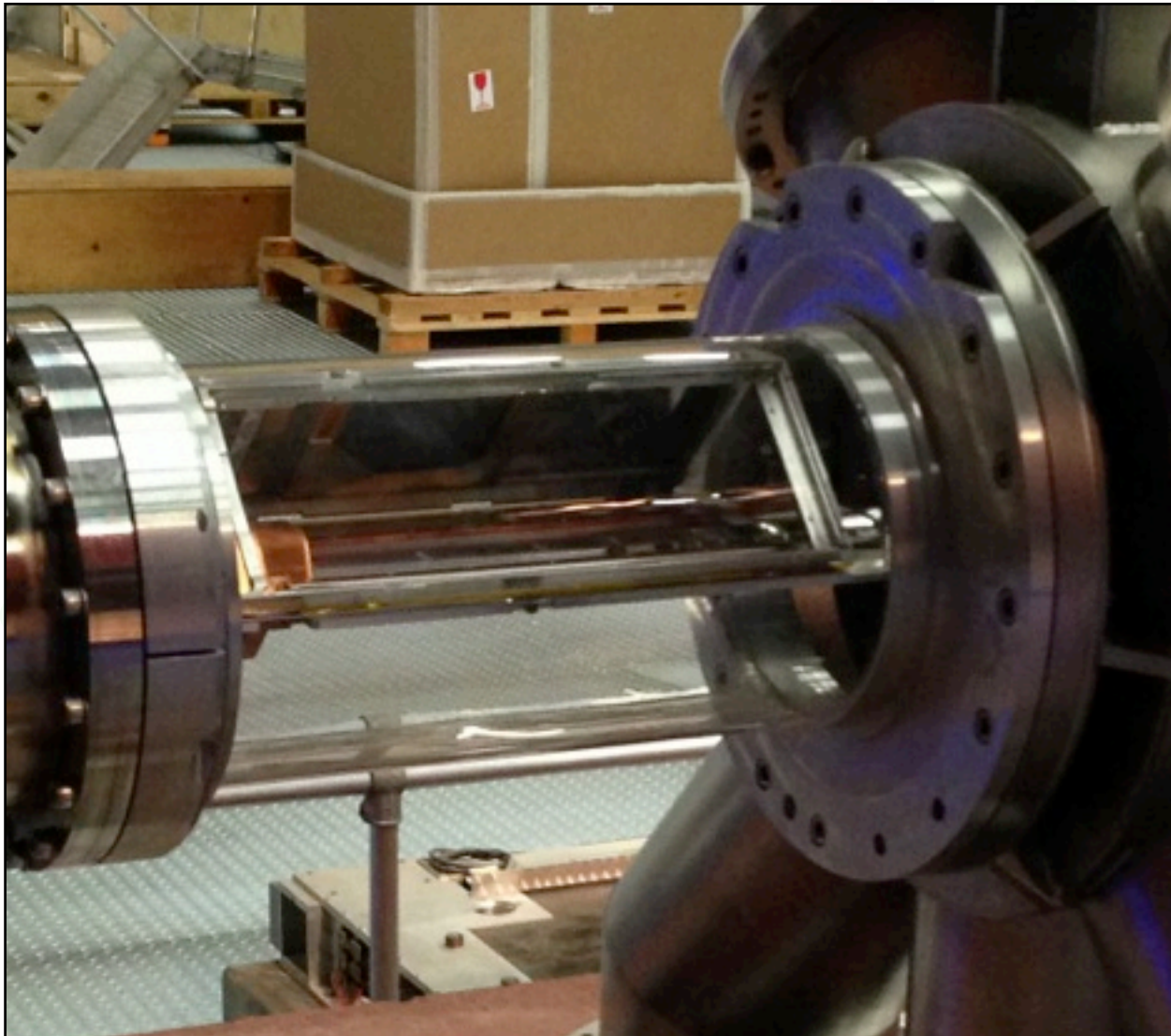
Schematic design of the scintillating fibre tracker (SFT)



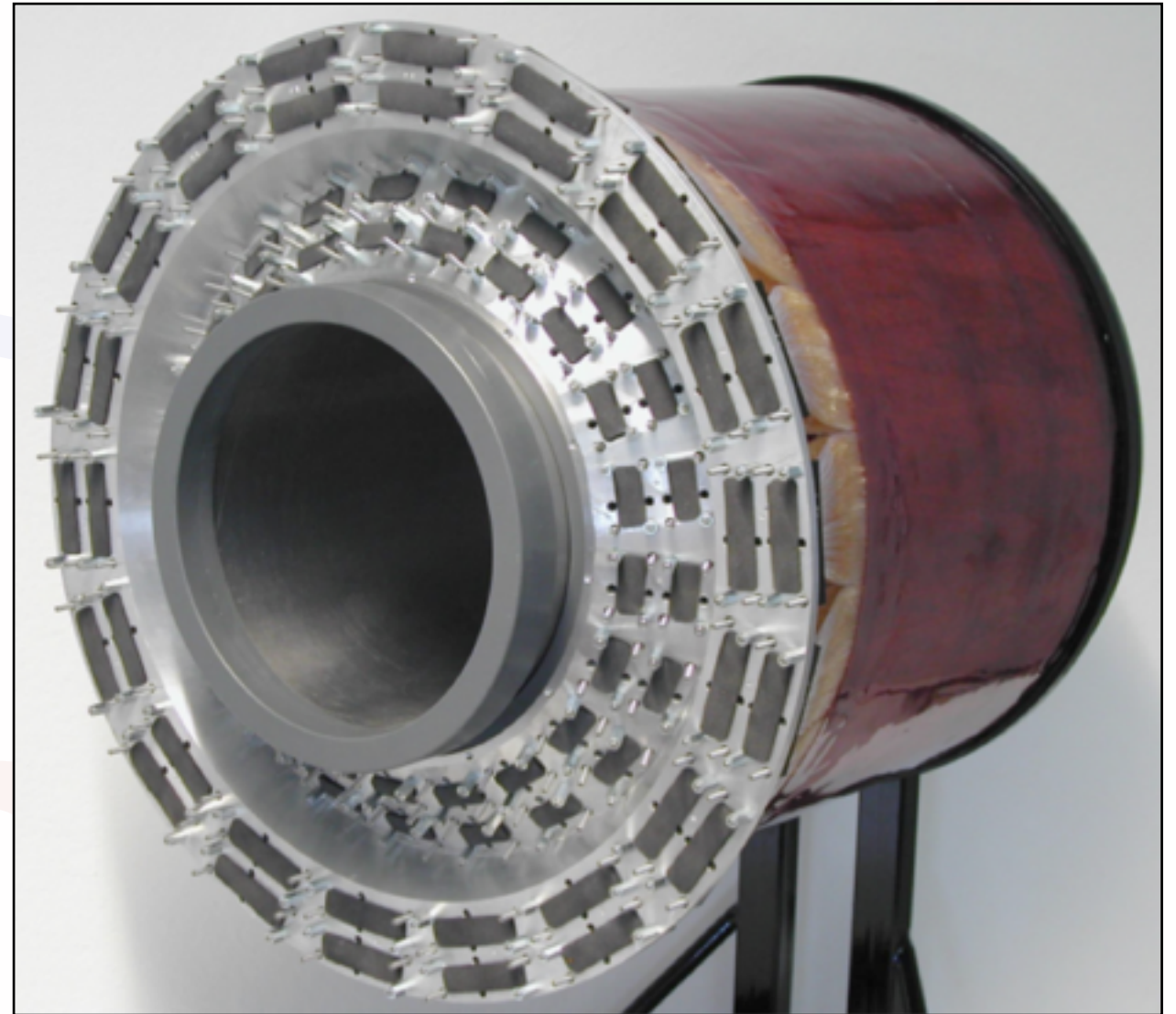


# The HERMES recoil detector

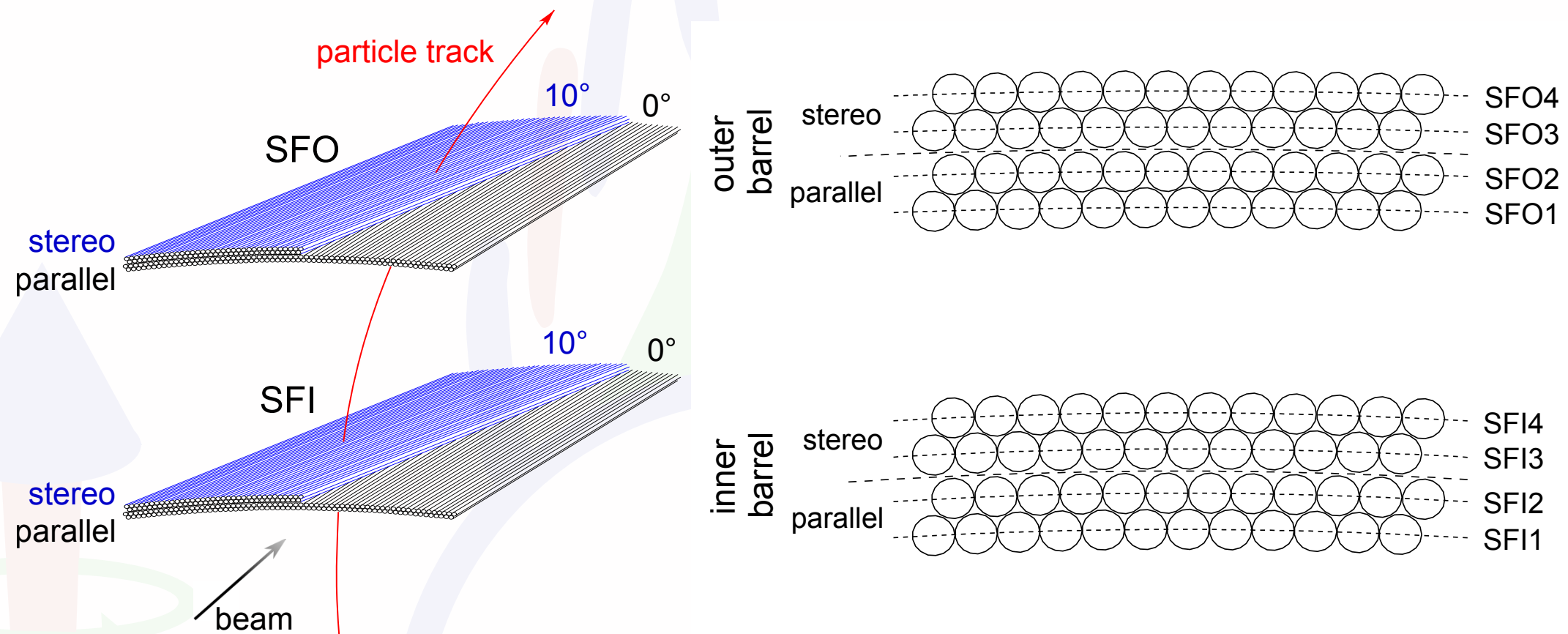
The silicon strip detector (SSD)



The scintillating fibre tracker (SFT)



# SFT (scintillating fibre tracker)

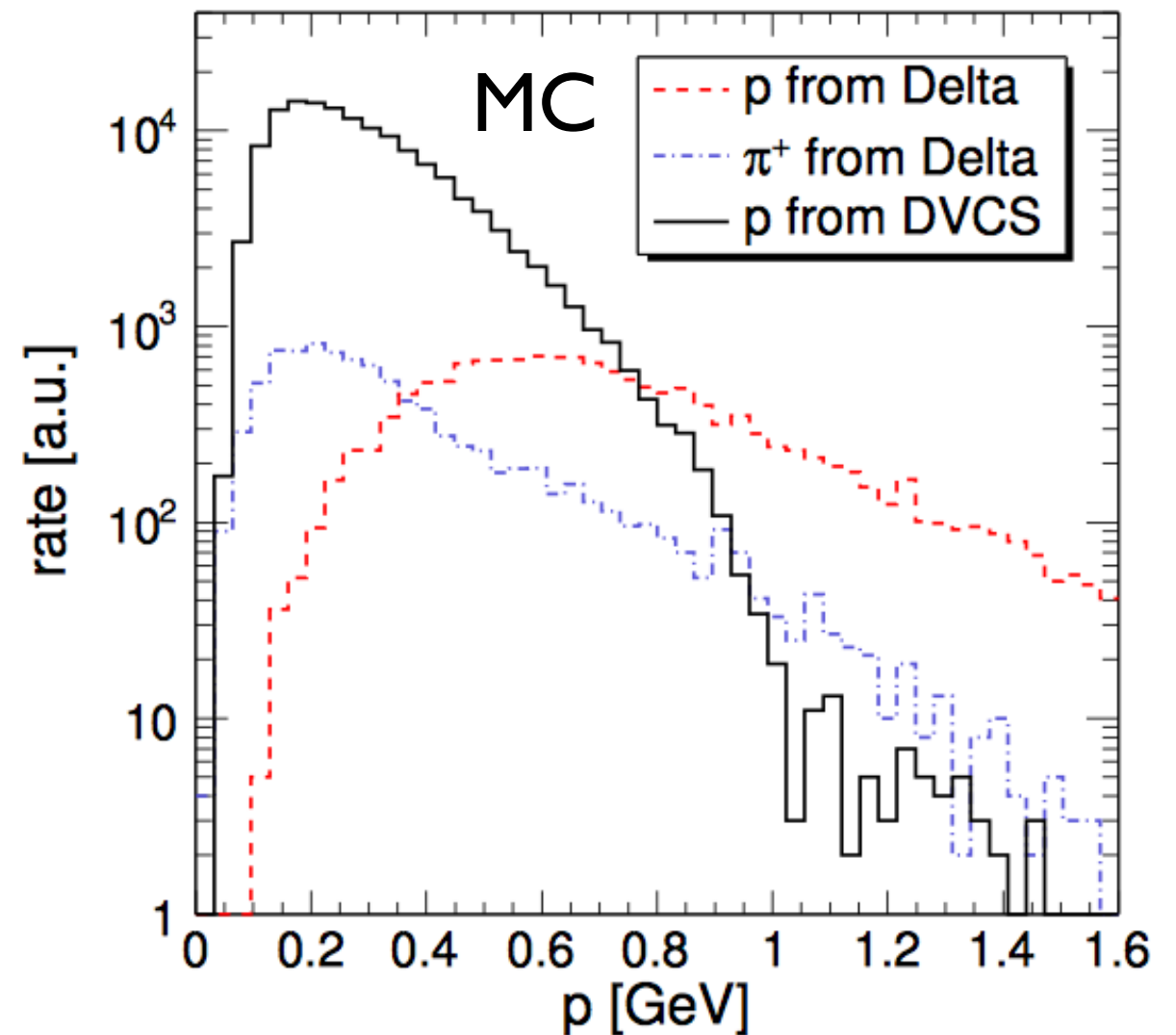
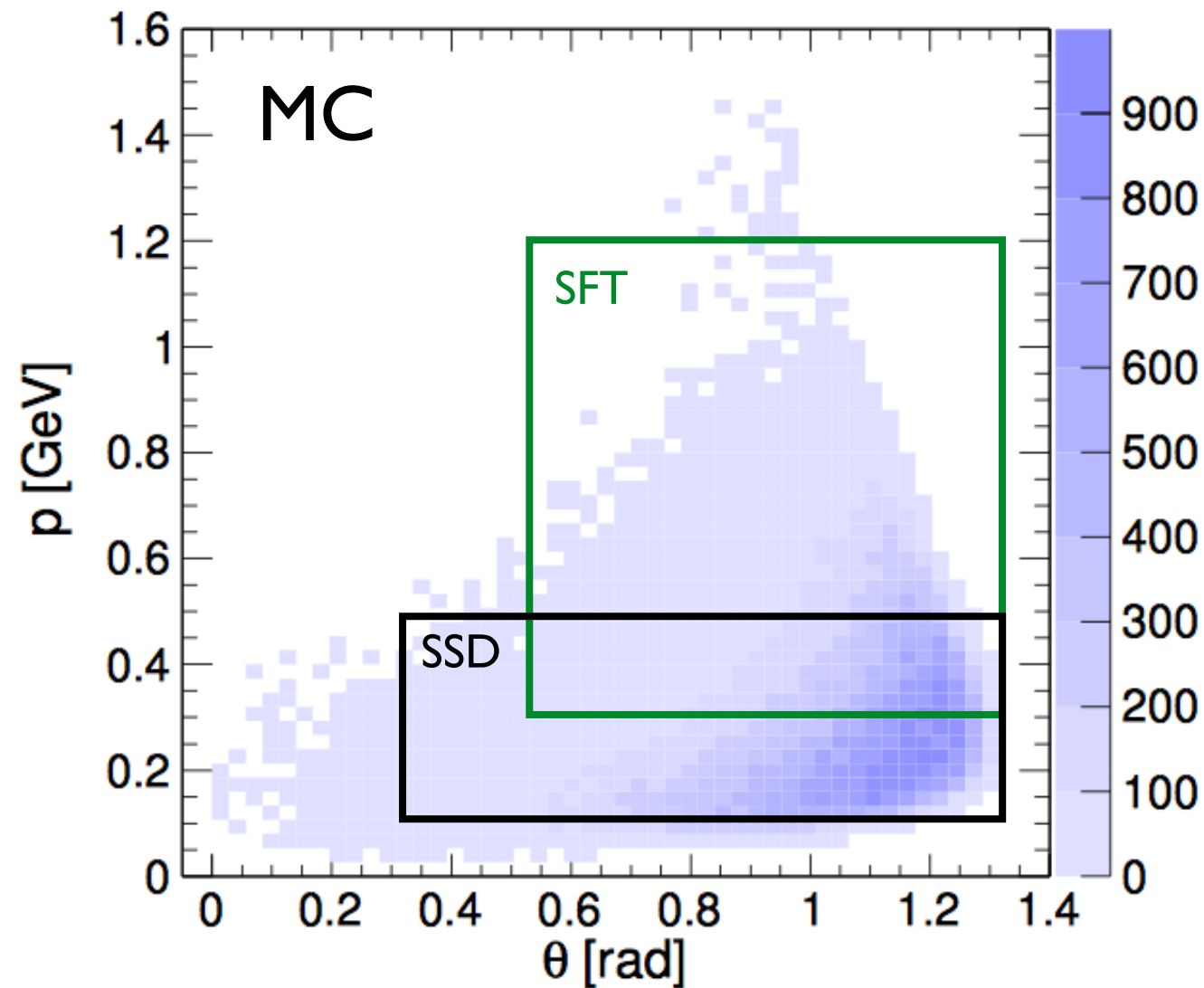


11.5 cm (18.5 cm) inner (outer) radius

1318+1320 (2198+2180) fibers with a diameter of 1 mm each

readout by 64-channel Hamamatsu H7546B MAPMTs

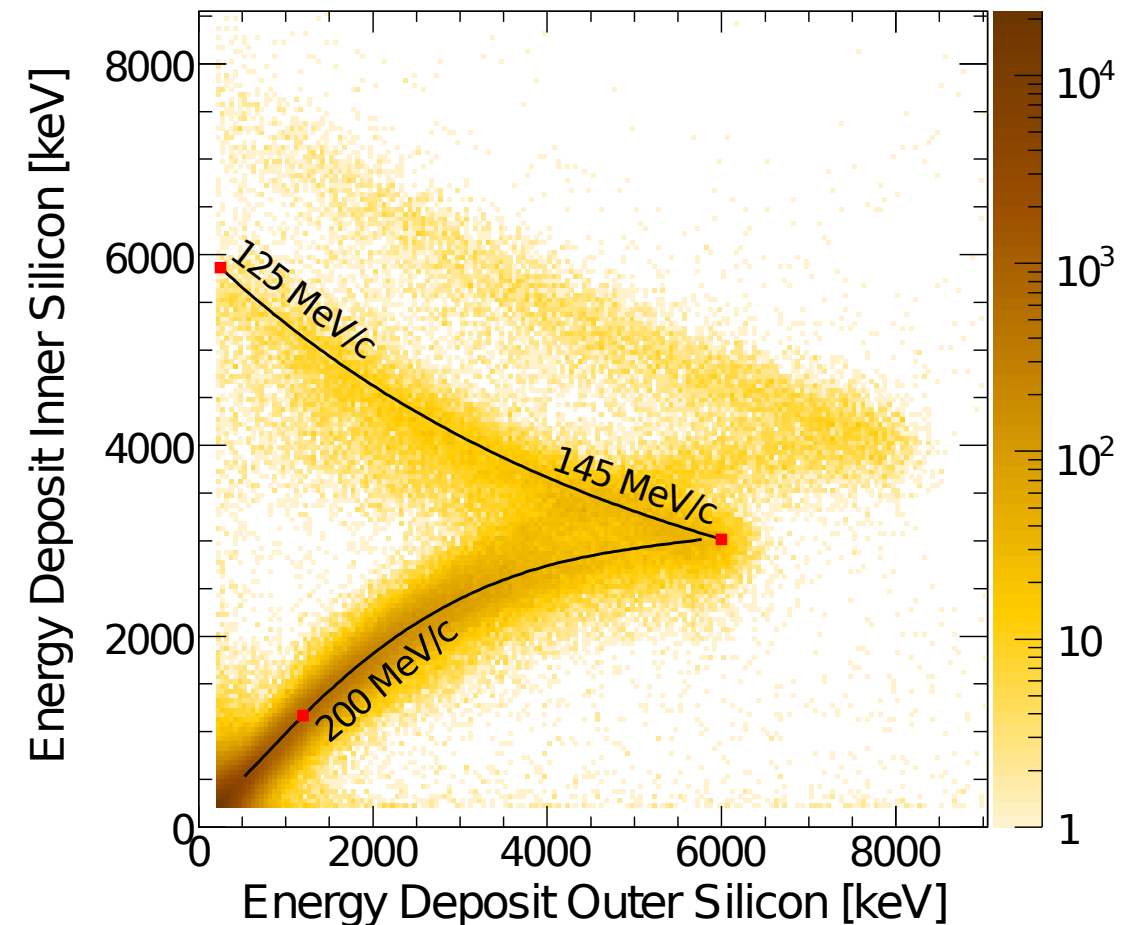
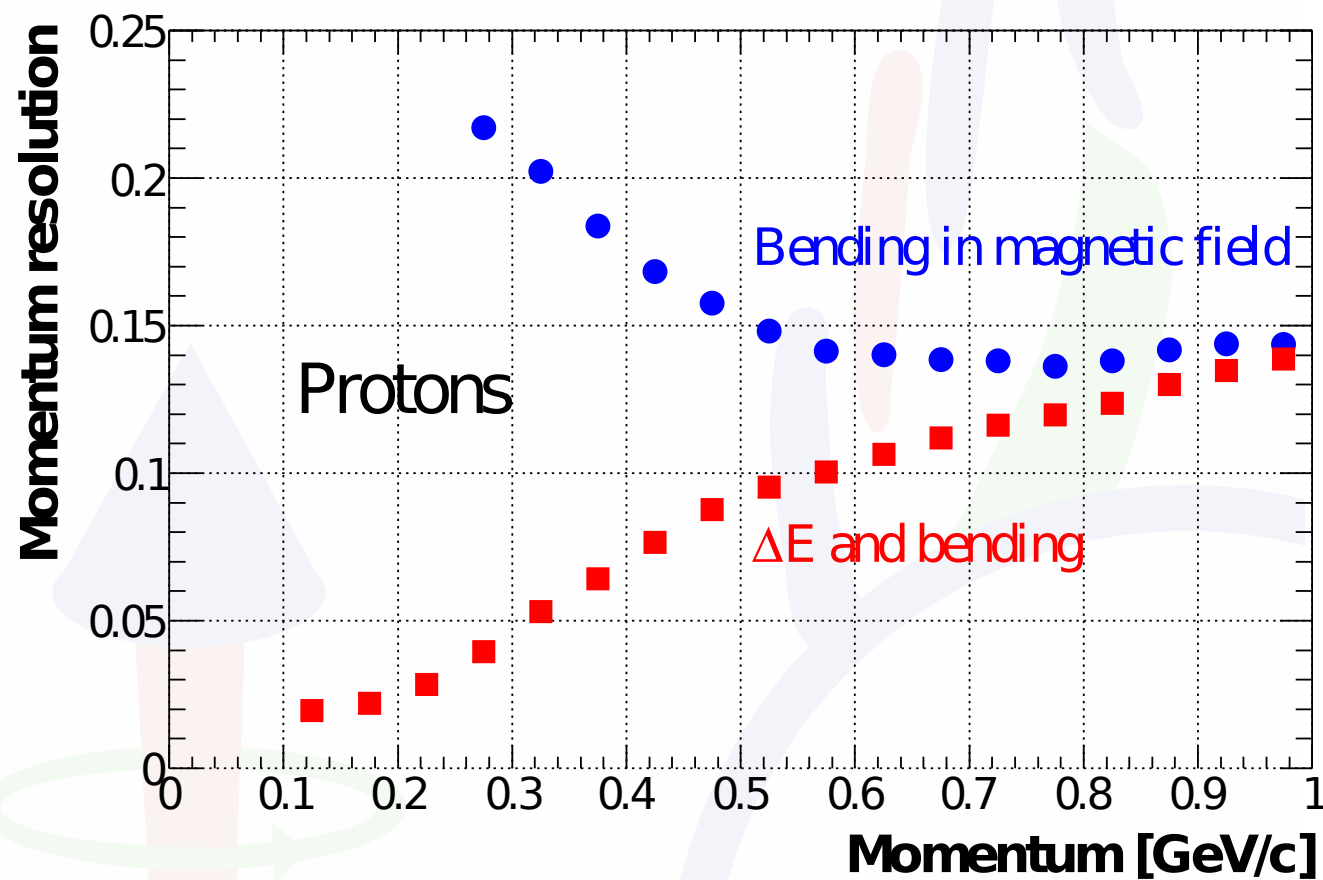
# Kinematic coverage of the HERMES RD



Scintillating fibre tracker (SFT) and silicon strip detector (SSD) complement each other

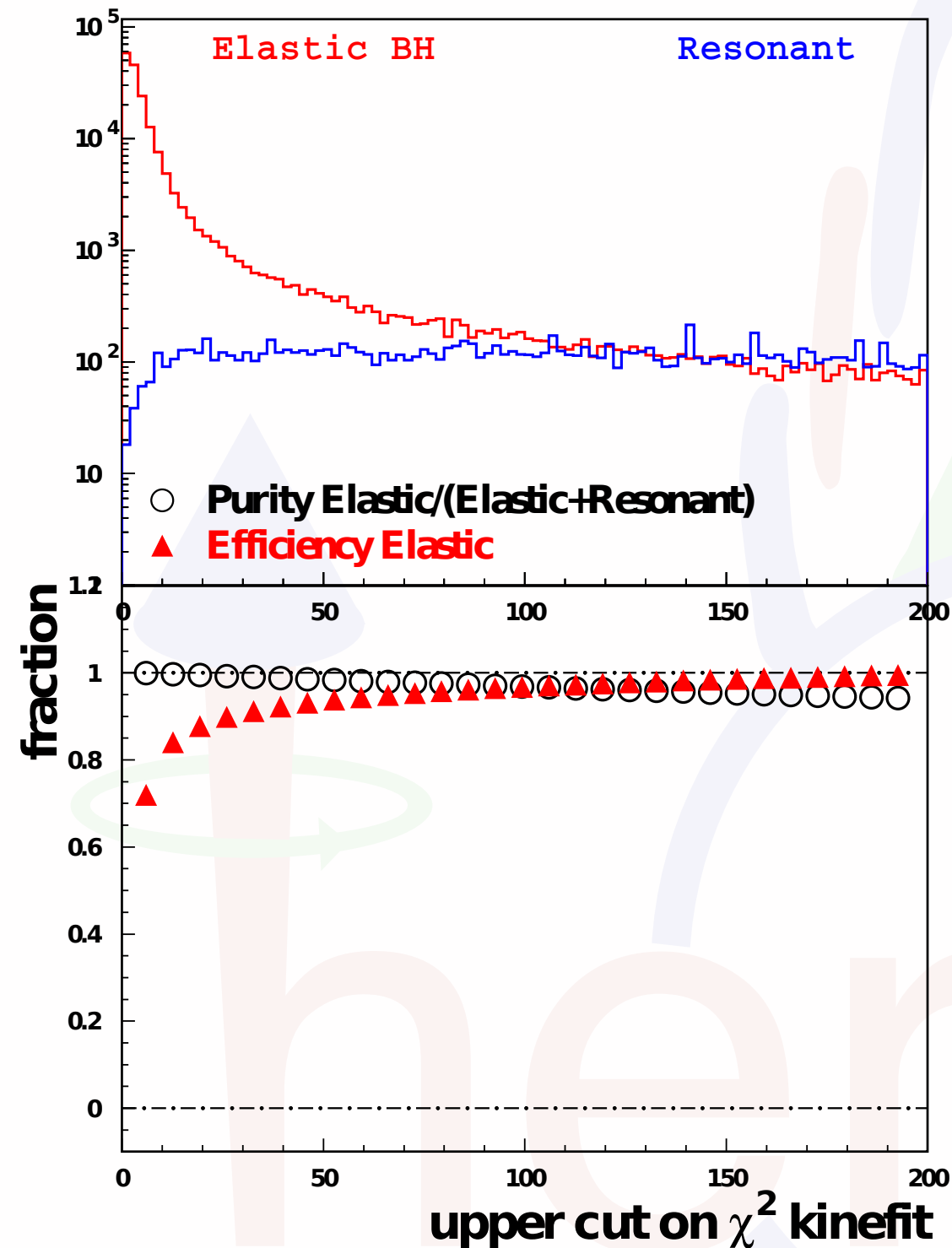


# Recoil-detector tracking



taking energy loss into account improves momentum resolution for low p  
azimuthal-angle resolution: 4 mrad  
polar-angle resolution: 10 mrad (for  $p > 0.5$  GeV)

# Kinematic event fitting

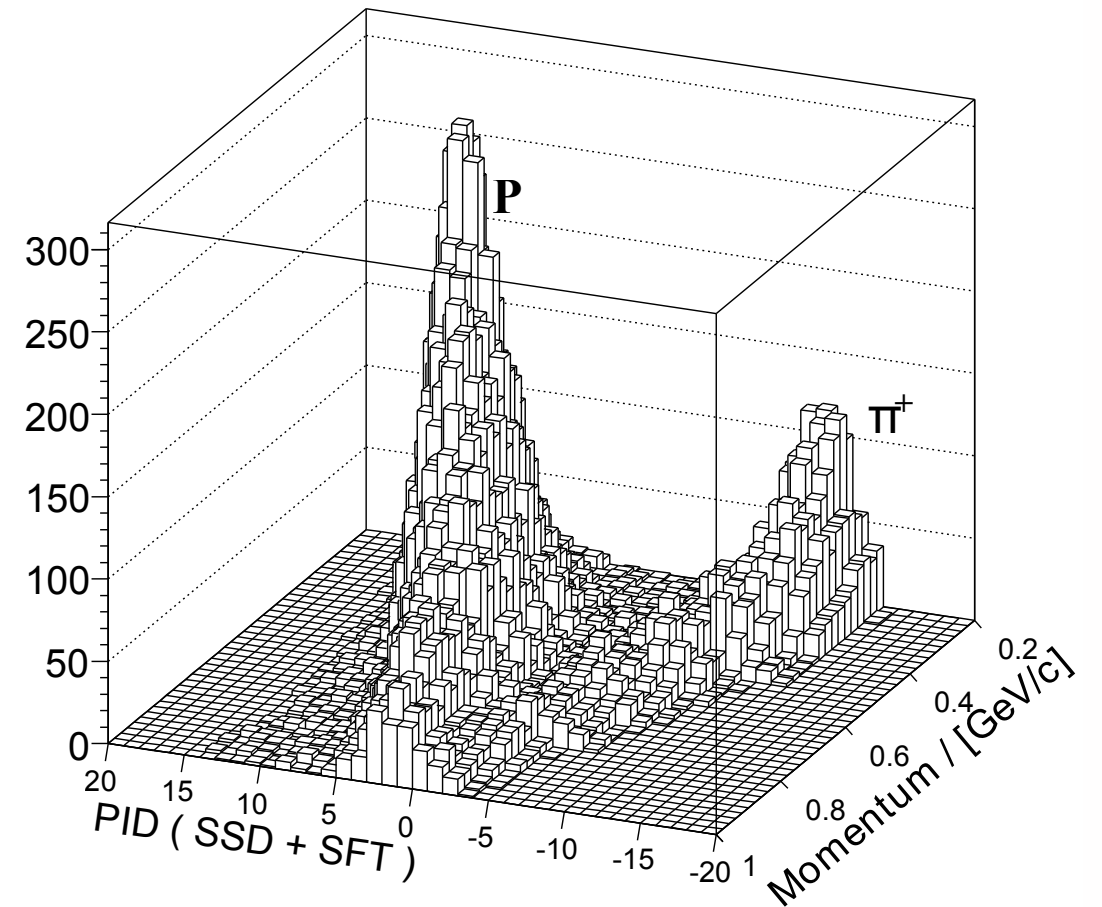
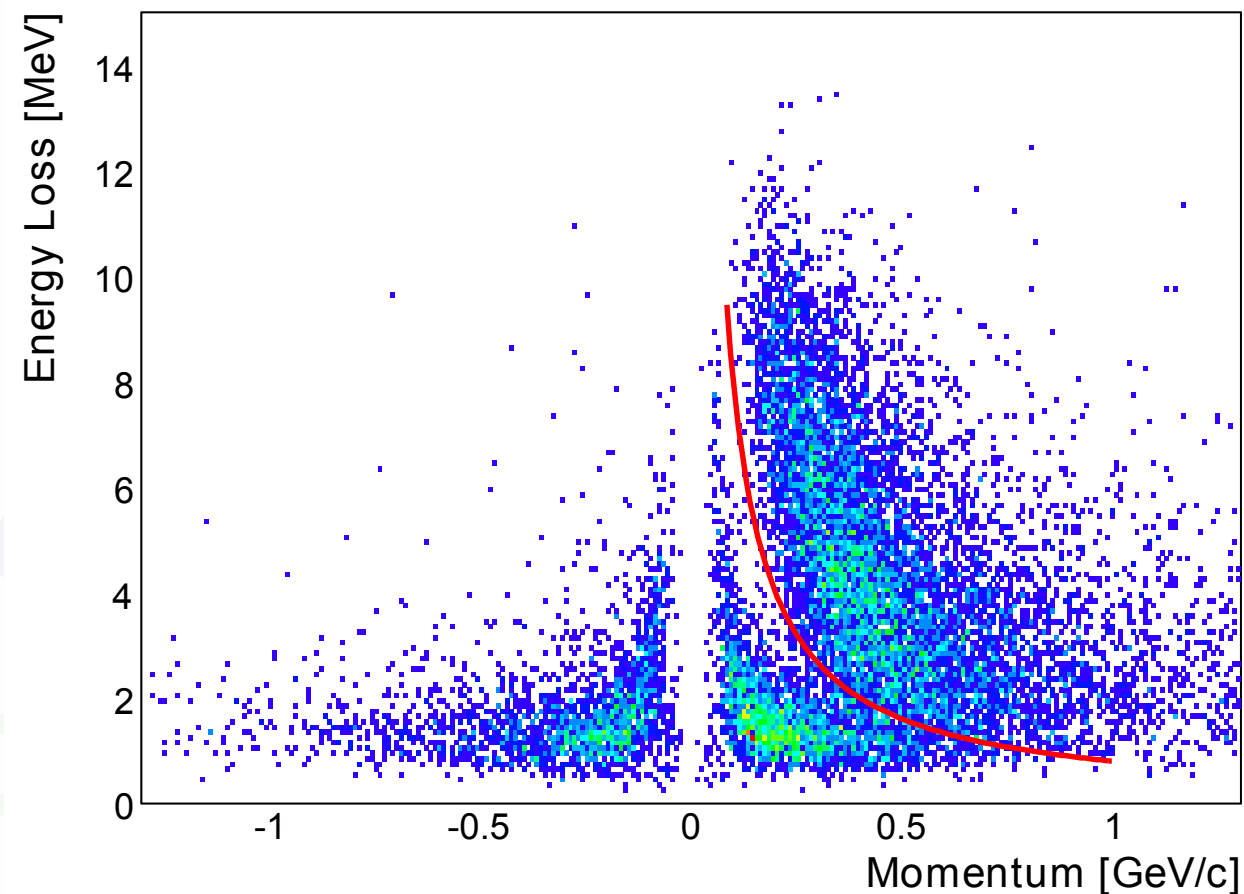


$$\chi_{pen}^2 = \sum_{i=1}^9 \frac{(r_i^{fit} - r_i^{meas})^2}{\sigma_i^2} + T \cdot \sum_{j=1}^4 \frac{[f_j(r_1^{fit}, \dots, r_9^{fit})]^2}{(\sigma_j^f)^2}$$

$\chi^2$ -value of interest penalty term constraints

- 4-momentum conservation as constraints
- lowest  $\chi^2$ -value in case of multiple recoil tracks per event
- minimum of 1 % fit probability required, which corresponds to  $\chi^2 < 13.7$

# Recoil PID

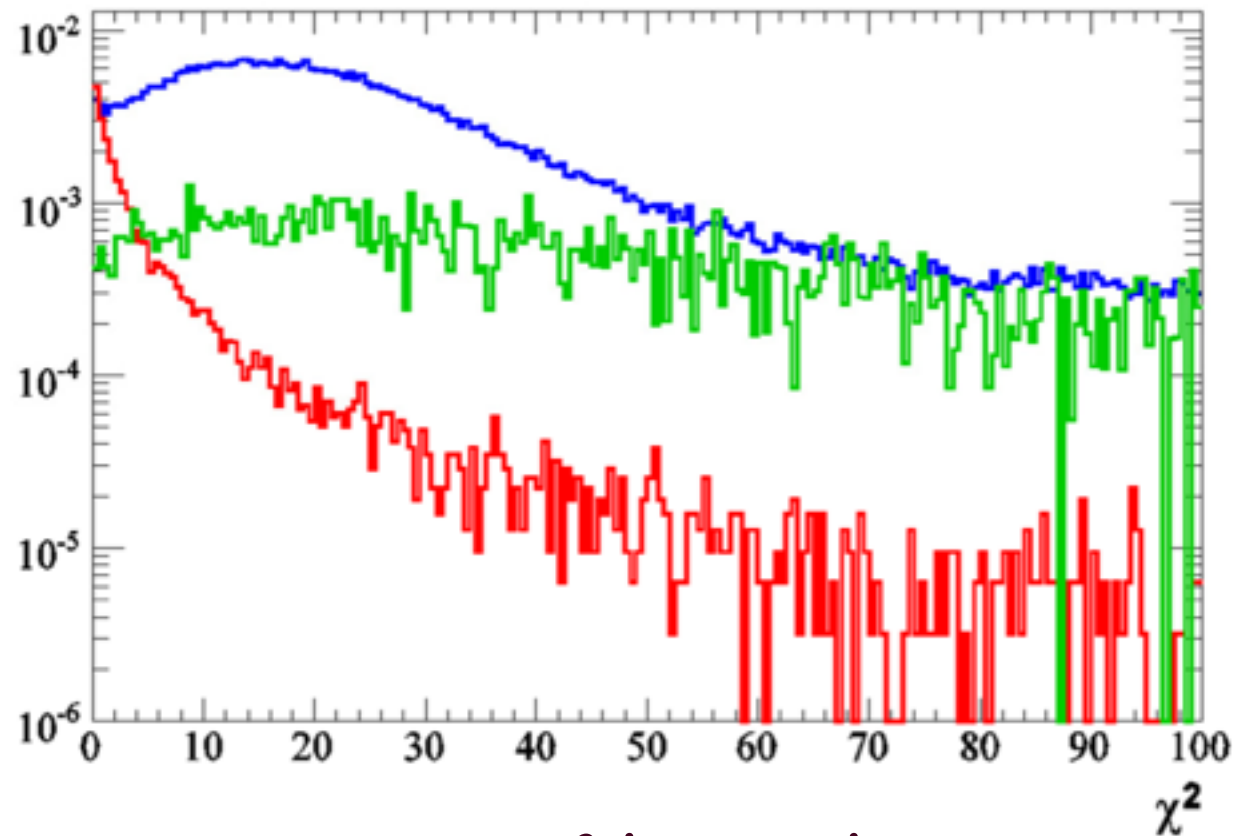


discrimination between protons and positively charged pions  
parent distributions were crucial and determined experimentally



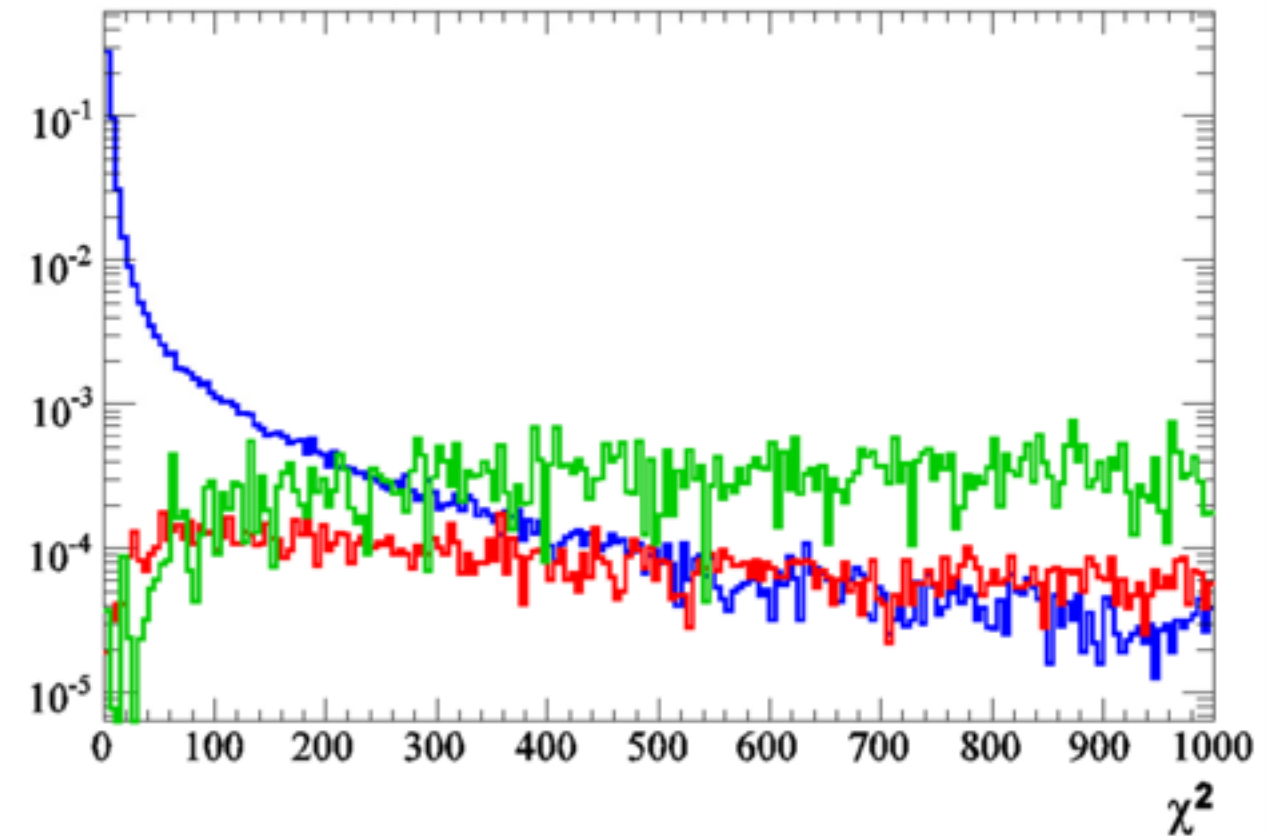
# Kinematic fitting for $ep \rightarrow e \gamma p \pi^0$

$ep \rightarrow e \gamma p \pi^0$   $ep \rightarrow e \gamma p$  SIDIS



$ep \rightarrow e \gamma p \pi^0$  hypothesis

$$\chi^2_{ep \rightarrow e \gamma p \pi^0} < 4.6$$



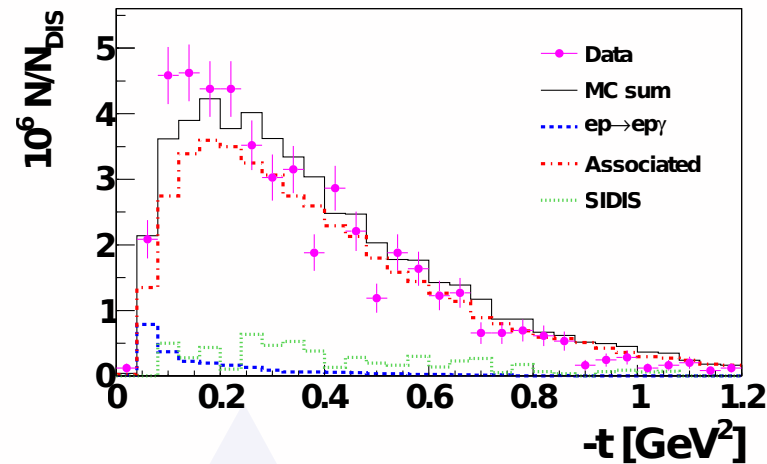
$ep \rightarrow e \gamma p$  hypothesis

$$\chi^2_{ep \rightarrow e \gamma p} > 50$$

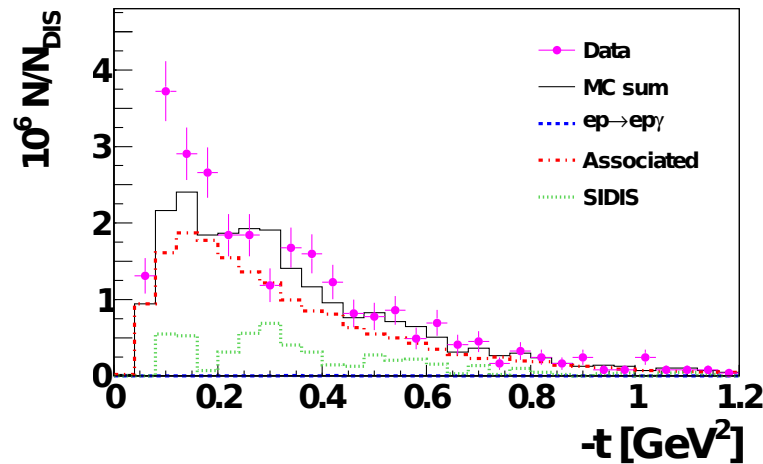
Using powerful kinematic fitting of  $ep \rightarrow e \gamma p$  hypothesis  
is crucial for the  $ep \rightarrow e \gamma N \pi$  analysis

# Selection of associated events

$$ep \rightarrow e\gamma p\pi^0$$

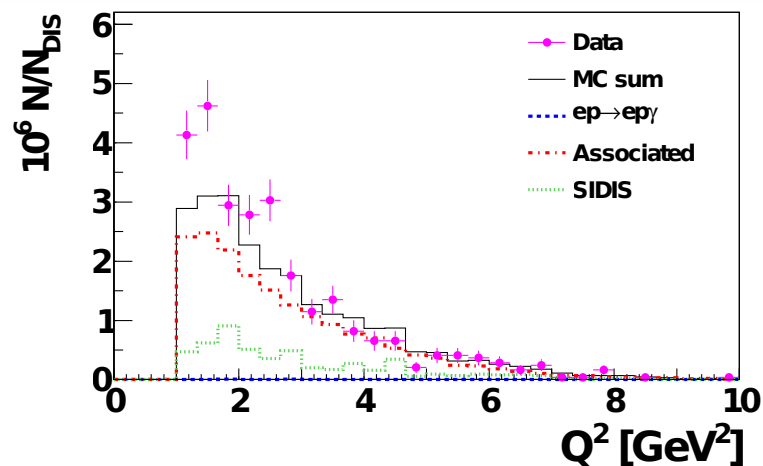
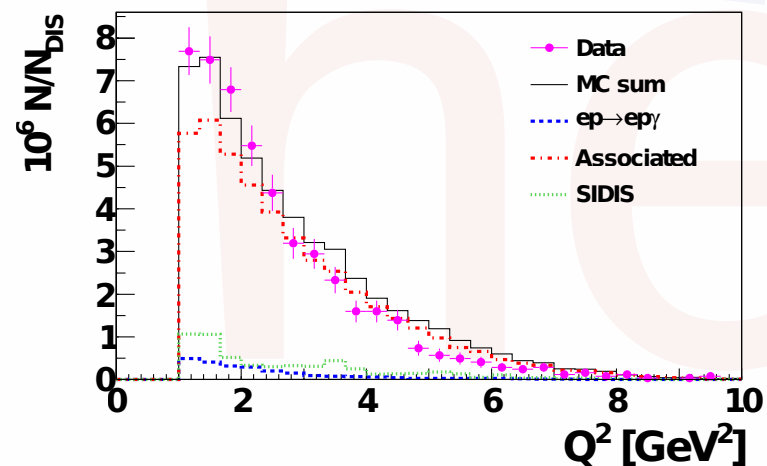
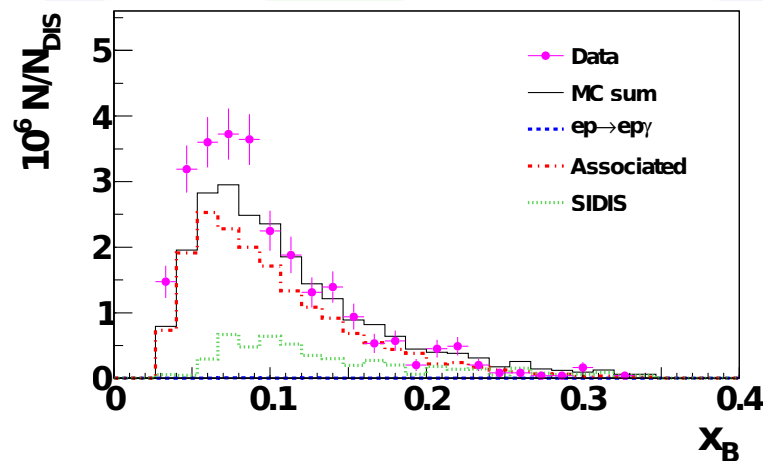
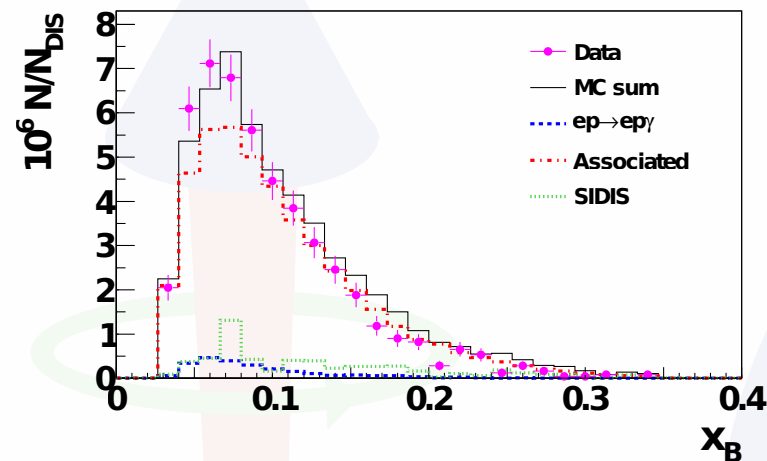


$$ep \rightarrow e\gamma n\pi^+$$



Uncharged particle  
remains undetected

Kinematic fitting in case  
of  $ep \rightarrow e\gamma N\pi$  hypothesis  
therefore not as strong



Additional selection criteria:

- Recoil PID information
- Lower-cut on  $ep \rightarrow e\gamma p$  hypothesis